An approach for using monitoring data to make a propulsion line model used for hardware-in-the-loop simulations

M. F. G. Vonk

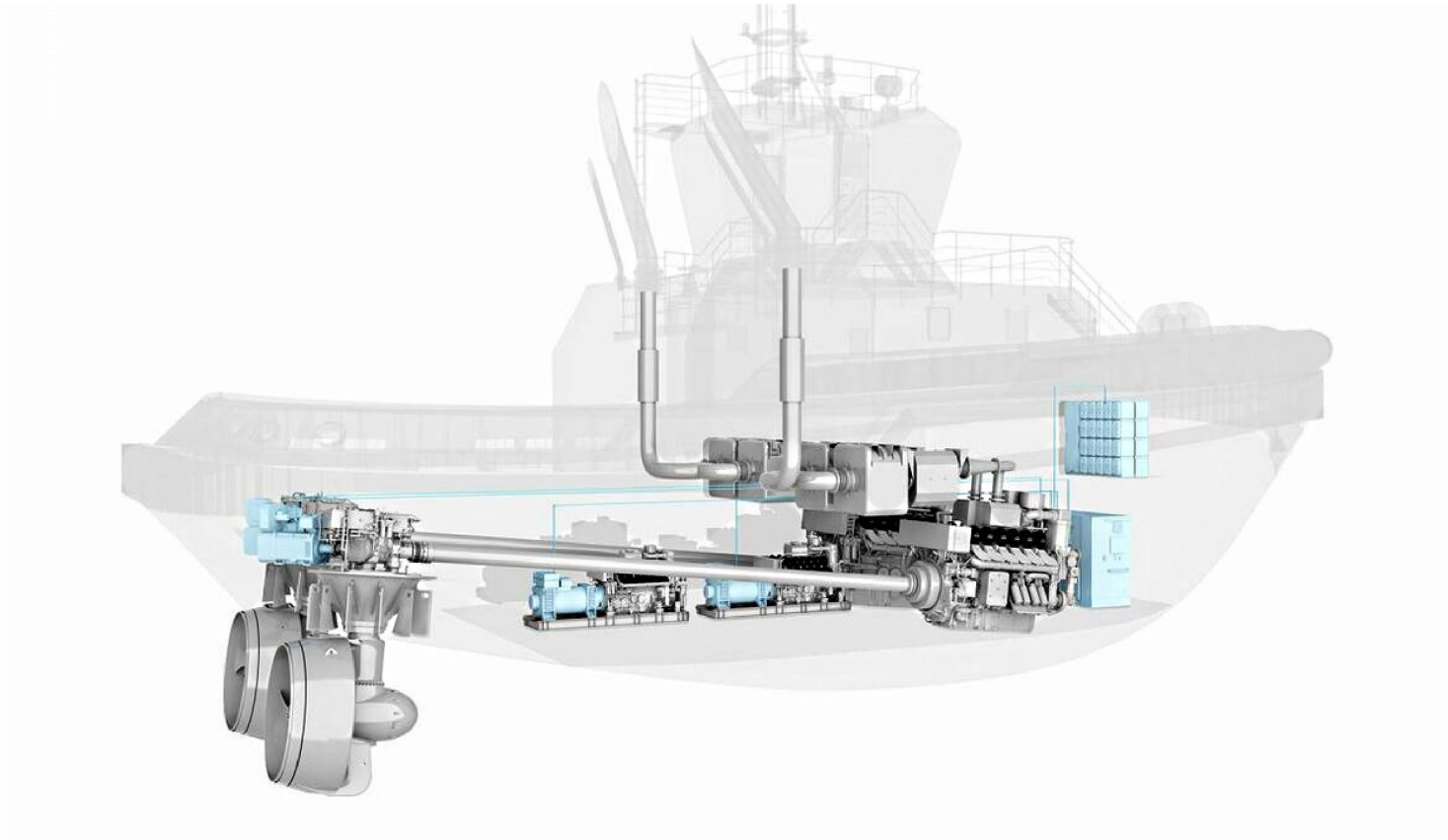

TU Delft

DAMEN

SDPO.20.027.m

An approach for using monitoring data to make a propulsion line model used for hardware-in-the-loop simulations

Master Thesis

by

M. F. G. Vonk

In partial fulfilment of the requirements for the degree of

Master of Science
in Marine Technology

at the Delft University of Technology,
to be defended publicly on Monday 02 November 2020 at 10:00 AM.

Report number:	SDPO.20.027.m	
Student number:	4287398	
Thesis committee:	Ir. K. Visser,	TU Delft
	Dr. ir. A. Vrijdag,	TU Delft, (supervisor)
	Dr. ir. I. Akkerman,	TU Delft
	Ir. J. Mobach,	Damen Shipyards, (supervisor)

An electronic version of this thesis is available at `http://repository.tudelft.nl/`.

TU Delft

DAMEN

Preface

With this report I present my graduation research. It is the final work of my time as a TU Delft student. This report is written to fulfil the graduation requirements for the master program, Marine Technology at the Delft University of Technology. Damen Shipyards Gorinchem offered me a subject for my graduation research that matched my interests and they supplied me with information and resources to fulfil the project.

The COVID-19 pandemic had a significant impact on my graduation research. I had to work from home for more than six months. Despite this though period the online communication with my supervisors remained very helpful and inspiring. There was a positive surprise: during this project I had the opportunity to give a webinar about my thesis for the Oceans 1 hackaton. An initiative of Oceans X to reduce the CO2 emissions of ships.

First, I like to thank the graduation committee. I would like to start by thanking my supervisor from the TU Delft, Arthur Vrijdag for the excellent guidance and support during this process. Our sometimes somewhat lengthy meetings helped me a lot to make progress in the project and to break new ground. I would like to extend my gratitude to Ido Akkerman for taking the time to take part of the graduation committee. I also would like to thank Klaas Visser for being the chair of the graduation committee and the elaborate feedback, first on the plan of approach and later on the draft version of this thesis.

I do like to thank Damen Shipyards Gorinchem. They gave me the opportunity to use their information, resources and do this thesis with an internship at their research and development department. In particular I would like to thank Joshua Mobach from Damen Shipyards as my daily supervisor, who was always ready to help and gave valuable feedback. Next, I do like to thank the simulations team for the welcome feeling, inspiring weekly meetings and the positive support during my time at Damen Shipyards Gorinchem.

Finally, I would like to thank my friends for the positive distraction and my parents and girlfriend for all the support, not only during this thesis project but also during the years for me as student. They motivated me to succeed and finish my study.

M. F. G. Vonk
's-Gravenhage, October 2020

Abstract

Due to constant changing environmental regulations, an increasing amount of vessels are being equipped with hybrid or electric propulsion and power systems. The use of those new energy sources and energy storage systems aboard of vessels increase the complexity of the power systems and controllers. Therefore hardware-in-the-loop simulations are more often applied in the shipping industry. Hardware-in-the-loop (HIL) testing is a technique where control signals from automation systems are connected to a virtual vessel, tricking the controller into thinking it is in the assembled product. With hardware-in-the-loop testing power systems and controllers aboard can be thoroughly tested and tuned before their integration in the final product, decreasing the amount of time spent finding errors and tuning controllers during the sea trial process. However, often models of virtual vessels are based upon the designer's gut feeling and are not calibrated or validated.

New technological developments enable full scale data monitoring and logging while a vessel is in operation. An increasingly amount of vessels are equipped with onboard data monitoring and logging systems that allow for wireless data transfer to the shore. Since nowadays remote data is becoming widely available and more convenient to use, the following research question arises: "How can the remote logged full-scale measurements be used to create a verified, calibrated and validated propulsion line model that can be used as a base for hardware-in-the-loop simulations?".

First, the raw remote logged data is processed into data that can be analysed and used for further application. With this analysis the following was noticed. There are limitations regarding the use of remote logged data for modelling purposes. Since the wireless data transfer connection is limited on the amount of information that can be send and received, the maximum achievable data sampling frequency is limited. The result is that the remote logged data cannot be used properly for the building, calibration and validation of dynamic models. The proposed solution is to extract only steady state data from the remote logged data in order to apply steady state operating points in the modelling, calibration and validation of the propulsion line model.

In order to apply the remote logged data for verification and validation of a propulsion line model, alternative modelling paths are created where equations within the component models are rewritten to control which output, input and assumptions are needed. By combining multiple assumptions and output variables, the model can be calibrated using remote logged data in the place of assumptions.

The effect of the calibration is examined by comparing the original model with the calibrated model and the remote logged data measurements. Finally, the model is validated by the use of remote logged data from another vessel of the same type. Validating with data from other vessel types, to check the modularity of the model is among other subjects discussed in the recommendations.

Contents

List of Figures

List of Tables

1 Introduction

In this chapter the problem definition is discussed and a possible solution is given. Next, the objectives that are required in order to apply this solution to the problem are listed. Thereafter, the research questions are listed. Last, the scope of the research is determined and the outline of this thesis is given.

1.1. Problem definition

Automation systems on board of vessels are becoming increasingly advanced and complex. During commissioning and sea trials often problems occur with interfacing and software functionality. The main reason for these issues is that during commissioning and sea trials all systems work together for the first time. Hardware-in-the loop (HIL) is commonly used in the automotive industry to test systems and controllers before their integration into the final product. Hardware-in-the-loop testing is a technique where control signals from automation systems are connected to a simulated vessel, tricking the controller into thinking it is in the assembled product. Nowadays this simulation technique is being used in the shipping industry to test systems before their integration in the final product. At Damen Shipyards Gorinchem, hardware-in-the-loop simulations are mainly used to test automation systems for propulsion. The aim of hardware-in-the-loop simulations is to decrease the amount of time spent finding errors and tuning PLC's during the sea trial process. The hardware-in-the-loop simulations make testing scenarios and operations that are dangerous to human and harmful to equipment possible in a virtual environment without any risk. Therefore more possible testing scenarios can be performed, resulting in a better tested and therefore a better final product. Sometimes, hardware-in-the-loop is also used to test dynamic positioning systems, analyse the electrical grid behaviour or to test system behaviour during operational switching. However, for every project the components in the simulation model are built or heavily adjusted to create a one-off virtual vessel that is able to perform simulations with specific needs. This virtual vessel is modelled and tuned by the model designer based on the model designer's experience and gut feeling. The models that are used are not validated and calibrated. Therefore, no conclusions can be drawn on the accuracy of the current made models. To reduce the time spent building a new propulsion line model for a specific vessel and to increase the accuracy of the modelled components used in the modelling of the propulsion line, the demand for a calibrated and validated propulsion model, as base for hardware-in-the-loop simulations is high. The use of widely available remote logged data to create a validated and calibrated model is researched in this project.

Until recently it used to be very expensive and time consuming to measure data on full-size vessels. One available method was performing towing tank tests, where a small physical model is tested and measurements are scaled to full scale. Towing tank tests have their limitations. One is that the test is performed over a short period of time resulting in a limited amount of data. Towing tanks allow for testing solely hydrodynamic behaviour and properties. Another available method for calculating variables that describe the vessel behaviour is with the use of computational fluid dynamic (CFD) computer programs. CFD is mainly used for testing hydrodynamic behaviour and properties. Also, CFD is limited by the maximum available computing power of the system and therefore sensitive to errors due to simple flow models or simplified boundary conditions. Both methods are based on predicting the behaviour of the full-size vessel and cannot always guarantee a good accuracy.

New technological developments enable full scale data monitoring and logging while a vessel is in operation. Many of the new-built vessels from Damen Shipyards are equipped with onboard data monitoring and logging systems that allow for wireless data transfer to the shore. A modern engine for instance, can have up to 4000 sensors. Data from about 250 of these can be monitored at the bridge, with information from about 70 measurements being displayed to the captain [35]. For every vessel that is equipped with an onboard data monitoring and logging system the information of approximately 250 sensors is stored in the a database on shore. The advantages of onboard data monitoring and logging systems with respect to traditional measurements are listed below:

- Data Logging can be done in remote or dangerous situations.
- Data logging can be carried out 24 hours a day, 365 days of the year.
- Since the data logging system is integrated into the vessel, no additional measurement setups are required.
- No need to have a person present taking measurements.

With the possibility to log data 24 hours a day, 365 days of the year as long as the vessel is in commission, Damen can provide service and assistant throughout the entire life cycle of the vessel, from lead to decommissioning. The benefits of this can be divided into multiple areas as listed below. When looking from a ship owner's point of view, improving efficiency and increasing income are important benefits. Improving efficiency can be achieved by monitoring and optimising fuel consumption, crew scheduling and navigation. Increasing income can be thought of in terms of maximise up-time which increases the amount of jobs that can be performed by the vessel per day. Monitoring the running time and load of installed components, can be used to check the condition of the component in order to accurate plan maintenance. At last, remote logging and monitoring could help with achieving plans for the future as autonomous shipping.

- Improving efficiency
  - Savings in fuel consumption.
  - Optimised crew scheduling.
  - Optimised navigation.
- Increasing income.
- Condition based maintenance.
- Autonomous shipping.

At this moment, remote logged data is mainly used for improving efficiency, increasing income and condition based maintenance. Since nowadays remote data is becoming widely available and an increasingly amount of vessels are equipped with onboard data monitoring and logging systems that allow for wireless data transfer to the shore, the following question arises: How can the widely available remote logged data be used to make a validated and calibrated propulsion line model?

As mentioned before, for each hardware-in-the-loop test the components in the simulation model are built or heavily adjusted to create a one-off virtual vessel that is able to perform simulations with specific needs. This virtual vessel is modelled and tuned by the model designer based on the model designer's experience and gut feeling. Since this model is based on the model designer's experience and gut feeling, a lot of assumptions are used in making this model. By the use the available remote logged data, a propulsion line model can be made, calibrated and validated. The verification, calibration and validation steps are well described by Sankararamana & Mahadevan [46] and shown in figure 1.1.

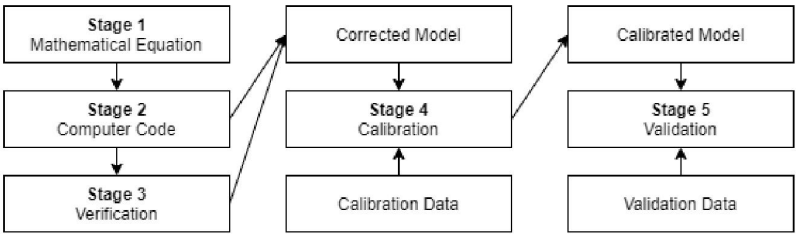

Figure 1.1: Stages in model development

In figure 1.1 the calibration data and validation data is used to calibrate and validate the model. Remote logged data can be used as the calibration data and validation data in order to calibrate and validate the model. By performing this calibration and validation steps the accuracy of the model is improved. Using such an calibrated and validated model as base for hardware-in-the-loop tests can result in several benefits. The expected benefits are listed below:

- When a calibrated and validated base model is used, making a propulsion line model to perform hardware-in-the-loop tests can be done more efficient and faster. When the hardware-in-the-loop test become more efficient, it becomes possible for more vessel projects to apply hardware-in-the-loop tests.
- A calibrated and validated model predict the behaviour of components more accurate which may increase the performance of ships due to better matching and tuning with hardware-in-the-loop simulations.

1.2. Objectives

The objective of this research is to make an approach for using remote logged data in such way that a propulsion model can be build, verified, calibrated and validated. The model is meant to be a base for the hardware-in-the-loop simulations. This means that the model has preferred requirements in order to achieve the expected benefits listed earlier. Those model requirements are:

- **Applicable for HIL simulations**
  The model must be able to be used as base for hardware-in-the-loop testing.
- **Modular**
  Modularity means here that a distinction between propulsion components is made in the model. This makes it possible to change components without affecting the overall model accuracy in order to simulate different vessels in the future.
- **Expandable**
  The model is the base upon which expansions can be made. In the future, the model could be expanded to include for instance: manoeuvring of the vessel, electrical system behaviour and different propulsion line configurations and components.

In order to use the remote logged data to reach the objectives, several steps must be performed. These steps are discussed in further detail in the project approach.

1.3. Research questions

The main research question of this research arises from the main objective and the question that was stated in the problem definition. The main research question is: "How can the remote logged full-scale measurements be used to create a verified, calibrated and validated propulsion line model that can be used as a base for hardware-in-the-loop simulations?".

This research question can be divided into multiple smaller sub research questions. If the sub research questions are answered, the main research question can be answered. The sub research questions can be linked to the steps that are described in the approach. The sub research questions are:

1. How is the remote logged data collected and what processing must be done in order to use it?.
2. What level of model complexity can be achieved by using the remote logged data and what corresponding variables are required?
3. To what extend is the remote logged data suitable for the calibration and validation of the model?
4. Can the application of validated models improve the accuracy and/or efficiency of the HIL tests?

1.4. Scope

The objective is to find out if it is possible to build, calibrate and validate a propulsion line model with remote logged data. Therefore only the remote logged data and known design parameters are used in this project. No extra measurements are used to reach the objective.

The data that is used in this project comes from the remote data logging aboard of tugs and the known design parameters. Besides tugs only a few other vessels are fitted with the system that makes remote data logging possible. Those vessels are mostly one of a kind vessels. Since several tugs are now equipped with onboard data monitoring and logging systems that allow for wireless data transfer to the shore, the propulsion line of a tug will be modelled in this project. Having remote logged data from vessels of the same series and different series of the same type, is preferred in order to apply the calibration and validation steps of the propulsion model.

As mentioned, only the vessel's propulsion will be modelled. First the components that are included in the propulsion line of the vessel are determined. In figure 1.2 a top-down view of the tug's engine room is shown. On this top down view the layout of the propulsion line can be observed. Two main engines are present, both connected to an Azimuth thruster via a shaft.

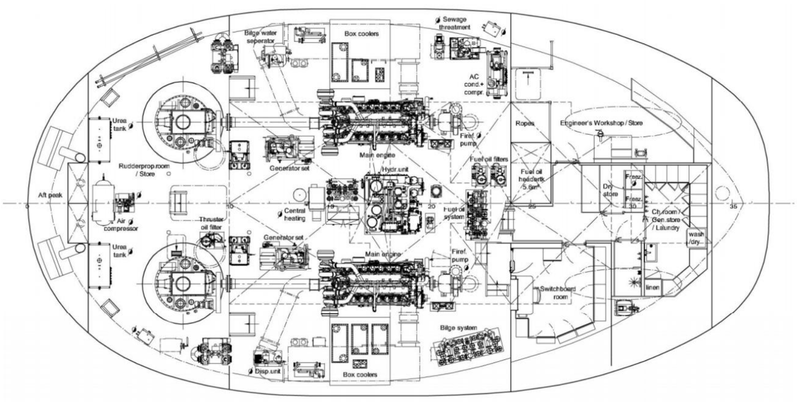

Figure 1.2: Schematic view of the general arrangement of the RSD tug

A schematic representation of the general arrangement of a tug is shown in figure 1.3. As discovered from the top-down view, the propulsion line consist out of two diesel engines as prime movers, each connected to an Azimuth thruster to propel the vessel. An azimuth thruster can be seen as a propeller and reduction gearbox in one. This means that the whole propulsion line of a tug can be modelled out of two identical propulsion

lines containing a diesel engine, reduction gearbox and propeller. Thus the suggested base model will also contain those three components twice. Besides the diesel engine, gearbox and propeller, the hull and it's resistance is also modelled. In figure 1.2 several other components are shown, such as generator sets, fuel oil systems, HVAC system components, bilge water pumps and hydraulic pumps. Those components do not contribute to the propulsion of the vessel and are therefore not taken into consideration in this research.

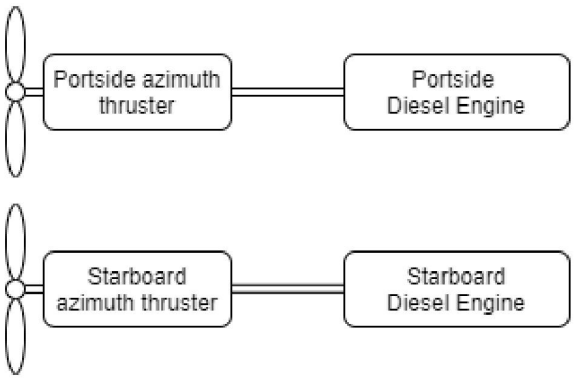

Figure 1.3: Schematic overview of the propulsion line

As mentioned, the model is preferably made with parameters known early in the design process, what makes it possible to extend and adapt the model to simulate multiple ship types in the future. The complexity of the model is determined by the available remote logged data. Model system boundaries determine the inputs, outputs and assumptions and with that the complexity of the model. The availability of the remote logged data determines the complexity of the model.

Because the computer program "Simulink" is used by Damen Shipyards Gorinchem to perform hardware-in-the-loop simulations, and the model aims to be a base for future hardware-in-the-loop simulations, the model will also be made in Simulink. Since Simulink is a part of MATLAB, MATLAB is used to process the remote logged data in order to make the integration of the processed data into the Simulink model possible.

1.5. Approach

The project is divided into six parts. Those parts are shown in figure 1.4. The first part is load and process data. In this part the data is downloaded in raw format and processed into data that can be analysed and used in the next steps. A selection is made which data set and which variables are visualised and analysed. The second part is data reduction where the processed data is reduced by means of selecting data that is useful for the modelling, verification, calibration and validation step. The third part is the modelling part which includes the making the propulsion line model. Step four, five and six are respectively the verification, calibration and validation of the model.

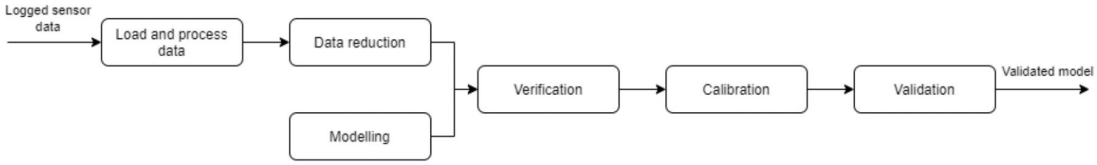

Figure 1.4: Flowchart of the project approach

To show the process of building, verifying, validating and calibrating the model, the systematic way as described by Vrijdag [51] will be used. In the paper by Vrijdag, a circular model is shown. Missing from this figure is the calibration step. In the in the paper “Modelling guidelines- terminology and guiding principles” by Schlesinger and adjusted by Refsgaard & Henriksen [22] the figure “elements of a modelling terminology” is shown in figure 1.5, which is the circular model including the calibration step. This figure is used to show the steps that need to be taken to build, verify, validate and calibrate a model and locate the steps were and how the remote logged data will be used.

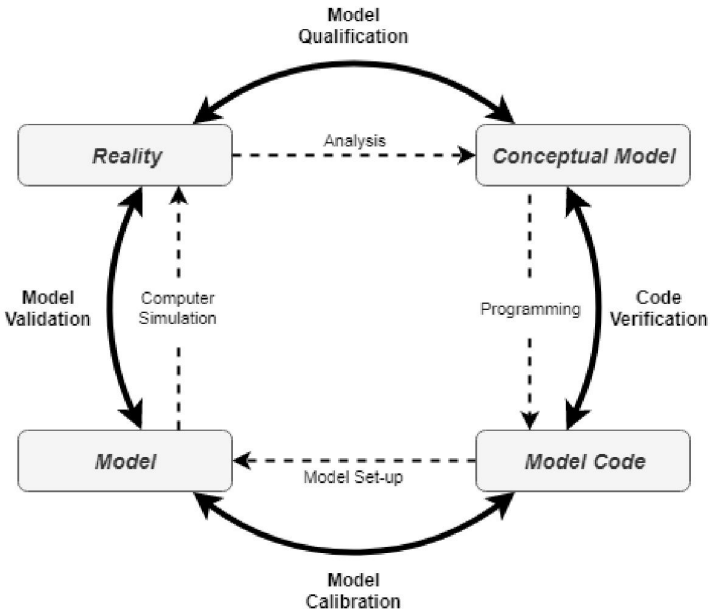

Figure 1.5: Elements of a modelling terminology

The first step is the model qualification step where the vessel is analysed. With this analysis, the complexity of the model is set. The analysis of the remote logged data determines what data actually is available and what data can be used. The data frequency and availability may limit the complexity of the component models that will be used to create the propulsion model. If the remote logged data causes limitations, it is preferred to use a more simple model where the remote logged data can be used, rather than a complex model where applying the logged data is not sufficient. The model must represent the propulsion line of a ship. This means a simple diesel engine, gearbox and propeller are included in the model. By placing system boundaries within this model, the variables such as inputs, outputs and assumptions are obtained.

The second step is the programming step. In this step, the model is made by combining models of components together into a whole propulsion line model. The model complexity must comply with the inputs, outputs and assumptions set by the remote logged data availability. The model consist out of different components, like the complete model, the components must be simple and must be chosen in such way that the remote logged data can be used. Literature research is performed on component models with different levels of complexity. Models from the literature research can be chosen and combined to create a propulsion line model.

The third step is using the remote logged data. Since the database where the data is stored is accessible through the Damen digital portal, the remote logged data is obtained by downloading comma separated values (csv) files from the portal. This data must be loaded and processed in order to use it for the intended purpose. This step includes the model calibration. The parameters that are chosen by placing system boundaries between propulsion components can be used to compare the remote logged data with calculations and known values in order to calibrate the model. Besides the remote logged data, known calculations with associated constants and known component data in the form of MATLAB lookup tables are used and inserted into the model. With the comparison of the model results and the remote logged data the model is calibrated.

The last and fourth step is the model validation. Now that the model is calibrated, it must be tested. Since the database where all remote logged data is stored, contains data from more than one vessel and vessel types, the first step is to check if the model complies for different vessels of the same type. If a different vessels contain different components but is from the same type, the modularity of the model is tested.

1.6. Outline

The report is structured as follows. In chapter two a literature review is presented where first the relevant research regarding hardware-in-the-loop and the usage of remote logging data in maritime technology and other fields is presented. Second, literature research is done to the modelling of marine propulsion lines including the different component models that are listed in the scope.

In chapter three the loading and processing of remote logged data is explained. The loading and processing of remote logged data is the first step as can be seen in figure 1.4 which is discussed in the project approach. In this chapter the processing of the raw data into data that is usable in a model and can be visualised is described. Processes that are performed are discussed and the scripts that are made for those processes are included in the appendix.

In chapter four the processed and visualised data is further processed. In this chapter the vast amount of data is reduced to a limited amount in order to use it for the modelling of the propulsion line and to use the data for calibration and validation purposes. The data reduction process can also be seen in figure 1.4 which is described in the project approach.

Chapter five can be divided into four parts. In the first part the modelling of the propulsion line model is explained. In the second path the model is verified with the use of theoretic formulas. In the third part the model is calibrated with the use of the processed and reduced monitoring data. After the model is calibrated, the fourth part describes the validation of the model.

Finally, this thesis finishes with conclusions and recommendations for further research in chapter six.

2

Literature

In this chapter, research is done regarding the main aspects of this project. First, hardware-in-the-loop and it's applications are examined. When the literature research is performed, the following questions about hardware in the loop are kept in mind.

- What are the applications for hardware in the loop?
  - How is hardware in the loop used in other industries?
  - How is hardware in the loop used in the marine industry?
- What are relevant developments regarding hardware in the loop in both industries?

The last main aspect of this thesis is the modelling of the propulsion line. Literature research is done on which modelling techniques are applicable and what the possibilities for modelling a propulsion line model are. Since the propulsion line model will contain the general components of the propulsion line of a tug, relevant literature regarding those components are examined. Literature of the following propulsion line components is researched :

- Diesel engine
- Gearbox
- Propeller
- Hull

In order to choose which modelling approach and component model complexity is suitable for the integration of the available remote logged data, different component models with different levels of complexity are researched.

In the search for relevant literature, multiple libraries are used. Not all literature libraries are free to use. Only free to use libraries and libraries that can be accessed with a Delft University of Technology account are used. The libraries that are used for this literature research are:

- https://www.google.nl/
- https://scholar.google.com/
- https://ieeexplore.ieee.org/
- https://www.academia.edu/
- https://repository.tudelft.nl/
- https://www.researchgate.net/
- https://www.sciencedirect.com/

2.1. Hardware in the loop

Hardware-in-the-loop (HIL) is a simulation technique where real signals from a controller are connected to a model that simulates reality. The principle of hardware-in-the-loop tests is tricking the controller into thinking it is in the assembled product. This way the real-time response and behaviour of the controller to the simulated reality can be tested. An important reason for applying this simulation technique is the possibility to test a product before it is finished. This way problems can be found early in the design process and changes are less costly to implement. Besides early testing, HIL can also be used to test in conditions that are unusual or dangerous, such as extreme weather. Hardware-in-the-loop testing also comes with challenges. According to Altosole, Campora, Figari, Laviola and Martelli [30] one challenge is running a model in real time mode and interfacing it with the real controller. One other challenge is the modelling of the main engine. The main engine is the most critical propulsion component to be simulated, requiring good precision and possibly a low computation time. Speed and accuracy are crucial for making an engine model capable for real-time simulations.

2.1.1. Applications of hardware in the loop

Nowadays, hardware-in-the-loop is more often used in several different industries. Besides the marine industry HIL is also applied in other industries. The industries were HIL is applied often are listed below.

- Automotive
- Power and energy systems
- Aviation and Aerospace
- Marine and offshore

Application in automotive

In the automotive industry hardware-in-the-loop test are commonly used to test control unit aboard of vehicles. A virtual vehicle is modelled and connected to a control unit that requires testing. Hardware-in-the-loop simulations allow developers to validate new hardware and software for the automotive industry without expensive and time consuming driving tests. One of the many applications of HIL in the automotive industry is the verification of the behaviour of a power-train controller module (PCM) by Raman et al. [47]. Besides the power-train controller module, the electronic control unit (ECU) is also often tested with the use of hardware-in-the-loop simulations. Palladino, Fiengo, Giovagnini and Lanzo [9] made a portable device that is able to perform hardware-in-the-loop tests of the engine management system of the ECU. The engine management system can also regulate the sequential turbocharging process. The application of hardware-in-the-loop test for validating and tuning the regulated turbocharging process is done by Du, Wang, Yang, and Wang [21]. Aparow, Hudha, Ahmad and Jamaluddin [19] used hardware-in-the-loop to test an ECU equipped with a x-by-wire system. The x-by-wire system is a new technology in the automotive where mechanical or hydraulic connections for steering, accelerating and braking are replaced by electrical wires.

Application in power and energy systems

Hardware-in-the-loop simulations are nowadays also applied to power and energy systems. Due to environmental regulations on emissions, renewable engine sources are becoming more popular. This change has an impact on the electrical power grid and on the dynamic behaviour of electrical power systems. Ahmad, Papadakis, Perilla, Torres and van der Meijden [34] used hardware-in-the-loop testing to test wind turbine controllers for transient stability enhancement. Grid damping control methods are examined and tested by Bhandia, Chavez, Cvetkovic and Palensky [39] and Al-Hammouri et al. [41]. Nguyen et al. [26] also investigated the impact of new energy sources on the grid by applying hardware-in-the-loop testing to test the power system stability. Besides electrical grid testing, HIL is also used in the design of renewable energy sources. Aregger et al. [43] used hardware-in-the-loop testing for autonomous airborne wind energy systems. Due to the hard to predict wind behaviour, theoretical calculations did not match with real life measurements. Hardware-in-the-loop is applied in order to keep the environmental test conditions the same.

Application in aviation and aerospace
Hardware-in-the-loop simulations is now widely used for testing aircraft and aerospace systems. Small unmanned aircraft, also called unmanned aerial vehicles (UAVs) are often tested using hardware-in-the-loop methods since physical testing brings a high risk of damaging the UAV. Lugo-Cárdenas, Salazar and Lozano [42], Kamali & Jain [45] and Abdulhamid, de Oliveira and d'Amore [40] all examined the applications of hardware-in-the-loop testing for UAVs. Coopmans, Podhradský and Hoffer [36] performed hardware-in-the-loop testing to verify a flight dynamic model and flight control system of an UAV. The design of a flight stabilizer for fixed-wing aircraft using HIL was researched by Akyurek, Ozden, Kurkcu, Kaynak and Kasnakoglu [5].

Besides the application of hardware-in-the-loop test in aviation, HIL testing is also often used for multiple aerospace applications. One of the applications is testing satellites in the design and planning phase of the project. A hardware-in-the-loop validation of the GPS/GNSS systems aboard of LEO Satellites was performed by Tsai, Chin, Lee, Goh and Low [27]. Fritz et al. [20] made a hardware-in-the-loop environment for the verification of the onboard software of a small satellite. The manoeuvring of a satellite was tested by Chesi, Perez and Romano [31] by making a dynamic three axis simulator to perform hardware-in-the-loop tests upon. Testing the manoeuvrability is also done upon rockets. Yamasaki, Matsumoto,Itakura, Miyamoto and Yonemoto [28] developed a HIL simulator to test the elevator control of a rocket and optimising the angle of attack and pitch angle in the ascend phase. Zhang, Yang, Jiang, Hu and Zhang [56] developed a hardware-in-the-Loop simulation for the validation of the control system for the THX rocket.

Application in offshore and marine engineering
In the offshore industry, ships are often equipped with advanced control systems dynamic positioning and power management. HIL makes extensive testing of a dynamic positioning system possible before the integration in the final product. Moreover, the use of HIL makes it possible to test the dynamic positioning system in simulated extreme environmental conditions. Skjetne & Egeland [37] proposed hardware-in-the-loop testing for the verification and validation of a dynamic positioning system. They presented concepts defining the primary target system for HIL testing. When sub-sea operations are performed, often not only the dynamic positioning system, but also a motion compensation system is responsible for keeping the position of the vessel and the position of the load steady. The application of hardware-in-the-loop testing for an active heave compensation system (AHC) of an offshore support vessel is examined by Luman, Roh and Ham [44]. To evaluate the applicability of HIL testing for a heave compensation system, it was applied to an offshore support vessel (OSV) crane.

Altosole, Benvenuto, Figari and Compora [52] presented a prototyping and testing procedure for the development of the propulsion controller of the new Italian aircraft carrier, using hardware-in-the-loop simulations. A complete dynamical model of the ship propulsion line was developed. Thereafter hardware-in-the-loop testing was applied to debug the controller software and to tune the controller before sea trials in order to reduce the time spent on tuning the control system during the ship delivery phase.

Due to changes in environmental regulations, an increasing amount of vessels are being equipped with hybrid or electric propulsion and power systems. The use of new energy sources and energy storage systems aboard of vessels increase the complexity of shipboard power systems and controllers. Perabo & Zadeh [32] examined the application of hardware-in-the-loop testing of a shipboard electric power system to verify the ship power management system (PMS).

Dubey & Subramanian [1] applied hardware-in-the-loop simulations in the design and validation of autonomous vessels. Studies on hydrodynamic behaviour were performed by modelling first order steering dynamics and the quasi-steady relationship between surge speed and the propeller speed. Towing tank tests and model scale turning circle test were applied in the modelling of the hydrodynamic behaviour. The HIL tests include manoeuvring such as sailing in a straight line, making a turn circle and performing a zigzag manoeuvre to validate the combined system performance.

Vrijdag [53] wrote an article on the potentials of hardware-in-the-loop simulations in the towing tank. The application of hardware-in-the-Loop in a towing tank or model basin is explored as a means to investigate to what extent, and in which cases, the dynamics of the shipboard systems affect the overall system behaviour. When free sailing tests in waves are carried out, the shaft torque or constant power are kept constant. How-

ever, neither of these options reflects realistic behaviour of the drive system, because in waves and during manoeuvres the propeller speed, torque and power are in fact variable.

A linearised model of the uncontrolled ship propulsion system which can be used for analysis of propulsion system behaviour in waves and for initial controller design and tuning is derived by Vrijdag & Stapersma [2]. In their research the behaviour of the ship propulsion system in the frequency domain is investigated by derivation and analysis of the transfer functions. The basic core propulsion system is modelled out of multiple sub-models. The required richness of the sub-models depends on the goal that one has with the overall model.

The potentials of hardware-in-the-loop simulations in the towing tank were further investigated. The Propeller-engine interaction in a dynamic model scale environment was investigated by Huijgens, Vrijdag and Hopman [18]]. To fill the resulting knowledge gap, they further developed existing scale model tests into so-called dynamic model basin tests. These tests aim to predict dynamic behaviour of the ship propulsion plant in complex, dynamic environments in more detail, leading to improved propulsion systems and controls and ultimately, lower emissions, lower fuel consumption and increased manoeuvrability.

Hardware-in-the-loop simulations is nowadays also being applied by Damen Shipyards in the design of multiple different vessel types. Damen mainly uses hardware-in-the-loop simulations to test the propulsion performance of a vessel. Damen first commercially applied hardware-in-the-loop tests to a series of Offshore Patrol Vessels (OPV's). Those vessels had two engines per gearbox and a whole array of operational modes and changeovers in addition to two main controllers on the propulsion train from different suppliers. Software logic and the integrated functionalities were tested. A lot of issues were identified and resolved that before only were discovered and solved during sea trails. This significantly reduced time spent on commissioning and sea trials. for a walk-to-work vessel where a gangway is used to assist people in getting on board and getting off the vessel, the hydrodynamic model, dynamic positioning control system and gangway controls were simulated for the hardware-in-the-loop test. By performing a hardware-in-the-loop test for this vessel, the systems could be tuned, resulting in an increase of dynamic positioning capabilities from 70% to nearly 96%.

Damen also applied hardware-in-the-loop simulations to test systems, other than the propulsion system. The performance of the Energy Management System of a hybrid ferry was tested and optimised by emulating the behaviour of the on board machinery systems. It facilitated testing of the Energy Management System throughout the development period and helped to demonstrate the feasibility of a cost-effective, environmentally friendly, reliable and stable operation. Hardware-in-the-loop was also used to develop and test the six operational modes of Damen's Marine Aggregate Dredger. The modes automate and facilitate all the processes required for the vessel to shift from one operational cycle to the other.

At this moment several projects are ongoing at Damen shipyards Gorinchem where hardware-in-the-loop is applied. Also studies to whether hardware-in-the-loop is required and can improve the product are performed.

2.2. Propulsion line modelling

The most basic general propulsion line of a vessel consist out of a marine diesel engine, reduction gearbox and a propeller. The propulsion line model will be build by using models of these separate components. A literature research on those different models is performed.

- **Diesel engine**
  There are different approaches to model a marine diesel engine. All with varying complexity and applications. According to Altosole et al. [30], the main engine is the most critical propulsion component to be simulated,requiring good precision and possibly a low computation time. Geertsma et al. [25] categorised the diesel engine models by the level of dynamics and underlying physical detail.

  – Zero order models could model the engine torque and fuel consumption with the use of mathematical equations, from a number of measurement points or from a look-up table.
  – First order models are based on more complex underlying principles and can calculate turbocharger pressure or turbocharger speeds with the use of extensive experimental data.
  – High order mean value first principle models include air and gas flow dynamics. The six point Seiliger cycle to determine inlet and exhaust receiver conditions.
  – Zero-dimensional crank angle models simulate the thermodynamic state of air and combustion gas in the cylinder for a specific crank angle position.
  – One-dimensional fluid dynamic models are used to predict airflow within the cylinder, compressor, turbine, intercooler, inlet and outlet receiver.
  – Multi-zone combustion models predict airflow throughout the whole engine in three dimension with the use of CFD techniques.

  A zero order model is described by Klein Woud & Stapersma [10]. The engine's overall efficiency is used to calculate the amount of heat from the fuel that is converted into work. The only output is engine torque or power as function of just a few input parameters such as the engine rotational speed and fuel consumption. In these sort of models, the dynamics of engine and subsystems such as turbochargers are often not taken into account or taken into account by means of time constants.

  More complex models are based on the mean value first principle where the cylinder processes over one cycle are considered. As written by Loonstijn [33] the TU Delft in-house developed Diesel A and Diesel B models are both based on the mean value first principle (MVFP) models and they differ in their complexity and application. The Diesel A model provides a lower entry level model that requires only basic project guide parameters and some other well-known parameters. The Diesel B is more complex and requires detailed data of the turbocharger groups including the operating maps of the turbine and compressor. Loonstijn [33] suggested adjusting the existing Diesel A model in such a way to make it suitable to model advanced turbocharger strategies without the need for the more complex Diesel B model.

  Miedema & Lu [58] stated that there is a need for a model that is more advanced then a first order system and less advanced than the very complex models. Such a model has been derived, based on the Seiliger (thermodynamic) process.

  More recently, the most complex models include a fully thermodynamic actual cycle simulation approach, where the cylinder thermodynamic processes, including combustion, are calculated as function of the crank angle. Ishida et al. [16] analysed the use of a two-zone diesel model which consists of a burned zone and an un burned zone where the thermodynamic process is independent in each zone. Also quasi-dimensional combustion models, which includes the mixing, phases and flow of fuel in different zones within the cylinder are analysed by Qi et al. [55]. Furthermore computational fluid dynamics (CFD) analyses are applied to model the diesel engine by Reitz & Rutland [8].

- **Gearbox**
  The gearbox connects the diesel engine to the propeller. The rotational speed of the output shaft of the diesel engine must be reduced in order to reach the optimum shaft speed for the propeller. The reduction gearbox enables the engine and propeller to operate at their optimum speeds. There are multiple different types of gearboxes. The most common are single stage and two stage reduction gearboxes. Single stage reduction gearboxes have a fixed gear ratio. The reduction gearbox within an azimuth thruster is a single stage reduction gearbox. Research is done on gearboxes to reduce the heat losses and therefore increase the efficiency.

  As described in the book "Design of Propulsion and Electric Power Generation Systems" by Klein Woud & Stapersma [10], a reduction gearbox reduces the rotational speed and increases the Shaft torque from the engine towards the propeller. Klein Woud & Stapersma [10] describe that a common constant value for the transmission efficiency amounts 97 percent in the design condition.

  The percentual losses of a gearbox are usually assumed to be constant and between 2% and 4%. This is true for full load conditions. However, in low-load and part-load conditions, gearbox losses may be significant. In order to estimate the performance of maritime gearboxes, an evaluation of losses by applying a thermal network and creating an equation for calculation of gearbox losses was done by Godjevac, Drijver, de Vries and Stapersma [11]. They presented an equation in normalised notation to determine the torque loss within a gearbox. The presented equation is shown with formula 2.1

$$M^*_{loss} = a \cdot M^*_{in} + b \cdot N^*_{in} + c \tag{2.1}$$

  In this equation M*loss is the normalised torque loss of a gearbox, a is the fit coefficient related to the torque, M*in is the normalised torque going into the gearbox, b is the fit coefficient related to the shaft speed, N*in is the normalised shaft speed going into the gearbox, and c is the fit coefficient related to the constant torque loss.

  Fernandes, Marquesa, Martinsa and Seabra [24] split their research regarding marine gearboxes into three parts. Part one describes the losses in roller bearings, considering the influence of the gears, rolling bearings and seals, the influence of the operating conditions, lubricant formulation and the lubrication method. The second part of the study presents extensive experimental tests where an average coefficient of friction between meshing gears was obtained. The third part includes the application to a parallel axis and a planetary gearbox. The results from part one and two are applied to predict the power loss in a parallel axis and a planetary gearbox. The power loss model indicates that the power loss does not change that much with increasing torques for a fixed speed. The model also suggests that all gear oils have similar power loss performance and that the main power loss sources are the rolling bearings.

  Wemekamp & Luo [57] developed a simulation tool for analysing efficiency and thermal behaviour of gearbox applications. The modelling includes local bearing and gear contacts as well as gearbox housing and shaft lay-out. The model gives the possibility to do sensitivity and robustness analysis to study effects of variations in operating conditions, material and lubricant properties and internal bearing clearance variations on the gearbox performance.
  The application of CFD models to study the oil squeezing power losses of gears and the churning power losses of planetary speed reducers was performed by Concli [15]. More studies were performed concerning the application of CFD to the prediction of gear power losses. Marchesse et al. [4] applied CFD models to study windage losses of gears and validated their results by means of experimental tests.

  Finally, the vibrations caused by the gearbox are studied. Chang, Liu and Wu [29] analysed the influence of different parameters on vibration of a planetary gear system. The considered parameters included mesh stiffness, structure stiffness, moment of inertia and mass of the structure.

- **Propeller**
  The first theories describing the marine propeller are based upon the actuator disk theory. The actuator disk, at the propeller plane, is considered to absorb all of the propeller rotating power from the engine and dissipate this power by causing a pressure jump, and by doing so creating a pressure difference across the two faces of the disc resulting in a thrust.

  Carlton [7] presented an overview of the development of different methods used to simulate the performance of different propellers. In the book by Carlton [7] the calculations for a simple propeller model by using experimental obtained data, written in the form of coefficients from "wake adapted ducted propellers" by Oosterveld [38] among others is described. With these coefficients, the thrust and torque coefficients can be determined for a given propeller. These coefficient can be plotted against the dimensionless velocity 'J' to obtain the open water propeller diagram. The standard Wageningen B-series have been used over the years to provide diagrams or equations to assist in the selection of the marine propeller suitable for a given ship during the preliminary stages of ship design.

  Since experimental results showed that these mathematical models of propeller thrust and torque that are traditionally based on steady state and obtained in model basin tests, do not accurately describe the transient phenomena in a thruster, Blanke, Lindegaard and Fossen [50] published a dynamic model of propeller that includes the effects of transients in the flow over a wide range of operation.

  More complex hydrodynamic models are described by Durante, Dubbioso and Testa [6]. For instance the analysis of the unsteady loads delivered by a marine propeller due to working in a non-uniform wake field. Also the predicted propeller loads by a fully 3-D panel-method Boundary Element Method (BEM) solver and the use of Computational Fluid Dynamic (CFD) solvers is described.

- **Hull**
  In the modelling of the hull, the main aspect is the ship resistance. The resistance is the total force that is required to propel the vessel at a specific speed. The hydrodynamic resistance can be divided into two main components, frictional and residual resistance or the viscous and wave resistance. There are three different methods for the prediction of the resistance. Analytical methods, towing basin model tests and Computational Fluid Dynamics (CFD) calculations.

  Towing basin test are the first test performed to determine the resistance of a vessel. Froude [54] compared towing tank results with towing tests of actual vessels to determine scaling laws which can be used to accurately determine the resistance with the use of towing tank tests. Towing tank results are now used as validation and benchmark for the CFD calculations.

  There are also empirical or statistical methods to determine the resistance. The most common of these is the approximate resistance and power prediction method by Holtrop and Mennen [17]. Despite the sufficient accuracy of this method, the sample hull forms on which the method is based upon dates back to the 1970s and 1980s. Those older hulls are somewhat different from modern hull forms. The Holtrop and Mennen method is currently considered as one of the most accurate and efficient methods for the estimation of the resistance and propulsion power requirements of a mono hull vessel at the initial design stage.

  The majority of recent research on the resistance of a vessel includes the application of computational fluid dynamics (CFD) methods. CFD solvers solve the reynolds averaged navier strokes equations over the entire hull in small and finite volumes. CFD methods can analyse flow problems in resistance estimation. Jasak, Vukcevic, Gatin and Lalovic [23] among many others use the CFD for validation and grid sensitivity studies. The application of CFD to calculate the resistance is done with three types of turbulence models, which are k-epsilon, k-omega, and shear stress transport (SST). Each turbulence model has its own strengths and field of application.

3

Load and process data

In this chapter, the loading and processing of remote logged data is conducted. This is the first of the six steps that are described in the project approach. The "load and process data" step that will be performed in this chapter is coloured green in figure 3.1. This figure is the same as the general flowchart of the project as discussed in the introduction.

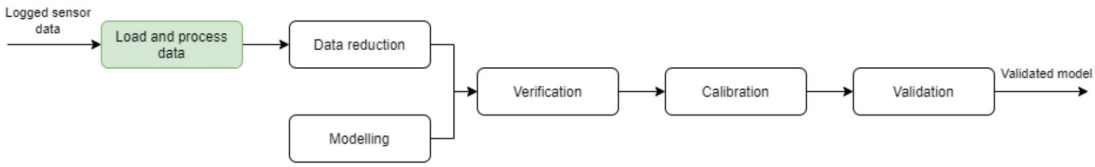

Figure 3.1: General flowchart

The load and process data step can be split up into multiple steps. In this chapter the available remote logged data is discussed. Thereafter, the data is loaded and processed in order to visualise the remote logged data. The steps that are required in order to do so are presented in figure 3.2.

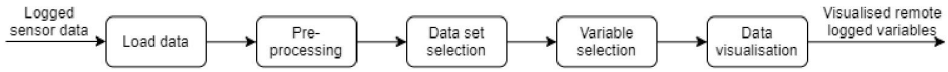

Figure 3.2: Flowchart of steps in the 'Load and Process data' chapter

The 'load data' step is divided into three smaller steps. The first is downloading the data from the Damen database. The second step is to split the large data files into smaller files in order to be able to load the data into MATLAB. The third step is the importation of the data files into MATLAB. Pre-processing can be divided into two different steps. The first step is combining the numbered headers of the data set with the corresponding sensor names. Thereafter all the empty lines of the data are removed.

3.1. Remote logged data

Data logging during sea trails is a common way of gathering performance data from a vessel. However, data that is gathered this way is almost always stored locally, often on separate systems and data is logged for only a limited duration. Nowadays, many of the new-built Damen vessels are equipped with onboard data monitoring and logging systems that allow for wireless data transfer to the shore. With this connection, it becomes possible to log data for an unlimited duration. This logged data is used to monitor the vessels behaviour and systems.

Not all the new build vessels are equipped with onboard data monitoring and logging systems. Besides tugs only a few other and mostly one of a kind vessels are equipped with such data monitoring and logging systems. Most new build tugs are however equipped with data monitoring and logging systems. Since six months now, data is logged from 10 tugs. The logged data from six of those is available via the database. This means that from three RSD 2513 tugs the data is available, from only one ASD 2811 the data is available and finally from two ASD 2813 the data is available. The tugs with corresponding yard numbers that are equipped with a monitoring and logging system and where the database can be accessed are listed below. As mentioned in the scope of the project, the use of remote logged data of these similar tugs is beneficial.

- RSD 2513 (Yardnumbers: 515001, 515002 and 515006)
- ASD 2811 (Yardnumber: 513202)
- ASD 2813 (Yardnumbers: 513301, (513302)

An installed automation system is responsible for collecting data from around 800 installed sensors. This collection is done with the use of the MODBUS Protocol. The MODBUS Protocol is a messaging structure, widely used to establish master-slave communication between devices. A schematic representation of the working principle of the MODBUS protocol is shown in figure 3.3. The master sends a message which includes the data request and the slave's (sensor) address where the data request is send to. The targeted slave (sensor) responds with a message containing the current measured sensor value and the current timestamp. Because the data request are targeted and only one sensor answers a request at a time, the whole system can be connected in series by using a serial interface such as RS232, RS422, or RS485.

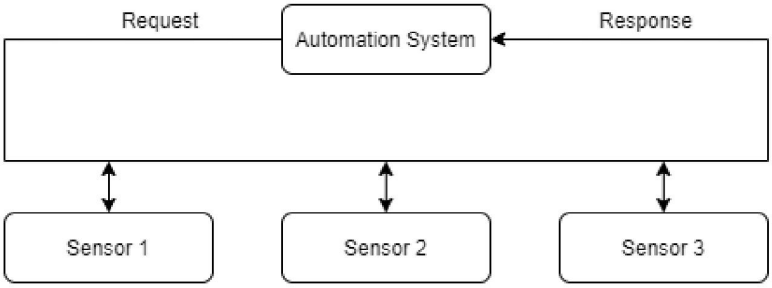

Figure 3.3: Schematic overview of the automation system

After the sensor data is obtained by the automation system, it is sent to the database using a wireless connection to shore. This database contains the logged data points with corresponding timestamps for all different sensors. Since the MODBUS protocol does not allow all messages to be sent at the same time, the data from the sensors is requested by multiple messages sent in a row. This means that the timestamp is different for each sampled sensor. This can be seen by the time difference between the timestamp of a sampled sensor and the timestamp of the next sampled sensor, which may differ up to two to three milliseconds. Since every timestamp is placed on a new row in the database, this different timestamps for different sensors result in a lot of empty spaces between each sampling loop. The time difference in the timestamp of successive data of one sensor amounts 1000 milliseconds. Since only the Damen digital portal data is available, it is not possible to determine from this data if this difference is caused by a sampling time of 1000 milliseconds by automation system, or a frequency of which data is transferred from the vessel to the database by using an internet connection. However, for the data we have, this means that data from a sensor is logged every 10 seconds and therefore the sampling rate is 0.1 samples per second.

In order to use the data for vessel monitoring, around 350 of the most common used sensors are picked from the database, processed and stored and shown in the front-end of the Damen Digital Portal. The transformation of the data includes removing the 2 a 3 milliseconds difference in timestamp between each different polled sensor resulting in all sensors having the same timestamp for one sampling loop. By doing so the spaces between each sampling loop, can be removed and the data can be neatly sorted without any empty spaces. The transformation of data also includes the naming of the sensors. All sensors are saved by their address number. The address numbers are replaced by sensor names in order improve the usability of the data.

Using the already transformed data from the portal is tempting, but a lot of sensors are excluded from that data-set, and since, before the analysis of the processed data, the choice for a certain set of parameters and the making of the Simulink model it is not known which sensors are required to build the model or validate in a later phase of the project, the raw database data is used for this thesis in order to be sure that all sensors are available to use. By using the raw data, the difference of two a three milliseconds between the sampling of successive sensors is not neglected.

3.2. Load data

Load data is the first process listed in the flowchart discussed in the introduction of this chapter. As mentioned, this process can be divided into three steps. Downloading data, splitting large files and loading data into MATLAB are discussed next.

Download data

The first step is downloading the remote logged data. For a given vessel build number and a given time domain the data can be downloaded from the database. The file format of the data is "comma separated values" (csv). This is a text file where all data points are separated by a comma. The text file consists out of rows and columns, creating a matrix where the data is placed in. The first row is the header, which includes the column notations and all address numbers which correspond to the different connected sensors. All other rows include the timestamp data and sensor data corresponding to the address numbers. Each connected vessel has its own csv file, and therefore for all 10 different build numbers the csv files are available. However, since the structure of all different csv files are the same, only one csv file is picked in order to make the MATLAB script and approach for processing the remote logged data.

Split files

The csv files are so large, around 800 megabytes, that issues arise when they are viewed or edited on a normal laptop. Opening these large files in a text editor results in the graphic card memory filling up, resulting in performance problems. Opening the files in MATLAB results in the RAM memory filling up and an error in the program. In order to use this program, some pre-processing of the data is needed.

To use and process this data files, first the large text files are split up into several smaller files using windows PowerShell. A PowerShell script written and published by Wright [14] is used to open the large text files and split them into multiple smaller text files, each containing 100.000 rows resulting in a significant smaller sized files of around 60 megabytes each. Now that the large csv files are split into multiple smaller files, there are no issues anymore regarding viewing and transforming this files.

Load files

Now that all large files that contain data are split into multiple smaller files, this files can be imported into MATLAB. As mentioned in the scope of the project, MATLAB is the program that is used for further processing, visualise and analyse the remote logged data. Since the data is split up into multiple files by the PowerShell script, they first need to be combined into one MATLAB matrix containing all data.

3.3. Pre-processing

After the 'load data' process, the pre-processing of the remote logged data can be performed. In the pre-processing, the data is prepared for visualisation and analysis. As mentioned in the introduction of this chapter, the pre-processing consist out of two steps. First the headers are renamed in order to improve the readability of the data. As second, the empty lines are removed in order to use the data for visualisation.

Rename headers

The first row of the data, containing the header is imported. The original header, which lists the address numbers is replaced with the corresponding sensor names. In order to do so, for a specific vessel build number an Excel file is provided by Damen Shipyards, where for each sensor the address, sensor description, sensor scaling factor and sensor range is given. The original header on the first row of the csv text file is imported into MATLAB. The Excel file is also imported and the corresponding sensor names for the address numbers that are listed in the original header are compared. The address numbers are replaced by sensor names to create a header with sensor names which makes finding and selecting preferred sensors easier.

Remove empty lines

Now that the data is imported and the header is replaced into a header which includes header names, the data can be processed further. Since the Modbus protocol causes the sensors not to be sampled at the same time, empty rows exist between the row including the sensor data and the following row including the consecutive data point of the same sensor. All empty spaces are removed, leaving only the rows that contain data. However, because the timestamp column in the data does not have any empty rows, there are no rows deleted from that column. Thus, when all empty rows between all sensor measurements are removed, the rows containing the timestamps are not associated with the rows containing the sensor data anymore. Therefore, for each data point, the associated timestamp must be found by comparing the original row number of the data-point with the timestamp rows.

3.4. Data set selection

One vessel must be chosen whose design characteristics are used to make an initial version of the propulsion model. In order to choose a vessel, a list of requirements and preferred points are listed below.

- The data must not contain logging errors or unpredicted extensive noise.
- All design parameters must be available, in the form of for instance product sheets.
- The amount of data and the variety of data logged from one sensor must be sufficient. This means that it must include for instance multiple trips with multiple different vessel speeds and steady state moments for those different speeds.

A starting data set will be chosen that complies the most with the requirements and preferred points listed above. In order to select the data set to start modelling a vessel, three aspects are looked into.

First, the remote logged data of all available vessels are analysed. The choice is made to look at the GPS data to compare the different vessels. With the logged data of the GPS speed, vessel movement can be analysed to be sure that there are enough trips with different GPS speeds to ensure that enough data is available for the calibration and validation steps further in this thesis. Decide what "enough" is, is hard to do in this state, but the comparison between all six available vessels can point to one vessel with "better" data. Besides looking at vessel movement, abnormal sensor behaviour can be detected by analysing this GPS data. Figures 3.4 to 3.9 show the GPS speed for all different vessel build numbers. From this figures the conclusions can be drawn that the GPS sensor data from vessel 515006 behaves abnormal after some time. Furthermore, the GPS data from vessel 515002, 515006 and 513202 seem to have a lot of noise. The vessels with build number 515001, 513301 and 513302 seem to have normal sensor behaviour. However, vessel 515001 seems to have more trips including more variety of GPS speeds and is therefore the most preferable vessel based on this aspect. Based on the conclusion, the decision is made to only look at this GPS data for now to choose a vessel for the initial model.

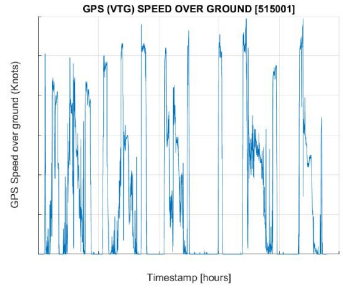

Figure 3.4: GPS speed 515001

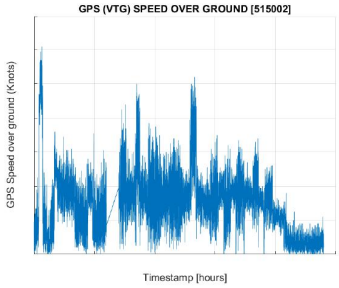

Figure 3.5: GPS speed 515002

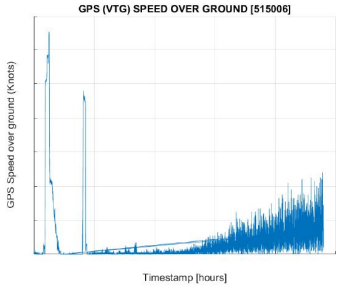

Figure 3.6: GPS speed 515006

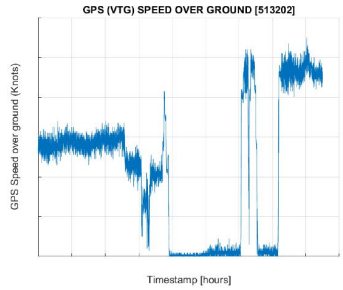

Figure 3.7: GPS speed 513202

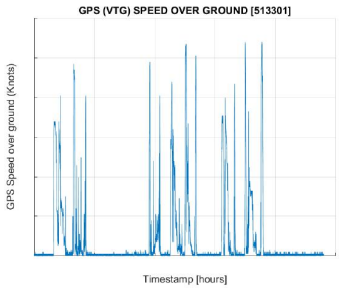

Figure 3.8: GPS speed 513301

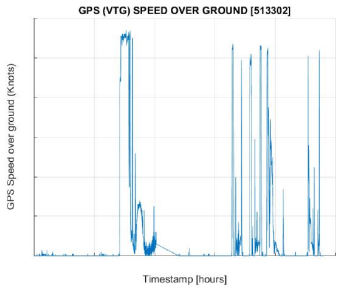

Figure 3.9: GPS speed 513302

The second aspect that is considered is the amount of available design parameters. The first build vessel of the series, having a build number ending with -01, usually has the product data sheet publicly available. Having the product data sheets available reduced the amount of guessing or assumptions in the modelling process. Also, the extended sea trail and bollard pull measurement and logging results are often available only for the first built vessel of the series. This logging data can provide extra information if needed.

The third aspect the amount of usable data. The RSD tug with yardnumber 515001 seems to have more trips including more variety of GPS speeds than the other vessels. Having the most trips including more variety of GPS speed result in "enough" data. Since the time domain of 24 hours is arbitrarily chosen, it can be increased to capture more data and thus increase the amount of data and the variety of data logged.

Considering all three aspects, the data from the RSD tug with yardnumber 515001 seems to have no errors or unexpected extensive noise. Also, the RSD tug with yardnumber 515001 seems to have the design parameters public available. At last the amount of data and the variety of those data seem "enough". The RSD tug with yardnumber 515001 is therefore the most preferable vessel whose data will be used to build the initial propulsion line model.

The RSD tug with yardnumber 515001 is a reversed stern drive (RSD) 2513 Tug. The product sheet of this vessel can be found in appendix A.2. The RSD tug is a harbour tug with two diesel engines producing 4480 kW power at a rotational speed of 1800 rpm and driving two azimuth thrusters. This means that remote logging data from both engines, shafts, gearboxes and propellers can be analysed.

3.5. Selection of variables

As mentioned before, a table including the names of the remote logged sensor data is shown in the appendix A.1. What sensor data is needed depends on the complexity of the model. Some sensors are more important than others when a propulsion line model must be made, calibrated and validated. As discussed before, the speed through water sensor and the engine load sensor are not available. All other blue coloured sensors from the table in the attachment are analysed and can be used for the model. The diesel engine speed and fuel rate of the port-side and starboard side diesel engine will be processed in order to find steady state moments. Also the port-side and starboard propeller rotational speed and GPS vessel speed are processed in order to use the data as steady state in the model.

Moreover, some sensors seem to be listed by their corresponding address number in the header of the original csv files but are always having a value of zero. This can be caused when the sensor has actually measurement data which is zero, or when the sensor is listed in the original header, but not actually connected or built into the vessel. One of those sensors listed, but not containing data is the engine load sensor. The engine load can therefore not be obtained from the remote logged data. Another of those sensors without data is speed through water. Speed through water gives the speed of the vessel relative to the water's velocity. Since the speed through water data is always zero, it cannot be used further in this thesis. The disadvantage of using GPS speed instead of speed through water is that GPS speed shows the vessels movement with respect to the ground. When water current is present, the speed through water differs from the speed over ground. When looking at resistance calculations where always speed through water is used, the use of GPS speed results in an error. However, since speed through water and current speed is not available, the ship speed is considered to be equal to the GPS speed for further calculations.

Apart from the speed through water and the engine load sensor, the rest of the blue coloured sensors from the table in the attachment contain useful data. The data from these sensors is plotted to a graph and shown in the data visualisation section next. In order to avoid very large files, the data is saved in those figures which take a lot less space. Those figures can then be saved on a laptop and later be used later in the project.

3.6. Data visualisation

Now that the data is processed to the extent that plots can be made with the remote logging data on the y-axis and timestamp on the x-axis, the graphs are shown and discussed. For all blue coloured cells from the list which contain non-zero data, a plot can be made by using the matrix that contains all data points and plotting the timestamp on the x-axis and the sensor value on the y-axis.

The engine speed of the port-side diesel engine is plotted and shown in figure 3.10a. The engine speed of the starboard diesel engine can be seen in figure 3.10b. The engine speed is given in rpm "rotations per minute" and the on the x-axis, the corresponding timestamps are given. At around 500 rpm the engine tends to have a limit according to both plots. This means that this is the idle speed of the diesel engines. According to the product sheet, the maximum speed of the diesel engines is 1800 rpm. This maximum speed can be found in the plots, however this speed is almost never reached.

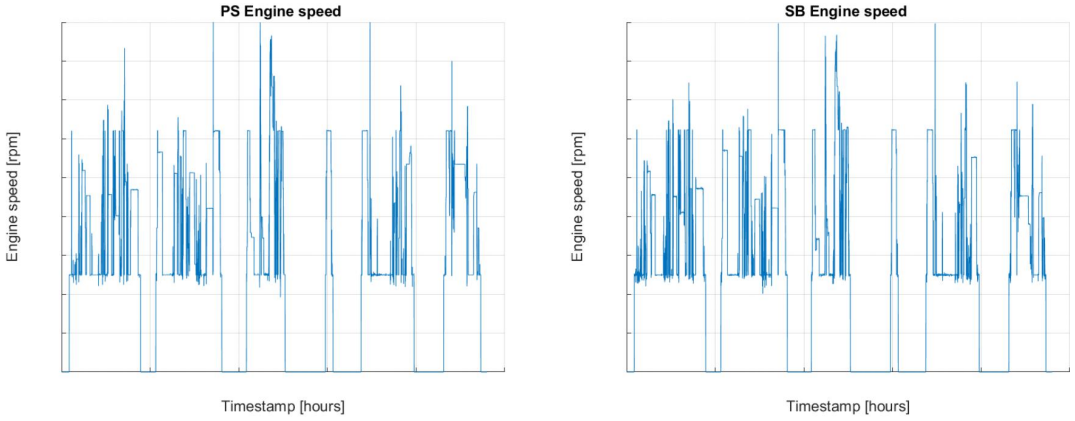

(a) (b)

Figure 3.10: Remote logged data of the engine speed

The fuel rate is also remotely logged for both installed diesel engines. The fuel rate of the port-side diesel engine is shown in figure 3.11a while the fuel rate of the starboard diesel engine is shown in figure 3.11b. The fuel rate is expressed in litres fuel per hour. As with the plots of the engine speed, on the x-axis, the corresponding timestamps are given. Both plots of the fuel rate seem to follow the engine speed well.

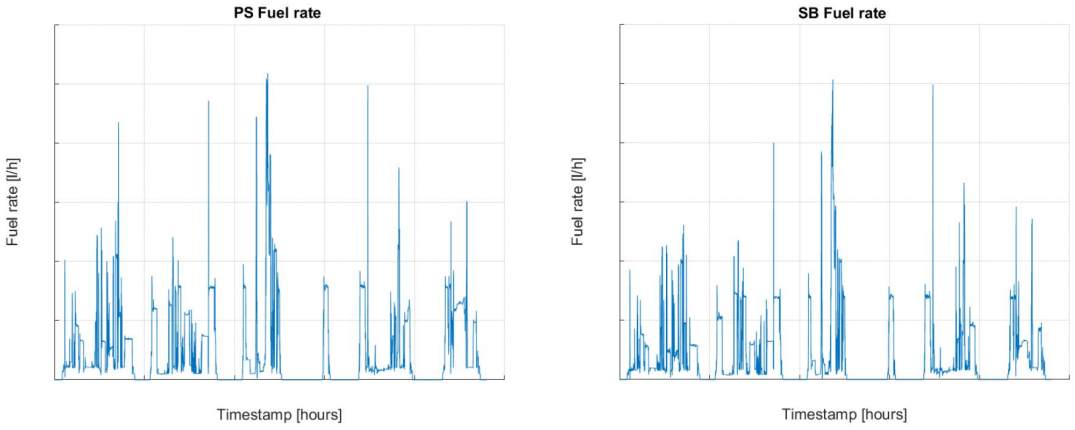

(a) (b)

Figure 3.11: Remote logged data of the fuel rate

The rpm command set value is the requested propeller rpm value. This value is determined by the throttle lever position set on the bridge of the vessel. The rpm command set value of the port-side propeller rotational speed is shown in figure 3.12a and the command set value of the starboard propeller is shown in figure 3.12b. Instead of a specific rpm value, this command set value is expressed in percentages. A value of 100 percent corresponds to the nominal propeller rotational speed. This nominal propeller rotational speed is for this vessel rpm.

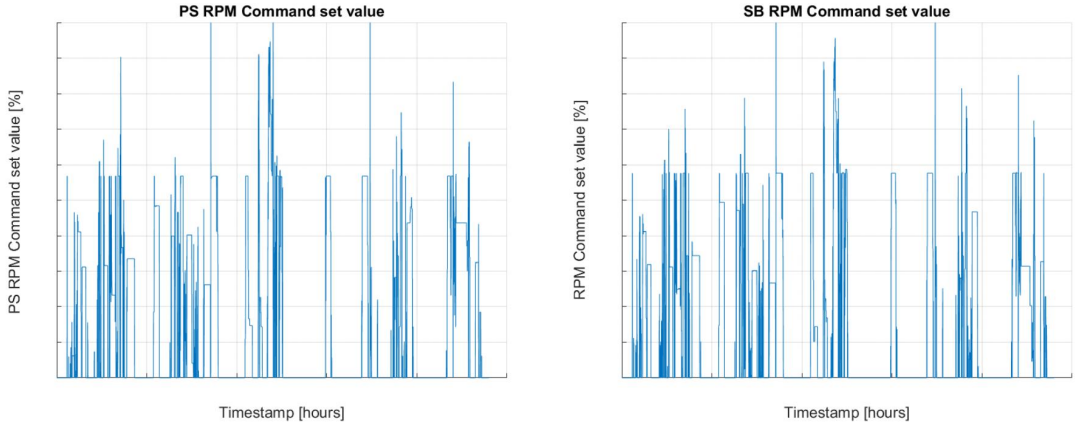

(a) (b)

Figure 3.12: Remote logged data of the rpm command set value

In figure 3.13a the plot of the port-side propeller rpm measurement is shown. The plot of the starboard propeller rpm measurement is shown in figure 3.13b. Both propeller rpm measurement plots look a lot like the rpm command set value. As with the rpm command set value, this propeller rpm measurement data is given in percentages with respect to the nominal propeller rpm. However, a rpm command set value of zero corresponds to a propeller rpm measurement percentage of around percent of the nominal propeller rotational speed. This means that a command set value of zero results in the diesel engines running at idle speed. If the clutched is engaged when the engines are running at idle speed, the propellers will also run at a minimal rotational speed. This minimal propeller rotational speed that corresponds to the diesel engine idling speed of 500 rpm matches percent of the nominal propeller rotational speed.

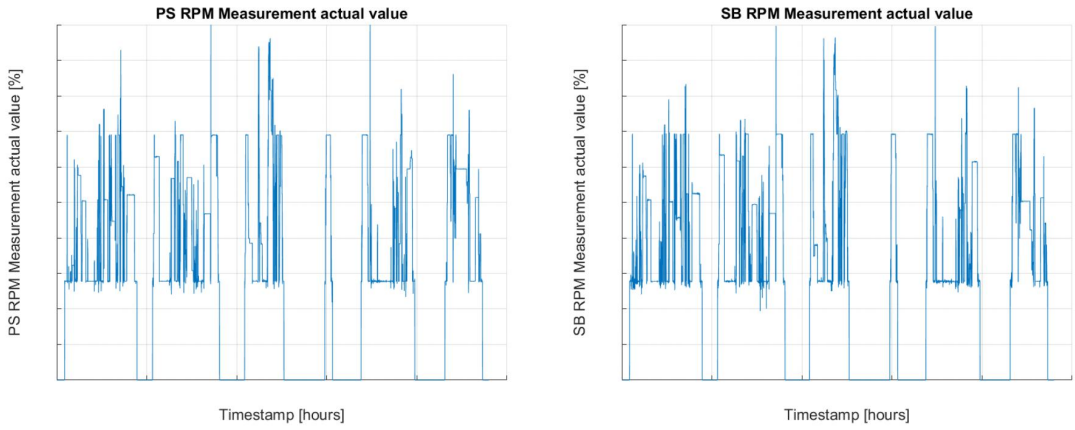

(a) (b)

Figure 3.13: Remote logged data of the propeller measured value

In figure 3.14a the plot of the port-side propeller rpm is shown. The plot of the starboard propeller rpm is shown in figure 3.14b. For the most part these plots are equal to the propeller rpm measurement plots. However, in these plots, the rpm tends to go lower than the percent minimum propeller rotational speed. These lower propeller speeds can be obtained by partially engaging the clutch. Having the clutch not fully engaged results in a slipping clutch and thus a lower propeller rotational speed.

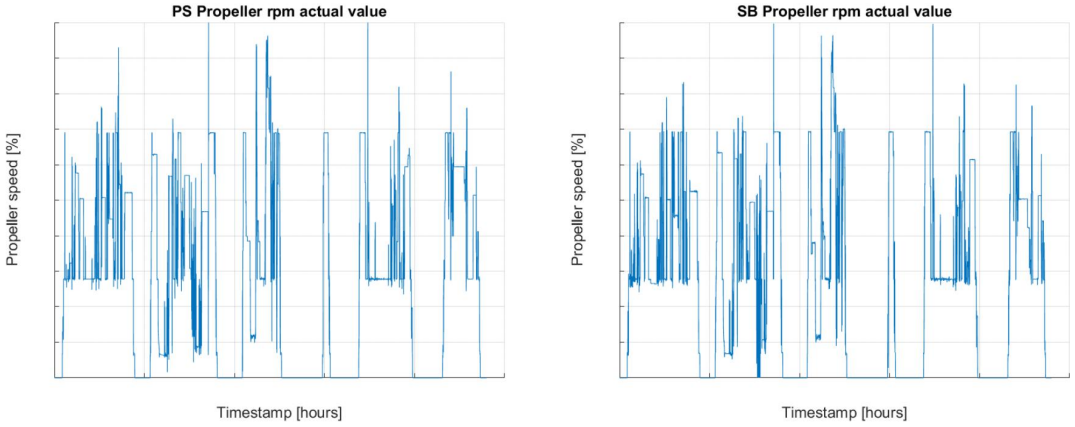

(a) (b)

Figure 3.14: Remote logged data of the propeller actual value

As mentioned while processing the data, due to bandwidth limitations the sensor data is uploaded only once every 10 seconds to the database. The low logging frequency means that dynamic behaviour cannot be seen in the presented figures of the data. Cylinder processes and accelerations within the diesel engine and the acceleration of the diesel engine speed and the propeller rotational speed cannot be caught with this frequency.

Because of the low logging frequency of the remote logged data, dynamic system behaviour cannot be made, calibrated or validated by the use of this data. Therefore the decision is made to use only the steady state data. Further processing is required for this data reduction in order to obtain and use the steady state data to make, calibrate and validate a model with the use of the remote logged data.

4

Data reduction

In this chapter, the data reduction is discussed. This data reduction step is the second step in the general flowchart discussed in the approach. The data reduction step that will be discussed in this chapter is coloured green in figure 4.1. Figure 4.1 is general flowchart of the project as discussed in the introduction.

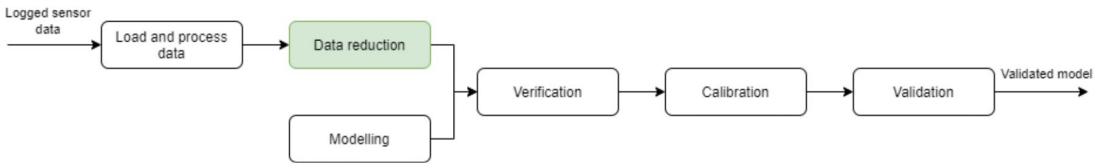

Figure 4.1: General flowchart

The data reduction can be divided into three smaller steps. The three steps that are required for data reduction are presented in figure 4.2.

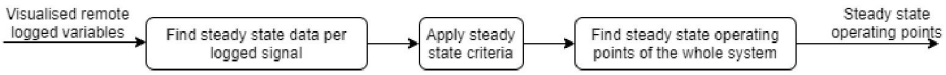

Figure 4.2: Flowchart of the data reduction process

First, the steady state data of each logged variable is obtained. These are all the data-points of a specific sensor that can be considered being in steady state. Further reduction and refinement is achieved by applying a list with criteria to the steady state data points. At last the refined steady state data points are combined to find the actual steady state operating points of the entire vessel that can be used further in the project.

4.1. Steady state data of each logged variable

Since the frequency of the remote logged data is low and is therefore unusable for describing accelerations of the ship's propeller, shaft and cylinder processes and accelerations within the diesel engine, the decision has been made to only look at the steady state operating points of the vessel.

In order to determine which remote logged data can be considered steady state, the chosen variables are processed even further. The finding of steady state data is based upon the following two points.

1. At a specific timestamp, the derivative can be taken to define the slope of the graph. This slope is compared with a set threshold value to determine if the data at this specific timestamp is in steady state.

2. Since the input data is not “live”, data from every timestamp can be selected. Therefore it is possible to look at the sensor data at its current timestamp, and compare it with sensor data at a timestamp that lies a certain distance in the future. The difference between those data points are an indication of how “steady state” that part of the data is.

In order to apply this method to the remote logged data, a script is made that imports MATLAB figures containing data from one sensor with timestamp on the x axis. This script can be found in appendix A.4. Figure 4.3a shows the graph of data that is imported into the steady state script. It represents the sensor data of the diesel rpm value over a time period of 24 hours. For illustration purposes, the figures 4.3a to 4.5 present the data of the port-side diesel engine only. In appendix A.3 the graphs of the other variables are shown.

At its current timestamp, the script takes the derivative to define the slope of the graph. This steepness of the slope is examined in order to determine if the data at that specific timestamp is in steady state. Due to noise in the data, taking the derivative of data containing noise will give unwanted high values. In other words, the noise can be seen as local very small but also very steep slopes between data points. To prevent that noise in the data causes unwanted high values of the derivative with the result of an incorrect conclusion of the steady state data points, the data is filtered first to obtain a more smooth line. A moving-average digital filter is a common method used for smoothing noisy data, and therefore used as filter for the remote logged data. In figure 4.3a the filtered data is coloured in red while the original imported data is coloured blue. Figure 4.3b shows the original and filtered data more up close. Now that the filtered data have less noise, the derivative is only high at places where the data is actually changing from steady state to non- steady state.

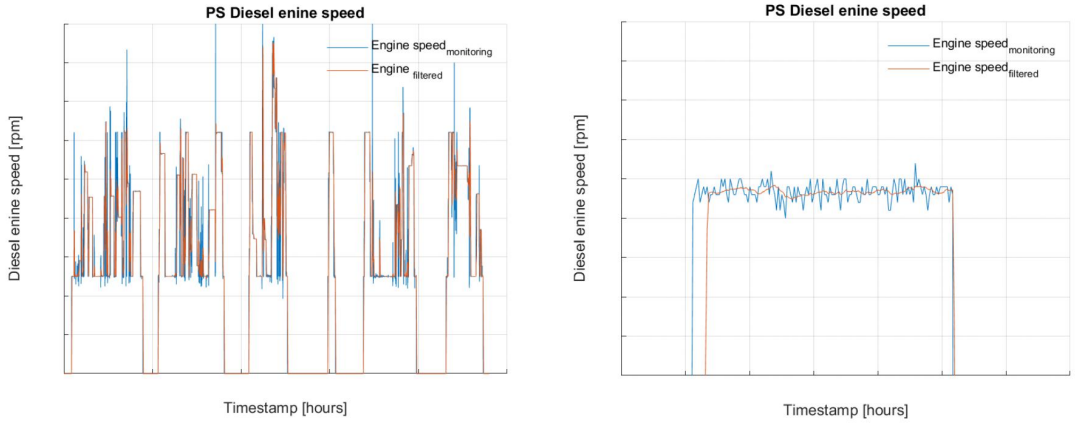

Figure 4.3: Raw and filtered remote logged data of the diesel engine speed

The second way to determine if a data point is in steady state, is to look at a specific timestamp, and compare it with sensor data at a timestamp that lies a certain distance in the future. The difference between those data points are an indication of how “steady state” that part of the data is.

Now that both the derivative at a specific timestamp and the change of rpm over a range of time are examined, they are combined to find the data points of a specific logged sensor that are in steady state. The data in steady state is expressed as a vector which has a value of one, if the data is in a steady state and a value of zero if the data is not in steady state. In figure 4.4a the filtered data is shown in red, while the steady state vector is shown in blue. For illustration purposes, all values in the steady state vector are multiplied by a scaling factor of 400 in order to be able to present the vector in figure 4.4a. Figure 4.4b shows the filtered data and steady state vector more up close. A steady state vector value of 400 in the graph means that the sensor data is in steady state while a value of zero means that it is not in steady state.

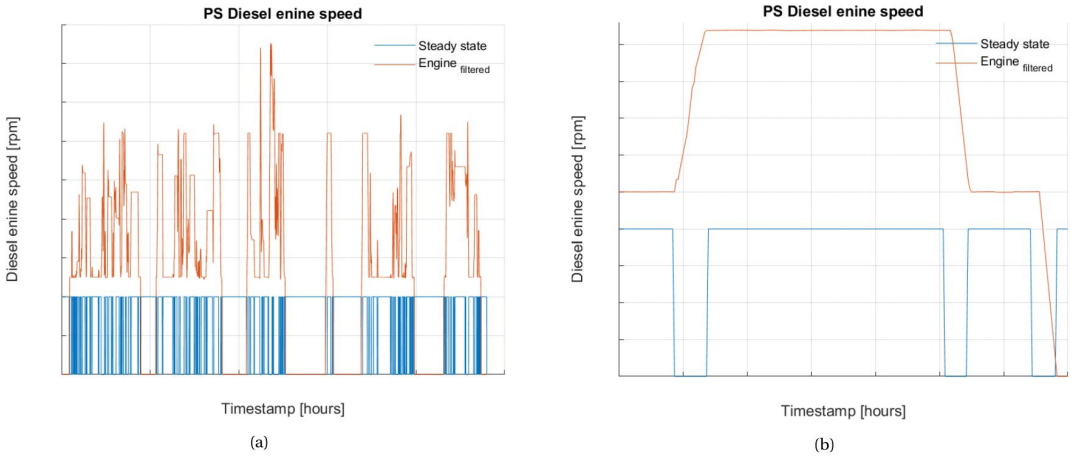

Figure 4.4: Filtered remote logged data of the diesel engine speed with the steady state vector

To avoid small peaks of steady state data, a minimum amount of connected data points being in steady state is set. By looking at the transitions between steady state and non- steady state data, the length of connected steady state data can be determined. If this length is smaller than the minimum required length set, all steady state data points within the specified range are deleted.

The application of the discussed aspects can also be expressed in mathematical form. Equation 4.1 shows the mathematical expression of the three aspects applied to obtain the steady state data for a certain sensor. In the mathematical expression the sensor is indexed by the letter n. The x value is the timestamp value of the data. From equation 4.1 can be seen that the 'SS sensor', the steady state vector of sensor 'n', has a value of one if all three aspects comply with the criteria. First, the value for the derivative at location 'x' must be lower than the threshold value. Second, the difference between the sensor value at location 'x + Δ' and the value at location 'x' must be below a set up threshold value and at last, the length of the connected steady state data point must be higher than a set up threshold value.

$$SS_{sensor,n}(x) = \begin{cases} 1 & if \quad \frac{\mathrm{d}}{\mathrm{d}x}(x) < threshold \\ & and \quad (Sensor_n(x+\Delta) - Sensor_n(x)) < threshold \\ & and \quad \left\| SS_{sensor,n} \right\| > threshold \\ 0 & otherwise \end{cases} \tag{4.1}$$

When the steady state vector is multiplied by the original port-side diesel engine speed data, the diesel engine speed in steady state remains while the data that is not in steady state is removed. Figure 4.5 shows the final diesel engine speed steady state data.

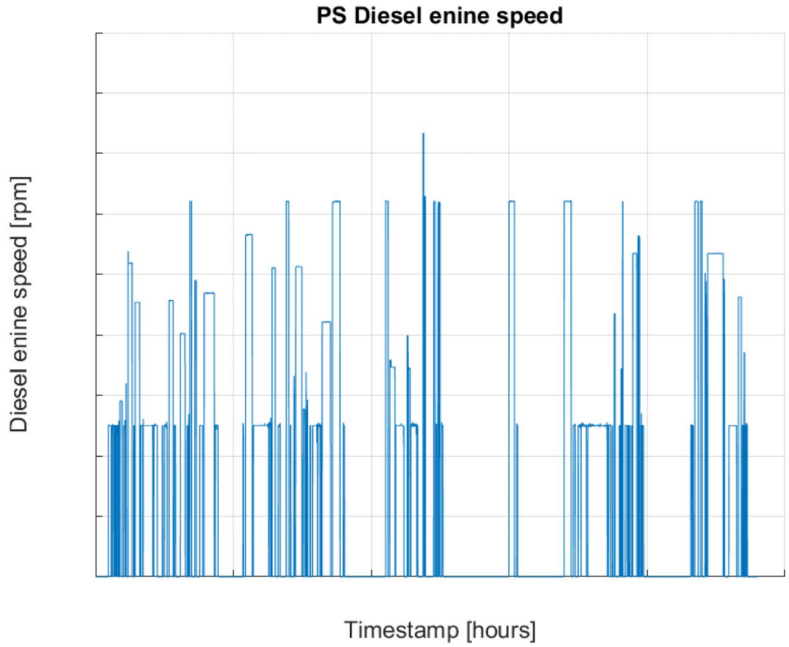

Figure 4.5: Steady state data of diesel engine speed

The data reduction step by finding steady state data within the remote logged data of a specific sensor is also done for other variables. For GPS speed, fuel rate, diesel engine speed and propeller speed the steady state data is obtained. The port side diesel engine is shown for illustration purposes. The steady state vector for GPS speed will look different than the steady state vectors from the fuel rate, diesel engine speed and propeller speed. The cause of this is that the acceleration of the vessel speed is much slower than the acceleration of the fuel rate, diesel engine speed and propeller speed. The result is that the vessel speed data is in steady state, some time after the other variables are in steady state. The filtered data and steady state vectors of the other variables can be found in appendix A.3.

4.2. Steady state criteria

Now that all the steady state data points of the separate variables are determined, the steady state of the whole propulsion line system is examined. First, we look at the steady state of the whole system when all separate variables are steady state at the same time. Then, criteria regarding water and weather influences are applied.

The steady state data from multiple sensors will be used together in the propulsion line model. This means that all variables that are within the propulsion line system must be in steady state at the same time. The system is only in steady state if all parts of the system are in steady state. If for instance a certain throttle position is set, the diesel engine makes the shaft and propeller accelerate to a certain speed. The ship also accelerates but with a delay. This causes the diesel engine, propeller and shaft to eventually be in steady state, but when the ship is still accelerating. In this condition the system is not in steady state. Therefore all steady state vectors must be multiplied by each other in order to obtain the steady state vector for the whole propulsion system. Figure 4.6 shows the result from the multiplication off all separate steady state vectors of different variables together.

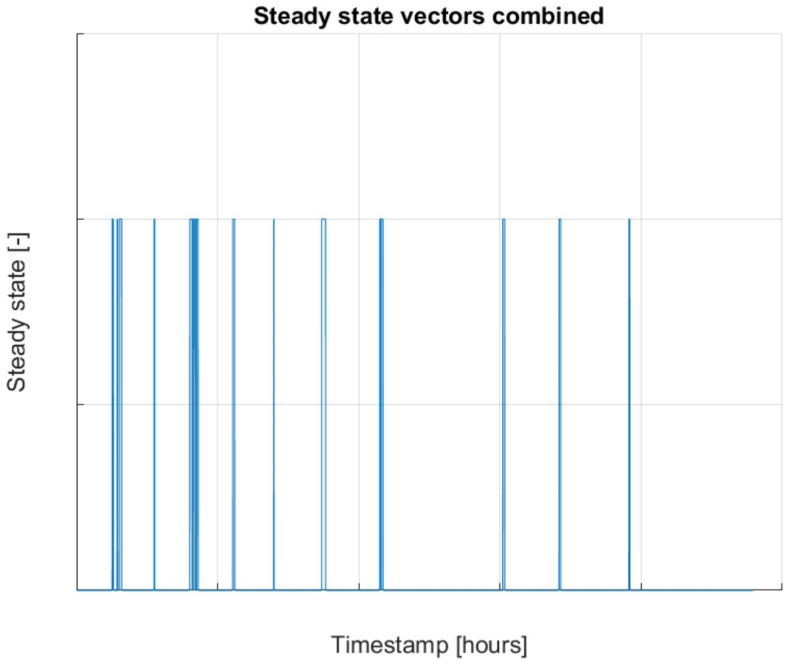

Figure 4.6: Steady state vectors combined

Like with the making of the steady state vectors for each variable, a mathematical expression can be made that described the criteria that all variables that are within the propulsion line system must be in steady state at the same time. This mathematical expression is shown by equation 4.2. The equation shows that the steady state vector of the whole system is one if all seven steady state vectors from the other variables are all one at the same time.

$$SS_{system}(x) = \begin{cases} 1 & if \quad \prod_{n=1}^{7} SS_{sensor\ n}(x) = 1 \\ 0 & otherwise \end{cases} \tag{4.2}$$

Making a model that includes weather and water influences is hard to do, especially If you want to make a simple propulsion line model. So instead of making a very complex model that includes those influences, a simple model is made were those influences are not included. The data that is used to verify, calibrate and validate this model is chosen in such way that the weather and water influences can be neglected. The remote logged data is logged while the vessel travels through different weather conditions, water current, shallow water, wind and also not always in a straight line due to manoeuvring or towing. Data from the wind speed and water depth are available. The rate of turn is not available but can be obtained by using the course over ground. As mentioned before, the current cannot be determined due the absence of the speed through water data.

In order to neglect these conditional influences, threshold values must be determined and compared with the remote logged data. If for instance the wind speed is above a certain threshold value, the data at that timestamp is considered to be not steady state. Not only the wind speed, but also the water depth and rate of turn are analysed below.

If weather conditions are neglected, we can only use the steady state data where the wind speed is low enough to be neglected. If the wind speed is above a certain threshold, the system is set as not steady state. In figure 4.7 the wind speed is shown.

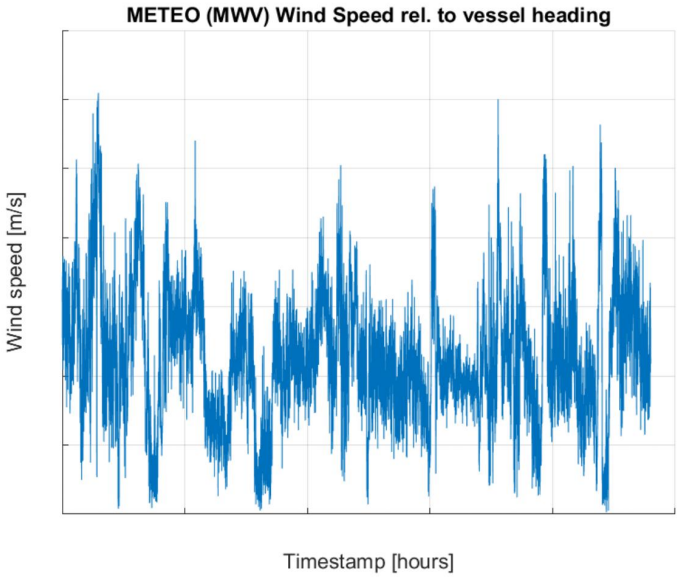

Figure 4.7: Wind speed sensor data

The threshold value that determines the maximum allowed wind speed is chosen to be 15 m/s in order to exclude data where the wind speed is high. This threshold value is arbitrarily chosen such that only high wind speeds are excluded. In figure 4.8a the wind speed data is coloured blue. The red line represents the maximum threshold value.

A vector is made that shows if the wind speed is below the chosen threshold value or above, by having a value of one if the wind speed is below the threshold value and zero if the wind speed is too high. This vector is shown in figure 4.8b.

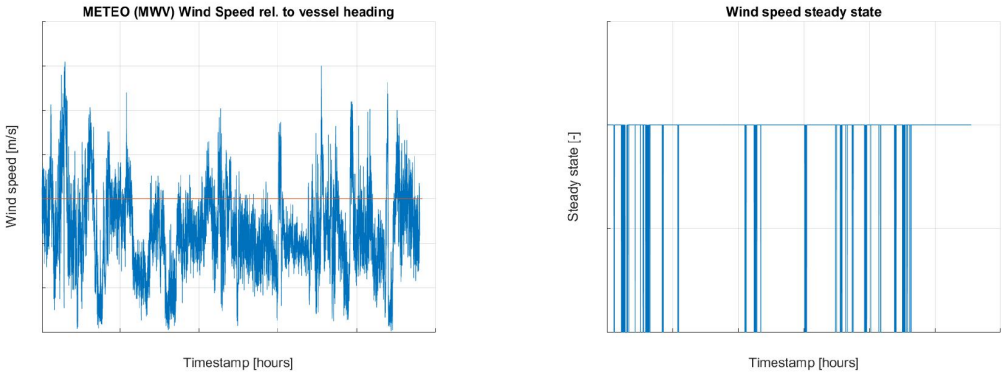

(a) (b)

Figure 4.8: Elimination of wind speed sensor data above the threshold value

The wind criteria can be expressed with the use of a mathematical equation. Equation 4.3 shows the wind speed steady state vector, which is one if the wind speed is below the threshold value. As mentioned before, the threshold value that determines the maximum allowed wind speed is chosen to be 15 m/s in order to exclude data where the wind speed is high.

$$crit_1(x) = \begin{cases} 1 & if \quad windspeed(x) < threshold_{windspeed}(x) \\ 0 & otherwise \end{cases} \tag{4.3}$$

As with wind, also the water depth influences the behaviour of the ship. If the vessel travels through shallow water, the resistance of the ship is influenced, resulting in data that not corresponds to the modelled steady state free sailing scenario. The water depth data is shown in figure 4.7. The water depth is measured with respect to the vessel's keel.

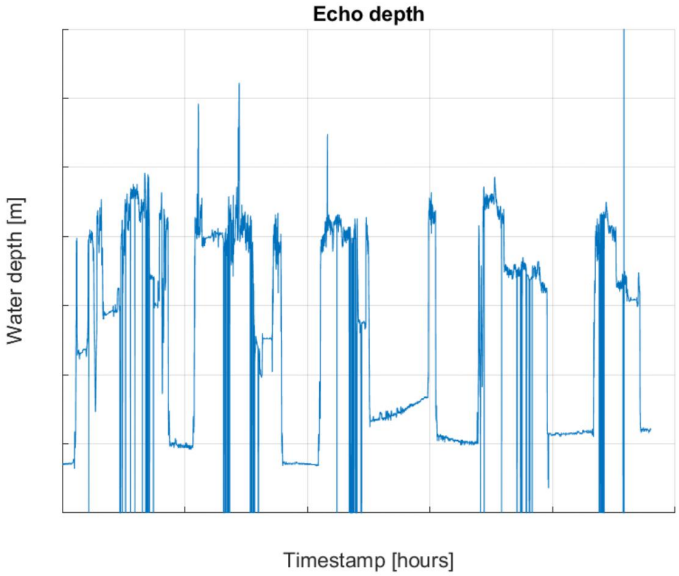

Figure 4.9: Water depth sensor data

Like with the wind speed a threshold value is arbitrarily chosen. For the water depth, a minimum value is taken to be able to neglect shallow water effects. The draught of the vessel is 3.2 metre, choosing a water depth of three times the vessel's draught should eliminate the major shallow water effects. In figure 4.10a the depth threshold value of 10 metres is shown with a red line. Like with the wind speed, a vector is made that has a value of one if the water depth is above the minimum threshold value and zero if the depth is below the minimum. This vector is shown in figure 4.10b.

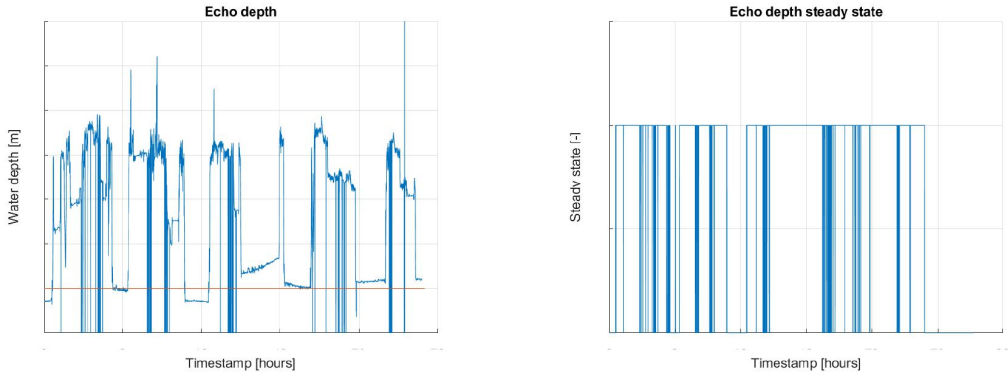

(a) (b)

Figure 4.10: Elimination of water depth sensor data below the threshold value

The water depth criteria can be expressed with the use of a mathematical equation the same way as the wind speed criteria. Equation 4.4 shows the water depth speed steady state vector, which has a value of one if the water depth is above the threshold value of 10 meter.

$$crit_2(x) = \begin{cases} 1 & if \quad waterdepth(x) > threshold_{waterdepth}(x) \\ 0 & otherwise \end{cases} \tag{4.4}$$

When the vessel makes a turn, this has an impact on the speed and the propulsion performance of the vessel. Only moving on a straight line is seen as steady state. Since the sensor showing the rate of turn is not available, the course over ground is used to determine if the vessel is manoeuvring. The course over ground is shown in figure 4.11. The sensor has a range from 0 to 360 degrees. When the vessel rotates from for instance 350 degrees to 10 degrees, it passes the point where 360 degrees transitions into zero degrees. When this happens, vertical lines appear in the course over ground graph.

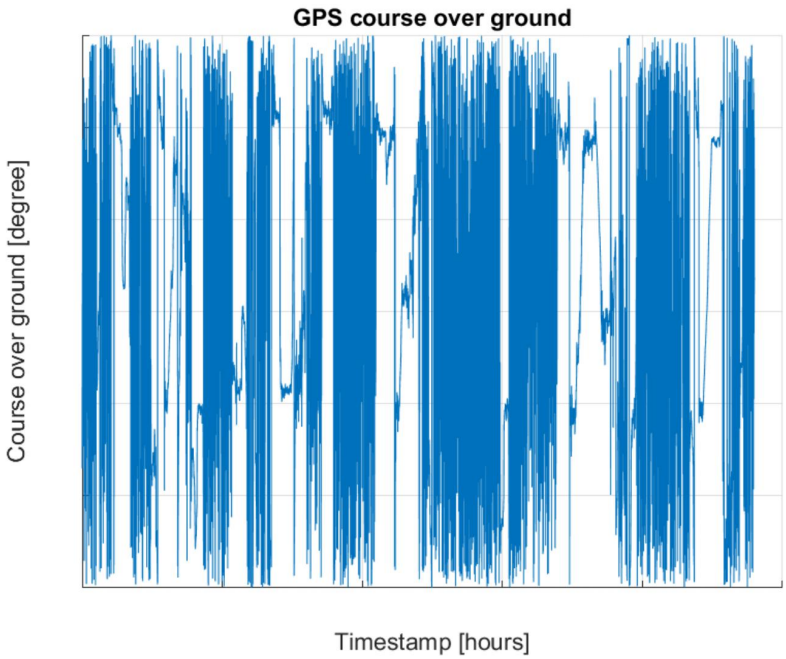

Figure 4.11: Course over ground sensor data

To transform the course over ground into the rate of turn, the angular difference between two successive course over ground data points is determined. This difference represents the change of course during one time step. By taking the angular difference, the vertical lines from 360 to 0 degrees also disappear. Figure 4.12 shows the rate of turn.

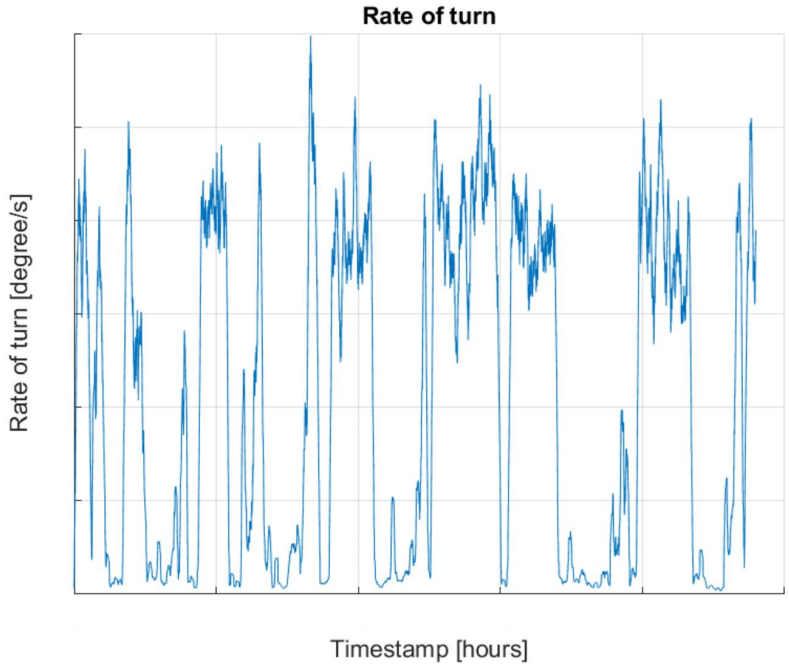

Figure 4.12: Rate of turn

Like with the wind speed and water depth, a threshold value is arbitrarily chosen. In figure 4.13a a rate of turn threshold value of 40 is shown with a red line. Like with the wind speed and water depth, a vector is made that has a value of one if the rate of turn is above the minimum threshold value and zero if the depth is below the minimum. This vector is shown in figure 4.13b.

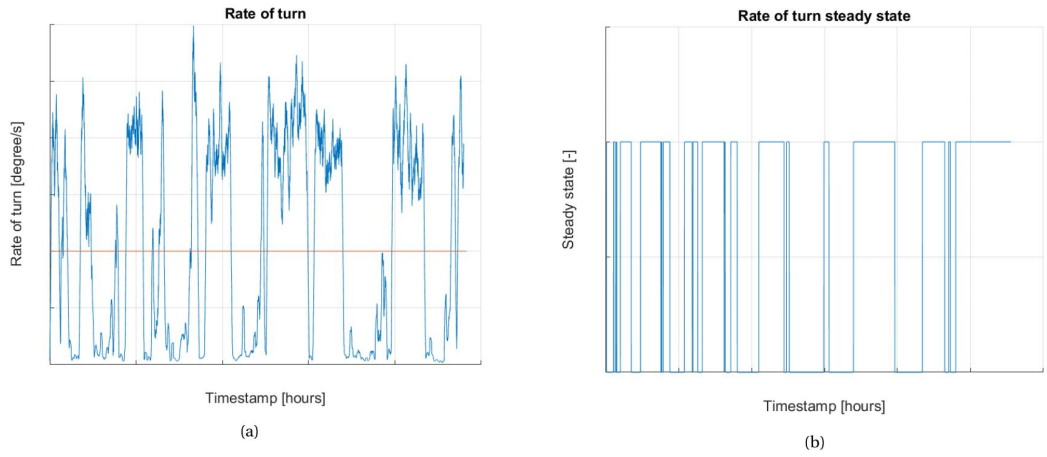

Figure 4.13: Elimination of rate of turn data above the threshold value

Also the rate of turn criteria can be expressed with the use of a mathematical equation 4.5. The rate of turn steady state vector has a value of one if the value for the rate of turn is below the threshold value.

$$crit_3(x) = \begin{cases} 1 & if \quad rate\,of\,turn(x) < threshold_{rate\,of\,turn}(x) \\ 0 & otherwise \end{cases} \tag{4.5}$$

Besides looking at the rate of turn, the difference between the engine speed of the port-side and starboard diesel engine is analysed. A maximum difference of 50 rpm is arbitrarily set as threshold value. All moments where the speed of both diesel engines differ more than 50 rpm are considered to be not steady state.

From the analysis in chapter 3.3 the remote logged data from the rpm measurement and propeller actual value are presented. The difference in propeller rpm between those two sensors are caused by a slipping clutch when the diesel engines are running at idle speed. A slipping clutch means that the speed of the propeller is not linear to the speed of the diesel engine. This can result in the GPS speed not matching with the propeller speed or diesel engine speed. Therefore, a minimum value of 550 rpm is set for the speed of both diesel engines. Since clutch slipping only occurs at the idle speed of 500 rpm, this minimum value eliminates the slipping effects from the steady state data.

It is hard to determine if the vessel is performing a towing operation. Sensors that show if doors are open or closed and sensors regarding the winches on the vessel are analysed, however they all seem to have no data or the same data values over the entire timeline. This means that there is no remote logging data available that tells directly if the vessel is performing a towing operation. Therefore, multiple sensors are combined in order to exclude towing operations from the steady state data. The criteria for maximum rate of turn, maximum speed difference of both diesel engines and the minimum speed for the diesel engine are considered to be sufficient to eliminate all manoeuvring including towing operations.

All separate criteria with the created steady state vectors can now be combined by multiplying each vector to each other. Figure 4.14 shows the vector as result of this multiplication. At the timestamps where the vector is one, the data complies to all criteria.

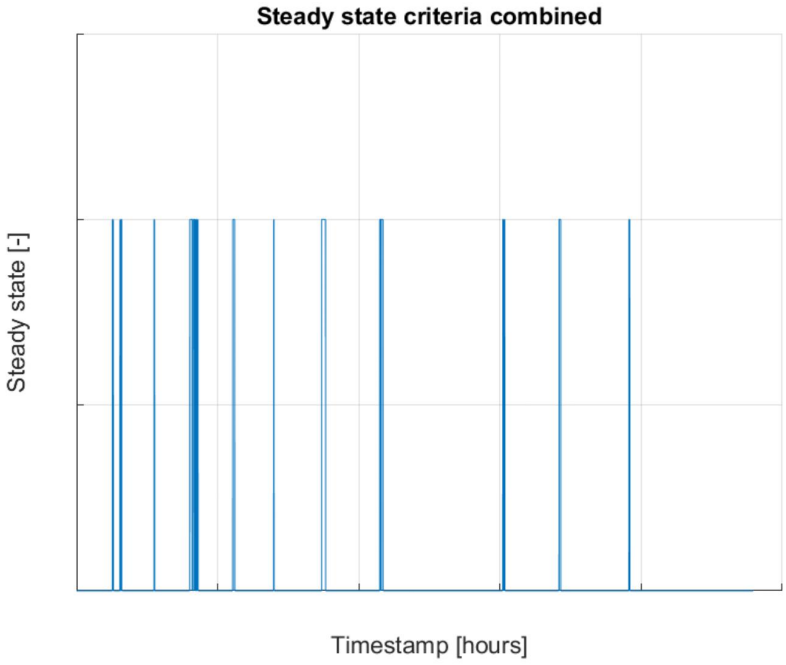

Figure 4.14: Steady state criteria combined

The combination of the steady state criteria are expressed in mathematical form in equation 4.6. The index value 'c' represents the three discussed weather and water criteria. When all steady state criteria vectors are one at the same time, the 'criteria combined' vector is also one.

$$crit_{combined}(x) = \begin{cases} 1 & if \quad \prod_{c=1}^{3} crit_c(x) = 1 \\ 0 & otherwise \end{cases} \tag{4.6}$$

The steady state data of the selected variable can now we multiplied by this criteria vector so that only data remains that complies to all criteria. For illustration purposes the steady state data of the port-side diesel engine speed, multiplied with the combined criteria vector is shown in figure 4.15.

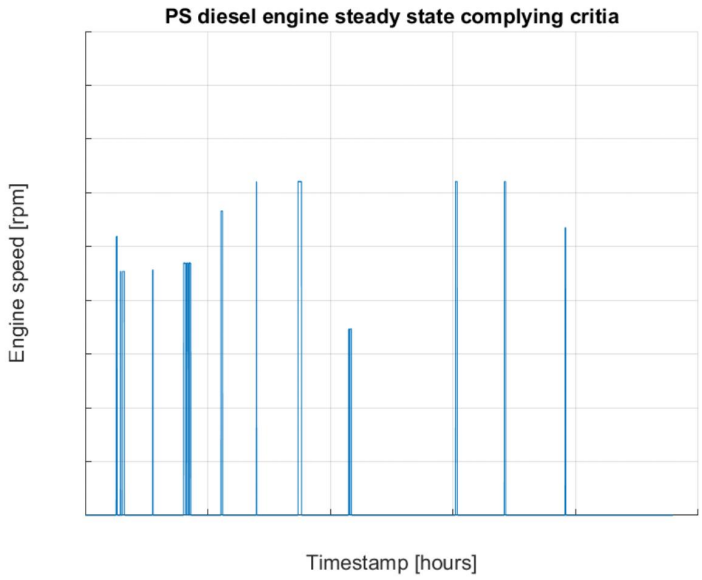

Figure 4.15: PS Diesel engine steady state data that complies with all criteria

Equation 4.7 shows the mathematical expression where the combined steady state vectors are multiplied by the combined criteria. This way, the steady state data points that comply to all criteria are obtained.

$$SS_{system,meetscriteria}(x) = SS_{system}(x) \cdot crit_{combined}(x) \tag{4.7}$$

4.3. Steady state operating points

The final step is to take the average value of the connected steady state data points. In order to do this all transitions from steady state to non- steady state and back are determined. After that, the average value of the data between the transitions is obtained. In total there are 15 steady state operating points left after applying all criteria. All those 15 steady state operating points for all seven variables can be seen in table 4.1.

GPS Speed [kts]	PS DE [rpm]	SB DE [rpm]	PS FR [l/h]	SB FR [l/h]	PS Prop [rpm]	SB Prop [rpm]

Table 4.1: All steady state operating points

5

Modelling

In this chapter, the modelling of the propulsion line is discussed. The modelling is the third step in the general flowchart discussed in the approach and is coloured green in figure 5.1. As mentioned in the approach, the verification, calibration and validation are also part of the modelling process and are therefore partly coloured green in figure 5.1. The modelling, including the verification, calibration and validation can be divided into a total of five parts. Those five parts can be seen in the flowchart in figure 5.2.

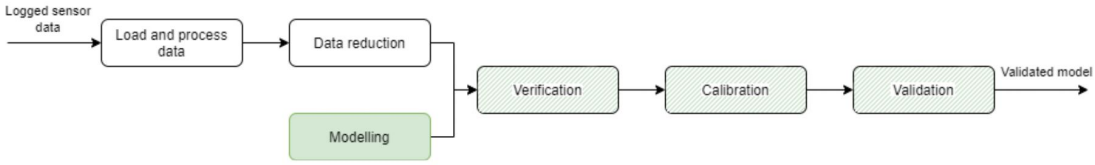

Figure 5.1: General flowchart

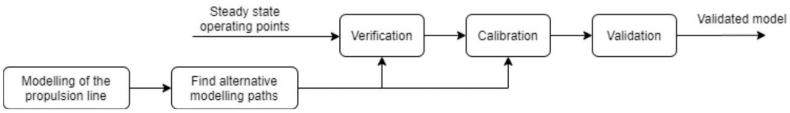

Figure 5.2: Flowchart of the modelling process

The first part is the modelling of the propulsion line model. This is also called the initial model since some additional models are made in the calibration step. The initial model is based upon the current models used by Damen Shipyards. The second part is finding alternative modelling paths. This alternative modelling paths are obtained by rewriting formulas in order to obtain alternative models with different inputs, outputs and assumptions. Those alternative models are used to verify and calibrate the initial propulsion line model. The third step is the verification of the model where model outputs are compared with theoretical formulas. The fourth step is using the alternative modelling paths to calibrate the model with the use of the remote logged data. In the fifth and last step the model is validated with the use of additional remote logged data.

5.1. Modelling of the propulsion line

In this section the model of the propulsion line is made. This model must be complex enough to be able to reproduce the steady state behaviour of a vessel and simple enough to be able to use the remote logged data for inputs and later for validation. In the chapter where the literature is presented, the simple and more complex models and research regarding different propulsion line components are listed. In the analysis of the processed data in chapter 3.4 the available parameters are determined. With the limited available parameters only a simple model will fit. This model includes a basic model of the diesel engine component, the gearbox component, propeller component and the resistance of the vessel.

The hardware-in-the-loop model as it is currently being used by Damen Shipyards is analysed. This model is a heavily adjusted and extended model to be able to fit the specific projects that require hardware-in-the-loop testing. However, despite the complexity, the model's base consist out of a diesel engine component, gearbox, propeller and ship resistance component.

First, a model is made that looks like the base of the current hardware-in-the-loop. This model contains a simple model of the diesel engine, gearbox, propeller and ship resistance. To make this simple model, the propulsion chain diagonal by Klein Woud & Stapersma [10], together with the model from the course by de Vos [12] are used as reference. The propulsion chain gives an overview of powers and efficiencies from resistance to brake power and is presented in figure 5.3. The similarity of the propulsion chain and the model is that they both have fuel flow as input and ship speed as output.

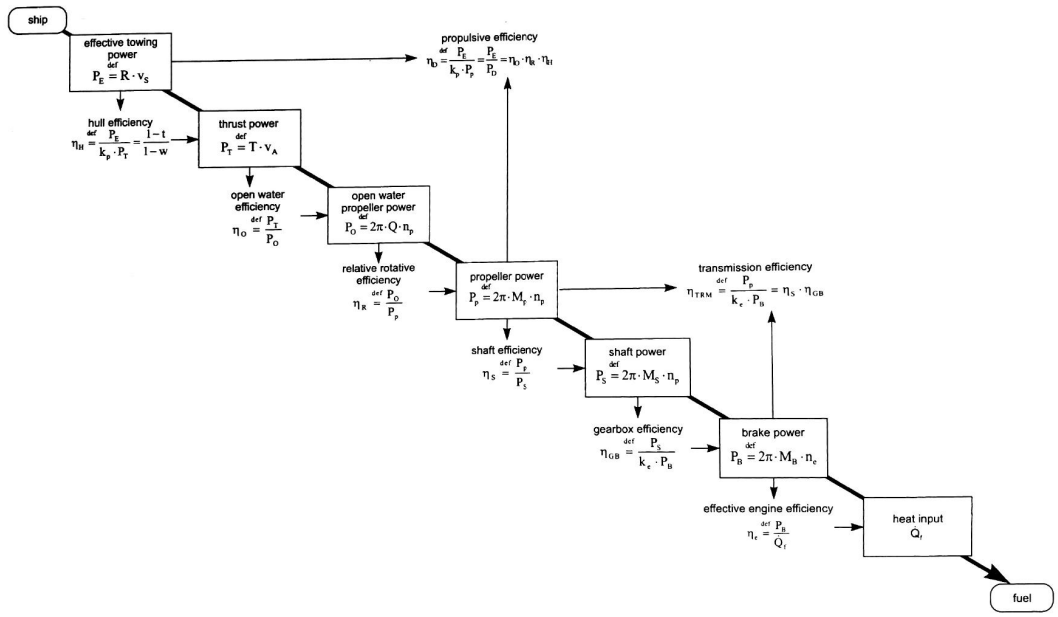

Figure 5.3: Propulsion chain diagonal

5.1.1. Diesel engine

The diesel engine is modelled using basic thermodynamic principles. Since there is very limited information available of the engine's cylinders, and mainly due to the lack of remote logging data of for instance engine inlet- and outlet- pressure and cylinder temperatures, more complex models which include in- cylinder processes of the diesel engine are not applicable.

The use of Pressure charging is also not included into the diesel engine model. Besides having limited information about the compressor and turbine ,from the remote logging data only ambient pressure is known. no pressure at intake after compressing and also no exhaust pressure is available.

The model by de Vos [12] is also made with the use of basic thermodynamic principles and is therefore used as reference. The formulas describing the thermodynamic process of converting fuel into mechanical energy can be found in the book "A fundamental approach to performance analysis, turbocharging, combustion, emissions and heat transfer" by Stapersma [49] and "Design of Propulsion and Electric Power Generation Systems" by Klein Woud & Stapersma [10].

The governor regulates the amount of fuel that is injected into the engine by comparing the actual engine speed with the required engine speed often with engine limits included. Since the regulating of the governor acts solely on the dynamic behaviour of the diesel engine and for now only steady state is considered, the governor is not included into the model.

Now that the governor is not included, the input to the diesel engine will not be an engine speed demand but the actual fuel rate as it is done in the model by de Vos and presented in figure 5.3 as found in the book from Klein Woud & Stapersma [10].

Model in- ,outputs and assumptions
Below a list of all inputs to the diesel engine model with units is presented. The engine speed is calculated in the gearbox block within the overall model while the fuel rate is an input from outside the model. The remote logged data is used as an input for the fuel rate.

- Fuel rate [litre/hour]
- Engine speed [revolutions/second]

below a list of all outputs from the diesel engine model is presented. The engine torque is used in the gearbox block further in the overall model. The brake power is an output that is only used for comparison and making plots, the brake power is not used in other blocks within the overall model.

- Engine torque [kNm]
- Engine brake power [kW]

Also some assumptions are made. The nominal specific fuel consumption is known from the manufactures product sheet. Assumed is that the specific fuel consumption is constant what results in a constant engine efficiency as it is shown in the model by de Vos [12]. In reality for part load conditions of the diesel engine the specific fuel consumption is higher than the nominal value.

The fuel properties are assumed to be constant and are chosen accordingly to the engine manufactures specifications. On the engine specification sheet the note is made that the given engine characteristics as specific fuel consumption, nominal speed, power and torque are only valid for fuel to DIN EN 590 specification with a minimum value for the lower heating value (h^L) of 42800 kJ/kg.

The density of diesel oil depends on the temperature. Accordingly to the DIN EN 590 fuel specification the density at 15 degree Celsius lies between 820 and 860 kg/m^3. Therefore the fuel density is assumed to be 840 kg/m^3.

Diesel engine Simulink model
From the given fuel rate, the mean fuel flow is determined. The fuel rate is given in 10 * litre per hour. First the fuel rate is divided by 10 so that the unit is litre per hour. Then the fuel rate is multiplied by the density of fuel, which according to diesel-net [13] amounts 0.84 kg per litre for the diesel oil specified by the diesel engine specification. To obtain the mean fuel flow the unit kg per hour must be converted to kg per second by dividing with 3600. Now the mean fuel flow in kg per second is obtained.

The heat flow and fuel flow are related by the Lower heat value (h^L) of the fuel. According to ISO 3046, which is used by manufactures in their product specifications, an value of 42800 kJ/kg can be used. Formula 5.1 is used to determine the heat flow from the mean fuel flow and the lower heating value.

$$\dot{Q}_f = \dot{m}_f \cdot h^L \tag{5.1}$$

Not all heat will be transformed into mechanical energy rotating the output shaft of the engine. Some heat will be lost in the conversion process. The engine efficiency relates the generated heat energy to the delivered mechanical energy. Formula 5.2 shows this relation. This formula can be rewritten into formula 5.3 in order to obtain the delivered brake engine power.

$$\eta_e = \frac{P_B}{\dot{Q}_f} \tag{5.2}$$

$$P_B = \dot{Q}_f \cdot \eta_e \tag{5.3}$$

The engine efficiency can be calculated by using formula 5.5. In this formula the specific fuel consumption of the engine is used to determine the engine's efficiency. The specific fuel consumption is the fuel consumption

related to the brake power delivered by the engine. The definition of the specific fuel consumption is shown in formula 5.4.

$$sfc = \frac{\dot{m}_f}{P_B} \tag{5.4}$$

When formula 5.4 is substituted into formula 5.1 and finally into 5.2, formula 5.5 is obtained. With this formula, the engine efficiency can be determined by the use of the specific fuel consumption and the lower heating value.

$$\eta_e = \frac{1}{sfc \cdot h^L} \tag{5.5}$$

The specific fuel consumption is expressed in g/kWh and the lower heating value is expressed in kJ/kg. Due to the different units, formula 5.5 can be rewritten into formula 5.6 in order to use the specific fuel consumption and heating value in the units as they are expressed in.

$$\eta_e = \frac{3600000}{sfc \cdot h^L} \tag{5.6}$$

Now that the engine efficiency is can be determined, formula 5.3 can be used to determine the engine brake power. With the use of the engine brake power and the engine revolutions per second, the engine torque can be obtained. Formula 5.7 can be rewritten into formula 5.8.

$$P_B = 2\pi \cdot M_B \cdot n_e \tag{5.7}$$

$$M_b = \frac{P_B}{2\pi \cdot n_e} \tag{5.8}$$

The formulas are inserted into MATLAB Simulink to form a model of the diesel engine. Figure 5.4 shows the Simulink block that represents the diesel engine. As mentioned earlier, the fuel rate and engine speed are the inputs for the this model. The engine torque and engine brake power are the output and are calculated with the use of the formulas discussed above. The fuel rate can be imported from the remote logged data, while the engine speed is calculated in the Simulink block that models the gearbox. The engine brake power is calculated but will not be used furthermore in other Simulink blocks.

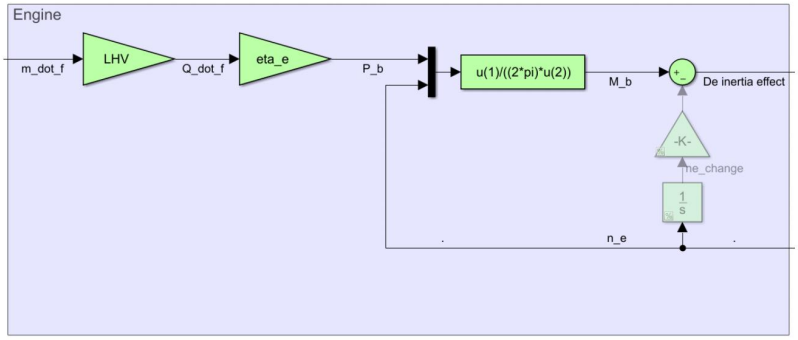

Figure 5.4: Model of the engine component

For now, only steady state is considered, therefore engine dynamics does not play a role in the overall model. As mentioned before, the governor is not modelled. The governor plays a significant role in the dynamic behaviour of the engine and must be included into the model when more than only steady state is considered. Furthermore the moment of inertia of for instance the crankshaft, camshaft, pistons and flywheel act on the acceleration of the engine speed. This dynamic behaviour influences the output torque of the engine as shown by the faded blocks in figure 5.4.

5.1.2. Transmission

The transmission transmits the mechanical energy from the diesel engine to the propulsor. The transmission consist out of a gearbox, shafts and bearings. To make a simple model, only the basic gearbox characteristics are modelled and all energy losses of different transmission components, such as bearings and the losses in the gearbox are combined into one transmission efficiency factor.

The RSD tug uses azimuth thrusters for propulsion. The gearbox and propulsor are combined inside the Azimuth thrusters. The gearbox that is installed in the azimuth thruster is a single reduction gearbox. The reduction gearbox reduces the speed of the engine to the speed that is required for efficient operation of the propeller. The reduction ratio of the gearbox is given by the manufacturer and amounts 7.516. The reduction ratio is the ratio between the input shaft and output shaft of the gearbox and is determined by the amount of tooth per gear. Since the present gearbox is a single reduction gearbox, the reduction ratio is fixed.

Model in- ,outputs and assumptions

Below a list of all inputs to the transmission model with units is presented. The engine torque is calculated in the model discussed above while the required propeller torque will be calculated in the propeller model which will be discussed further on.

- Engine torque [kNm]
- Required propeller torque [kNm]

below a list of all outputs from the transmission model is presented. By comparing moments on either side of the gearbox, the shaft speed can be determined. Since the reduction ratio of the gearbox is known, both the diesel engine speed and propeller speed can be obtained.

- Engine speed [rps]
- Propeller speed [rps]

Also some assumptions are made. The losses of all separate components of the transmission are combined into one efficiency and is assumed to be constant over different shaft speeds and loads.

Transmission Simulink model

As mentioned earlier, the reduction ratio of the gearbox is given. Formula 5.9 shows the effect of the reduction ratio and engine speed on the propeller speed.

$$i_{GB} = \frac{n_e}{n_p} \tag{5.9}$$

As a result of the speed reduction the torque has increased. Formula 5.10 shows the relation between the engine shaft torque and the propeller shaft torque.

$$M_s = \eta_{trm} \cdot i_{GB} \cdot M_B \tag{5.10}$$

The η_{trm} term is the transmission efficiency which causes a power loss. According to Klein Woud & Stapersma [10], the power loss of gearbox for single step reduction gearbox is around 1 to 2%, however this is just the efficiency of the gearbox component and does not include the bearing losses and shaft losses that are included in the transmission efficiency. Moreover is the efficiency of a azimuth thruster is generally lower than the efficiency of a single reduction gearbox. Damen uses a transmission efficiency of 92% for general calculations. For this simple model this constant transmission efficiency will be used.

In the Simulink model of the transmission a moment balance is made. The delivered torque by the diesel engine is compared with the required torque of the propulsor. If the delivered torque is equal to the required torque, the moment is in balance and in steady state. If there is a difference between the delivered torque and required torque, a net torque will appear which causes the propeller and diesel engine shaft to increase or decrease in speed. Formula 5.11 shows the moment balance and result on shaft speed.

$$n_p = \int \frac{M_b - M_s}{2\pi \cdot I} dt \tag{5.11}$$

The inertia (I) is the rotation inertia of the whole propulsion line. This includes the inertia of all rotating components attached to the shaft line such as the flywheel of the engine, crankshaft, shaft, gears and propellers. Since the inertia of all those components is hard to determine and the remote logged data can only be used in steady state moments where the acceleration of the shaft is zero, the inertia is set to a very low value to eliminate the acceleration and deceleration effects.

The formulas are inserted into MATLAB Simulink to form a model of the transmission. Figure 5.5 shows the Simulink block that represents the transmission. For now the inertia is set to a very low value. In the future, the inertia of all components can be determined to include also non steady state remote logging data in the model.

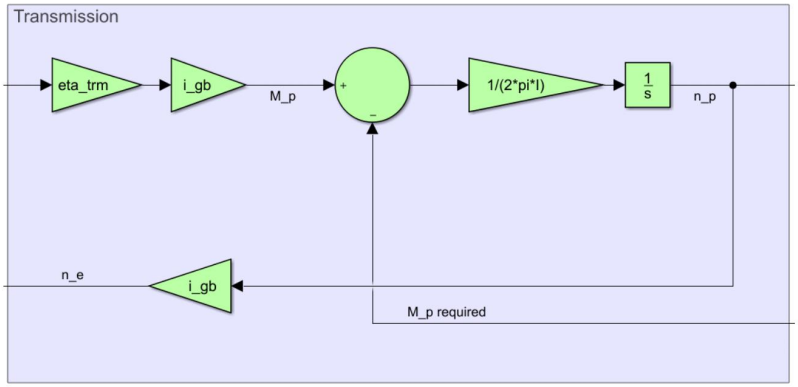

Figure 5.5: Model of the transmission component

5.1.3. Propulsor

The RSD tug is propelled by two azimuth thrusters. In the previous section was explained that the azimuth thrusters include a gearbox and a propulsor. The propulsor attached to the azimuth thruster is a propeller. The propeller is enclosed by a nozzle in order to generate a higher bollard pull capability. The dimensions and specifications of a propeller are determined in the design of the vessel and are given in table 5.1.

	value	unit
Propeller diameter	2.70	meter
Number of blades	5	-
A0/Ae ratio	75	-
P/D ratio		-
Propeller series	ka	-
Nozzle profile	19 a	-

Table 5.1: Propeller specifications

Model in-, outputs and assumptions

Below a list of all inputs to the propeller model with units is presented. The advance velocity comes from the Simulink model that models the vessel's velocity and resistance. From this velocity, the advance velocity 'va' is obtained.

- Propeller speed [rps]
- advance velocity [m/s]

below a list of all outputs from the propeller model is presented. By applying the propeller performance characteristics together with the propeller dimensions and calculated speeds, the propeller delivered thrust and toque are be obtained.

- Propeller Thrust [kN]

- Propeller Torque [kNm]

In order to model the propeller and obtain the propeller torque and thrust the open water propeller diagram is used. Using this open water propeller diagram is an assumption, since the data in this diagram is obtained by experimental tests. The assumption is that the data from the open water propeller test can be used as data of the real propellers installed in the RSD tug.

Propeller Simulink model
To obtain the propeller performance and especially the propeller torque and thrust, the open water propeller diagram can be used. The open water propeller diagram expresses the propeller performance in three non-dimensional parameters: the advance ratio 'J', the thrust coefficient 'KT' and the torque coefficient 'KQ'. Formula 5.12 shows the equation to obtain the advance ratio 'J'. In this formula the advance velocity 'va' is used. This velocity will be calculated inside the Simulink model that represents the vessel's resistance. The advance velocity is made non-dimensional by diving by the propeller rotational speed and diameter.

$$J = \frac{v_A}{n_p \cdot D_p} \tag{5.12}$$

To obtain the thrust delivered and torque required by the propeller, the thrust and torque coefficients are required. By rewriting formula 5.13 into formula 5.15 and formula 5.14 into formula 5.16 the thrust and torque are obtained.

$$K_T = \frac{T}{\rho \cdot n_p^2 \cdot D_p^4} \tag{5.13}$$

$$K_Q = \frac{Q}{\rho \cdot n_p^2 \cdot D_p^5} \tag{5.14}$$

$$T = K_T \cdot \rho \cdot n_p^2 \cdot D_p^4 \tag{5.15}$$

$$Q = K_Q \cdot \rho \cdot n_p^2 \cdot D_p^5 \tag{5.16}$$

After rewriting, formula 5.15 can be used to obtain the delivered thrust and formula 5.16 to obtain the required torque. Now that the formulas are rewritten, the thrust and torque coefficients must be found. These coefficients can be read from the open water propeller diagram that represents the installed propellers. Since the installed propeller has five blades and an A0/Ae ratio of 0.75, the open water propeller diagram for the 5-75 propeller must be used. The used propeller is of the 'ka' series which corresponds to the propeller that is tested to obtain the propeller performance. Furthermore, a nozzle is applied. This nozzle has a profile that is named '19 a'. The open water propeller diagram of the ka 4-75 19a propeller matches the propellers used in the RSD Tug.

Since reading values accurately from the open water propeller diagram is hard, the original coefficients that are used to make the open water propeller diagram are used. In the thesis by Oosterveld [38], the lines of the thrust and torque coefficients from the open water propeller diagram are described using a polynomial equation. This polynomial equation uses multiple coefficients to create the right curves in the open water propeller diagram. Besides the coefficients, the P/D ratio and advance ratio 'J' can be inserted into the equation for the polynomial to obtain the corresponding thrust and torque coefficients. Formula 5.17 shows the polynomial for the thrust coefficient.

$$\begin{aligned} K_T = {} & + A_{0,0} + A_{0,1} J + \dots + A_{0,6} J^6 + \\ & + A_{1,0}\left(\frac{P}{D}\right) + A_{1,1}\left(\frac{P}{D}\right) J + \dots + A_{1,6}\left(\frac{P}{D}\right) J^6 + \\ & + A_{2,0}\left(\frac{P}{D}\right)^2 + A_{2,1}\left(\frac{P}{D}\right)^2 J + \dots + A_{2,6}\left(\frac{P}{D}\right)^2 J^6 + \\ & \dots \\ & + A_{6,0}\left(\frac{P}{D}\right)^6 + A_{6,1}\left(\frac{P}{D}\right)^6 J + \dots + A_{6,6}\left(\frac{P}{D}\right)^6 J^6 \end{aligned} \tag{5.17}$$

Formula 5.18 shows the polynomial for the torque coefficient.

$$K_Q = + C_{0,0} \quad + \quad C_{0,1} \quad J + - \\ - + C_{6,6} \left(\frac{P}{D} \right)^6 \quad J^6 \tag{5.18}$$

When the coefficients are substituted into the equations for the polynomials the values of the thrust and toque coefficients for a specific advance ratio 'J' can be obtained. Plotting those values over a range of J values, the open water propeller diagram is obtained. In figure 5.6 the thrust and torque coefficients are plotted over a range of J.

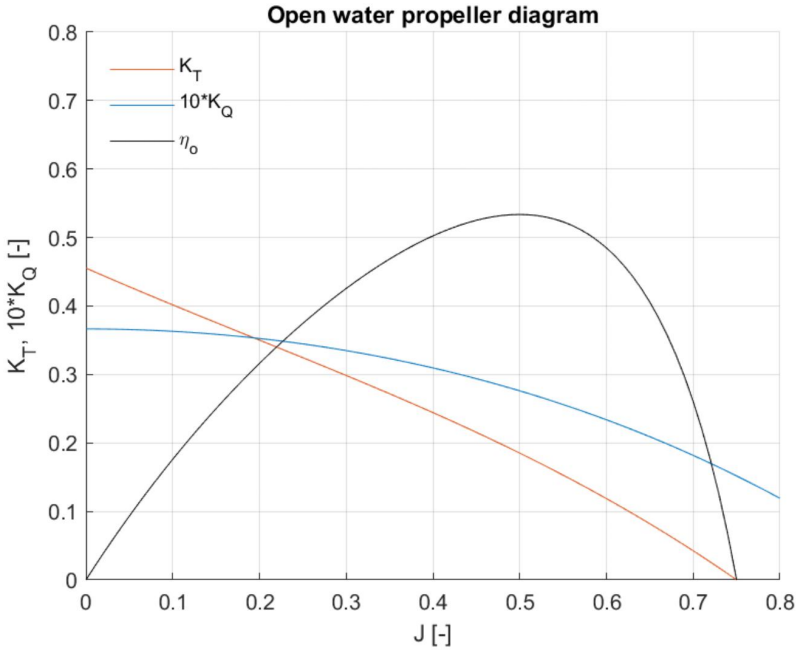

Figure 5.6: Open water propeller diagram of the ka 5-75 19a propeller

Using the thrust and torque coefficients in formula 5.19 makes it possible to obtain the open water propeller efficiency. This open water propeller efficiency is also plotted over a range of J and shown in figure 5.6 but not used in further calculations.

$$\eta_o = \frac{1}{2\pi} \cdot \frac{K_T \cdot J}{K_Q} \tag{5.19}$$

Now that the required torque for the propeller to deliver a certain amount of thrust is known, the torque that the engine must deliver can be obtained. Using the open water propeller diagram means that the results, the torque and thrust only holds for an open water environment. Since the hull is not present in an open water propeller environment, hull- propeller interactions are not taken into consideration. To obtain the required torque for the propeller when a hull is present, a hull- propeller interaction expressed as the relative rotative efficiency (η_r) must be taken into account. Formula 5.20 shows the effect of the relative rotative efficiency on the propeller torque. According to Klein Woud & Stapersma [10] the relative rotative efficiency normally does not differ much from unity. Values of the range of 0.98 to 1.02 may be encountered.

$$\eta_R = \frac{Q}{M_P} \tag{5.20}$$

The formulas are inserted into MATLAB Simulink to form a model of the propulsor. The coefficients and equations for the polynomials that describe the thrust and torque coefficients are programmed into a Simulink function block. Figure 5.7 shows the Simulink block that models the performance of the propulsor.

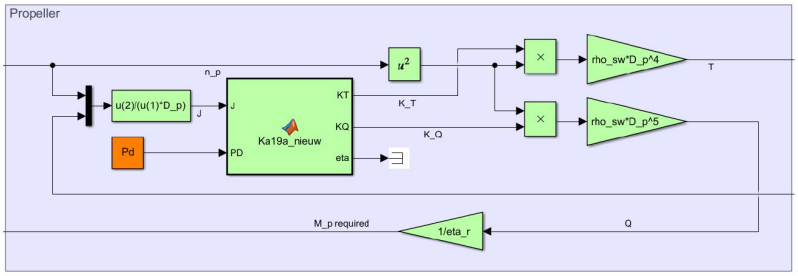

Figure 5.7: Model of the propeller component

5.1.4. Hull

The last Simulink model is made to model the energy transfer from the propulsor's trust into the water, resulting in speed. This model is called ship. The resistance of the ship depends on the speed of the vessel, the higher the speed, the higher the resistance. More resistance means more thrust is required to propel the vessel. A balance between the resistance of the vessel and the thrust delivered by the propellers can be made. This balance determines if the vessel is going to accelerate, decelerate or sails with a constant velocity.

Model in-, outputs and assumptions

Below a list of all inputs to the ship model with units is presented. Since there are two azimuth thrusters present on the RSD tug, two propellers deliver thrust. Because two propellers deliver thrust upon only one hull, the thrust of the port-side and starboard propellers are add together.

- Thrust [kN]

below a list of all outputs from the ship model is presented. The vessel velocity is converted to an advance velocity, which is used in the Simulink model of the propulsors.

- Advance velocity [m/s]
- Vessel velocity [m/s]

A couple assumptions are made, such as the thrust deduction factor. The thrust deduction factor is part of the propeller-hull interaction. The trust deduction factor is the part of the total delivered thrust that is required to overcome the added resistance due to the presence of the propeller behind the hull. With the design of the RSD tug, Damen Shipyards did estimate the thrust deduction factor for different vessel speeds. The estimate by Damen Shipyards is used as an assumption for the model. Figure 5.8 shows the thrust deduction factor for different vessel speeds. The thrust deduction values that represent this graph can be used in a lookup table within the Simulink model.

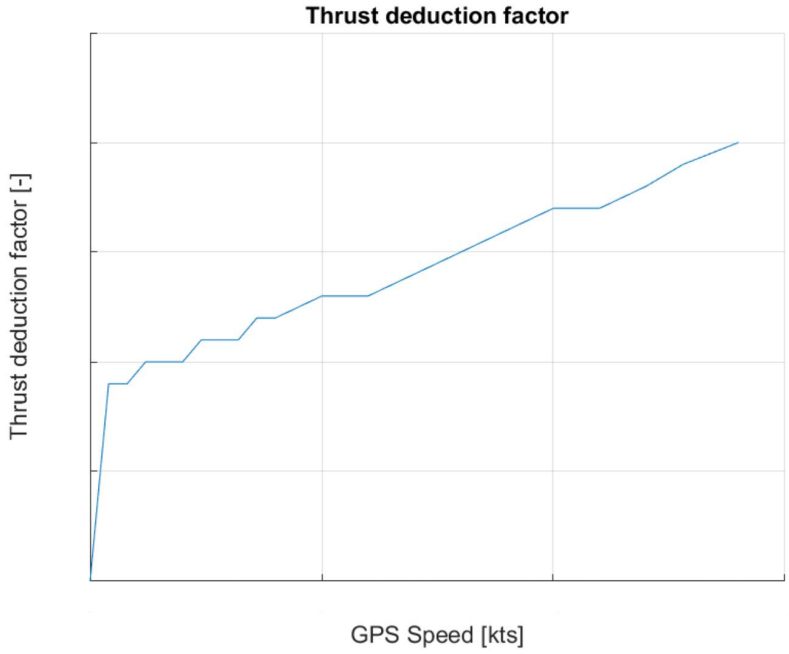

Figure 5.8: Thrust deduction factor lookup

Like with the thrust deduction factor, Damen Shipyards made an estimate of the vessels resistance for different vessel speeds. Like with the thrust deduction factor, the estimate by Damen Shipyards is used as an assumption. Figure 5.9 shows the resistance for different vessel speeds. The values that make this graph can be used in a lookup table within the Simulink model.

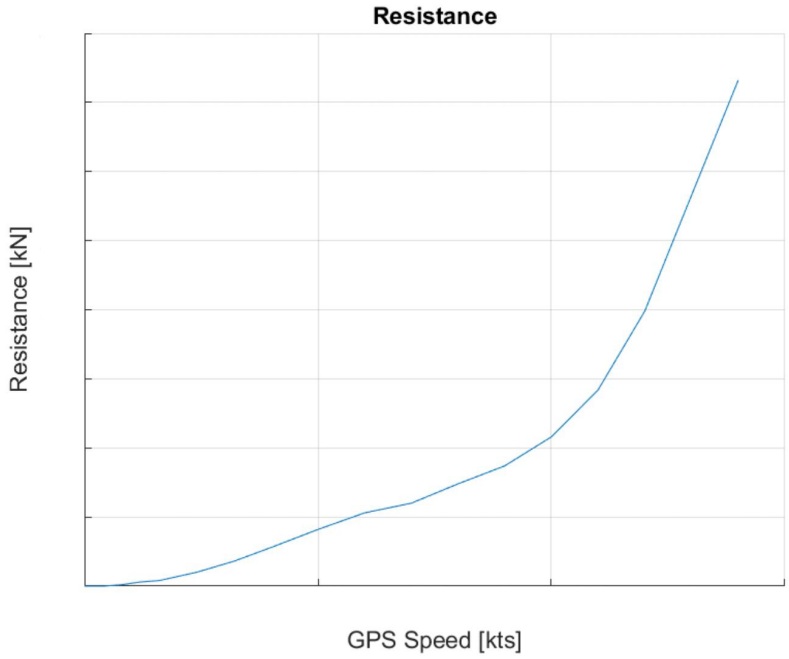

Figure 5.9: Resistance lookup

Besides the Resistance and the thrust deduction factor, the wake factor is also determined by Damen during the design process. The wake factor is assumed to be a fixed value.

Hull Simulink model

As mentioned earlier, a balance between the resistance of the vessel and the thrust delivered by the propellers can be made. If the delivered force by the propellers is equal to the required force to sail at a certain speed, the moment is in balance and in steady state. A difference between the delivered force and required force results in a resultant force that will causes the vessel to accelerate or decelerate. Formula 5.21 shows the force balance and result on vessel speed.

$$V_s = \int \frac{F_{prop} - F_{ship}}{m} dt \tag{5.21}$$

The mass (m) is the mass of the vessel and the surrounding water that induces added resistance. The mass and added mass determines the delay in acceleration or deceleration of the vessel. Since the remote logged data can only be used in steady state moments where the acceleration of the vessel is zero, the mass is set to a very low value to eliminate the acceleration and deceleration effects.

In order to determine the required force to sail at a certain vessel speed, formula 5.22 can be used. In this formula, the thrust deduction factor and resistance are used. Values for those are obtained by a lookup table where the values for the thrust deduction factor and the resistance are obtained for a certain vessel speed.

$$T = \frac{R}{1-t} \tag{5.22}$$

The Simulink block that represents the propulsor calculates the advance ratio 'J'. In order to do so, the advance velocity is needed. By the use of formula 5.23 the advance velocity can be calculated. The wake factor 'w' shows the difference of the vessel speed and the water speed at the location of the propeller. Since the propeller is located behind the hull in the boundary layer around the vessel it encounters a lower water velocity than the vessels velocity.

$$V_a = (1-w) \cdot V_s \tag{5.23}$$

The formulas are inserted into MATLAB Simulink to create a model of the vessel where the resistance, thrust deduction factor and wake factor are used in the force balance. Figure 5.10 shows the Simulink corresponding Simulink block.

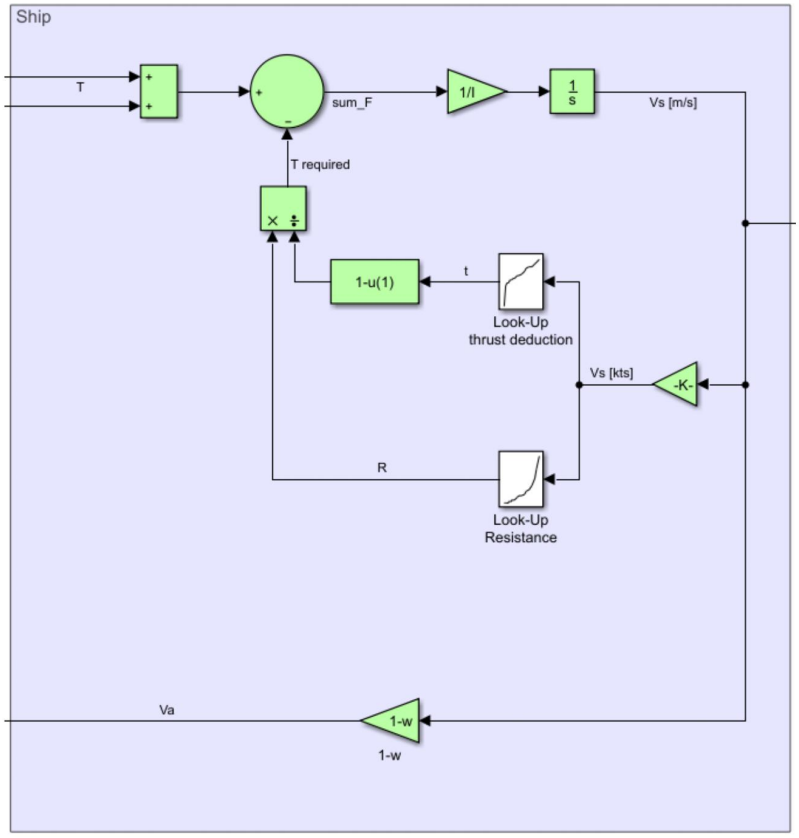

Figure 5.10: Model of the hull component

5.1.5. Complete model

Since the RSD tug is propelled by the use of two azimuth thrusters, two diesel engines, two transmissions and two propellers are present. Those three components are placed twice in the model to obtain the realistic configuration. A simple multiplication is not sufficient the starboard and port-side diesel engine can run at different speeds and under different loads. This means that also the starboard transmission and propeller speed and thrust can differ from port-side. Figure 5.11 shows all discussed Simulink models into one propulsion model that represents the propulsion line of the RSD tug.

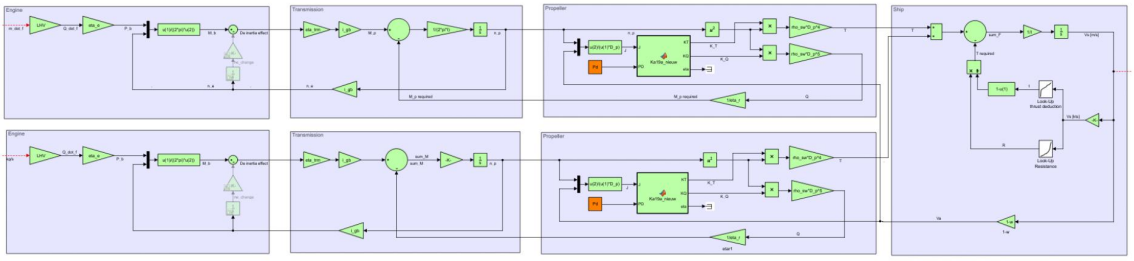

Figure 5.11: Complete initial propulsion line model

5.2. Find alternative modelling paths

In the previous section, an initial model is made. This propulsion line model is made by using the model by de Vos [12] and the propulsion chain diagonal [10] as reference. For each component within the propulsion line model, the in- and outputs are discussed. Those in and outputs, together with the assumptions made in the modelling of each component are shown in table 5.2. This table shows all inputs, outputs and assumptions of the whole initial propulsion model.

	Input	Output	Assumptions
Diesel engine	Fuel rate, Engine speed	Engine torque, Engine power	SFC
Transmission	Engine torque, Propeller torque	Engine speed, Propeller speed	η_{trm}
Propulsor	Propeller speed, Advance velocity	Propeller thrust, Propeller torque	KT, KQ, η_R
Hull	Propeller thrust	Vessel speed, Advance velocity	R, t, w

Table 5.2: Inputs, outputs and assumptions

In this table, often the output from one component is an input for another component. Therefore, this table can also be expressed in a flowchart where arrows connect the outputs with the inputs. Figure 5.12 shows the initial model in a flowchart diagram. The four main components, the diesel engine, transmission, propulsor and ship are placed as blocks. Arrows pointing into a block represents an input for that component while arrows pointing away from the block represents outputs. The assumptions are inputs and are therefore represented by an arrow pointing into a component and the name of the assumed parameter is coloured red. Parameters can also be an output, without being used as input for another block. An example is the break power in the diesel engine block. Output that are not used as input and go out of the model are represented by an arrow pointing away from the block and the output name coloured green.

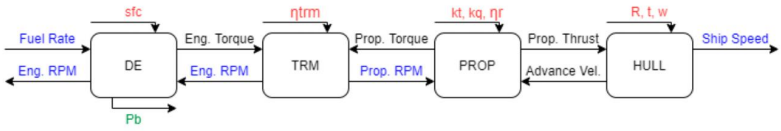

Figure 5.12: Possible Path 1

The input and outputs that are coloured in blue are the parameters that are obtained with remote logging. With the diesel engine block for example, the fuel rate is an input. The fuel rate is obtained with remote logging and is processed such that only the fuel rate of steady state moments is left. The engine speed is also coloured blue since it can be obtained using remote logging and processing. In this model however, the engine speed is an output and will be calculated within the model. This way, remote logging data is not used as in input and can only be used to compare the model output to the remote measured data.

It is possible to rewrite formulas in order to have another input parameter, which results in another output variable. This way, a remote logged measurement can be used as input to the model and reduce the amount of assumptions that are needed. Below a list is made with all different possible paths to make a propulsion line model with the available parameters.

- 2^{nd} path.
  Figure 5.13 shows an alternative model by means of a different parameter path. This path represent a model where formulas inside components are rewritten. Instead of calculating the engine torque in the engine component, the required torque is calculated in the gearbox component. The diesel engine rpm is calculated in the engine component instead of in the gearbox component. This path is also often used in common propulsion line models. The result of rewriting formulas is that the input and output arrows between the component diesel engine and gearbox are reversed.

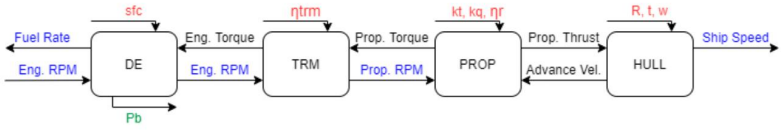

Figure 5.13: Possible Path 2

- 3rd path.
  As mentioned earlier, when an extra input is introduced it becomes possible to extract another output from the model. In the first and second path the propeller thrust, resistance, thrust deduction factor and wake factor were required to calculate the vessel speed and advance velocity. By inverting the direction of ship speed and use the remote logged measurements as input, one input value can be inverted into an output. This way the resistance for example can be extracted from the model. This path is presented in figure 5.14. It can be seen that using this path results in one less assumption needed.

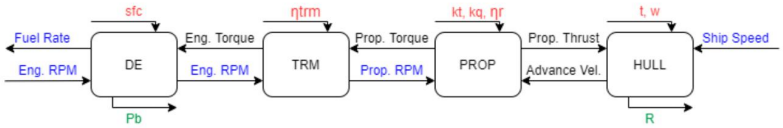

Figure 5.14: Possible Path 3

- 4th path.
  As with the third path, an extra input is provided to the diesel engine components. This means that an assumption can be changed into an output of the component. In this path the remote logged measurement of the fuel rate is used as an input, making it possible to change the assumption for the specific fuel consumption into an output. This path is based upon the 2th path, figure 5.15 shows that only input, output and assumptions of the diesel engine component are changed.

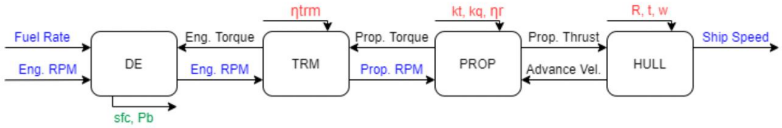

Figure 5.15: Possible Path 4

- 5th path.
  The changes done in path 3 and 4 can also be combined. Figure 5.16 shows a path that rewrites both the diesel engine component as the ship component. In this path both the remote logged data of the fuel rate and the vessel speed are used as input. This makes it possible to change the specific fuel consumption and the resistance into outputs. This way two less assumptions are needed for the model. As can be seen on the figure 5.16 all remote logged parameters are now an input into the whole propulsion line model.

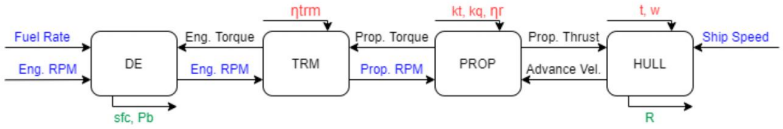

Figure 5.16: Possible Path 5

- 6th path.
  When the diesel engine block is rewritten and the fuel rate and engine rpm are an input to the diesel engine component, the specific fuel consumption can be taken as output. This is done in path 4. Now the specific fuel consumption is not taken as output and still is an assumption. This way the diesel

engine torque can now be inverted to an output. The result is that the diesel engine rpm and diesel engine torque are an output of the diesel engine component and thus an input for the gearbox component. Since engine torque is now not an output from the gearbox component anymore but an input, the gearbox has one extra input and the transmission efficiency can be taken as output. Figure 5.17 shows this path.

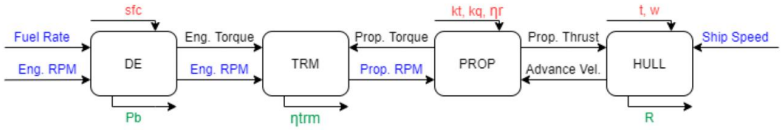

Figure 5.17: Possible Path 6

- 7^{th} path.
  Like done with path 6, the remote logged fuel rate, engine rpm and ship speed are all taken as input. Instead of rewriting the diesel engine and take specific fuel consumption as output like in path 4, or rewriting the diesel engine and add an extra input to the transmission model where the transmission efficiency is taken as output, both the diesel engine and transmission component are rewritten in order to create an extra input for the propulsor model. The ship component is also rewritten in order to add another input to the propulsor model. The result is that propeller thrust, propeller torque, propeller speed and advance velocity are all inputs to the propulsor model. Now that two extra parameters are an input into the propulsor model, two assumptions can be taken as output. As figure 5.18 shows, the thrust coefficient and torque coefficient are an output instead of an assumption.

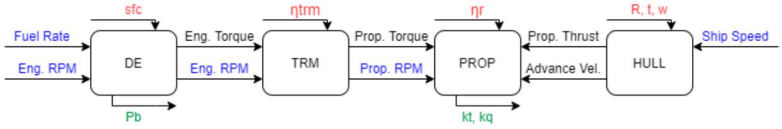

Figure 5.18: Possible Path 7

- 8^{th} path.
  Instead of using the propeller torque and propeller speed to output the thrust coefficient and torque coefficient like path 7, the thrust and torque coefficient are not taken as output in this path. When both the torque and thrust coefficients are still an assumption it becomes possible to invert the advance velocity. When the advance velocity is inverted and becomes an input to the ship component, not only the resistance but also the wake factor can be taken as output. This path is shown in figure 5.19

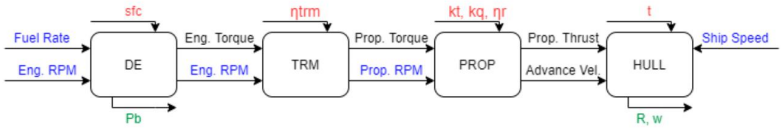

Figure 5.19: Possible Path 8

- 9^{th} path.
  This path is the same as path 8. However, now the thrust deduction factor is taken as output instead of the resistance. Figure 5.20 shows this path.

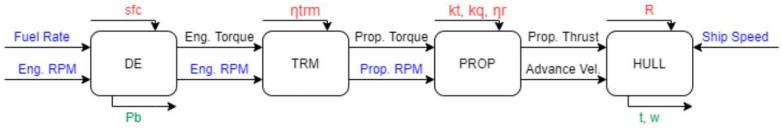

Figure 5.20: Possible Path 9

- 10^{th} path.
  From previous paths can be seen that some assumptions can be converted into an output by the use of the remote logged measurements as input and by rewriting formulas. Since the remote logged fuel rate, engine rpm and ship speed are all used as input, the only way to remove more assumptions is to combine the outputs. Formula 5.24 shows how the thrust is calculated in the ship Simulink model. The separate resistance and thrust deduction term can be combined into one term. This term than represents R/(1-t).

$$T = \frac{R}{1-t} \tag{5.24}$$

  Now that the resistance and thrust deduction terms are combined into one parameter, this new parameter can be taken as output like it is done for the resistance or thrust deduction term separately. This means that the thrust deduction and the resistance are not an assumption anymore. The downside is that the whole term R/(1-t) is the output, making it impossible to isolate either the resistance term or thrust deduction term alone without making an assumption for one of the two terms. This path were thrust deduction and resistance are combined is shown in figure 5.21.

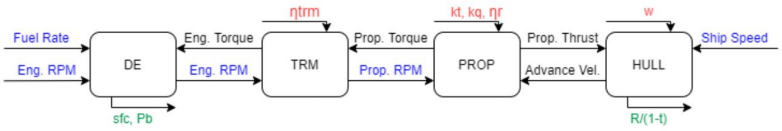

Figure 5.21: Possible Path 10

- 11^{th} path.
  Like with resistance and trust deduction, the transmission efficiency and the specific fuel consumption can be combined. Since the specific fuel consumption has been multiplied by, among other things, the efficiency of the transmission, those two terms can be combined by dividing the specific fuel consumption with the transmission efficiency. The drawback of this combination is that the specific fuel consumption and transmission efficiency are both located into different component models which makes both the diesel engine model and the transmission model dependable on each other. The advantage of combining those terms is that only four assumptions are needed for the whole propulsion model. The path were the specific fuel consumption and the transmission efficiency are combined is shown in figure 5.22.

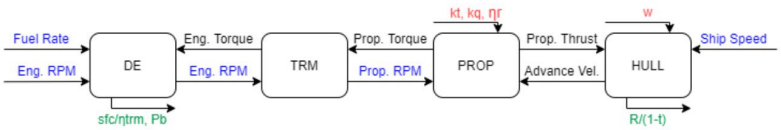

Figure 5.22: Possible Path 11

5.3. Verification

Now that the propulsion line model is made and alternative paths are created, these alternative paths can be used in order to check if the model behaves like expected. This is the verification step. Verification is done by comparing the simulation outputs from the model with theoretical expectations. In the verification step, the fit of the simulation results with the theoretical expectations is not the most important. However, the shape and trend of the simulation results are important and are compared with the shape and trend of the theoretical expectations.

The initial propulsion line model has three output variables. The output variables from the initial model are diesel engine speed, brake engine power and ship speed. By using an alternative modelling path as discussed in the previous section, formulas within the simulation blocks can be rewritten in order to change the input and output variables. Since the diesel engine speed and ship speed are remote logged variables, they can be used as input for the model to reduce the amount of assumptions. Looking at the alternative modelling paths where the remote logged data is used as input, it can be seen that without combining output variables, the maximum number of outputs is three. Alternative paths 5 till 9 are rewritten in such way that the remote logged data is solely used as input to create three output variables. In order to choose which alternative modelling paths are preferred to create output variables for the verification process, the different paths are examined. Two aspects are looked into.
First, can the output variables be compared to theoretical calculations or available values in order to succeed in the verification of the model?
Second, can it be expected that a good assumption is possible for the specific variable?
In the list below the variables are examined on the two mentioned aspects.

- The specific fuel consumption can be compared with available engine specifications. Assuming this variable seems difficult.
- The transmission efficiency can be difficult to compare with theoretical calculations or available data and is often an assumption in modelling.
- The thrust and torque coefficient are included in the open water propeller diagram. The open water propeller diagram is hard to compare to theoretical calculations and is often used as assumption based on the propeller characteristics.
- The relative rotative efficiency can be difficult to compare with theoretical calculations or available data and is often an assumption in modelling.
- The resistance can be compared with available resistance predictions. An assumption of the resistance can also be made with the use of theoretical formulas and constants.
- The thrust deduction can be difficult to compare with theoretical calculations or available data and is often an assumption in modelling.
- The wake factor can also be difficult to compare with theoretical calculations or available data and is often an assumption in modelling.

If for a certain variable it is possible to make a good assumption and the variable is hard to compare with theoretical calculations or other available data, the variable is preferred to be used as an assumption. Likewise, if a certain variable is hard to assume and it is possible to compare this variable with theoretical calculations or other available data, the variable is preferred to be an output of the model. Based on this preferences and the two aspect that were looked into when examining the variables of the alternative modelling paths, the preferred alternative modelling path to use is path 5. Path 5 is presented in figure 5.23.

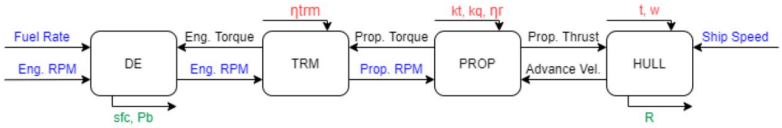

Figure 5.23: Possible Path 5

Using modelling path 5 means that the input variables differ from the initial model. In modelling path 5 the formulas in the hull component and diesel engine component of the model are rewritten in such way that for all external input variables, the remote logged data can be used. The blue coloured variables in figure 5.23 represent the input variables. Those input variables are:

- Diesel engine Fuel rate
- Diesel engine speed
- Vessel GPS speed

By rewriting formulas and changing the input and output variables, the assumptions change as well. The assumptions required for this modelling path are listed below.

- Gearbox efficiency is assumed to be constant.
- Thrust and torque coefficients are obtained from the open water propeller diagram of the corresponding propeller.
- Rotative efficiency is assumed to be constant.
- Thrust deduction is predicted by Damen Shipyards.
- Wake factor is assumed to be constant.

When alternative modelling path 5 is used , the output variables are the ship resistance, the engine brake power and the specific fuel consumption. With those three variables, multiple graphs can be made and compared to theoretical calculations or other available data in the verification of the model. The list below shows the plots that can be made with the use of the output variables from modelling path 5. The variable on the left will be plotted on the vertical axis against the variable on the right, that will be plotted on the horizontal axis.

- Resistance - GPS speed
- Engine brake power - Engine speed
- Specific fuel consumption - Engine brake power
- Engine brake power - GPS speed
- Engine speed - GPS speed
- Fuel rate - Engine speed

For each item in the list above, a figure is presented where an output variable of the propulsion line model is plotted together with the theoretical expectation. After that, The creation of the line in the graph representing the theoretical prediction is described with the use of formulas. At last the comparison between the output variable and the theoretical expectation is made.

Resistance - GPS speed
In figure 5.24 the resistance is plotted on the vertical axis and the GPS speed is plotted on the horizontal axis. The orange markers represent the resistance calculated by the propulsion line model with the use of 15 steady state operating points. The solid blue line represents the theoretical curve.

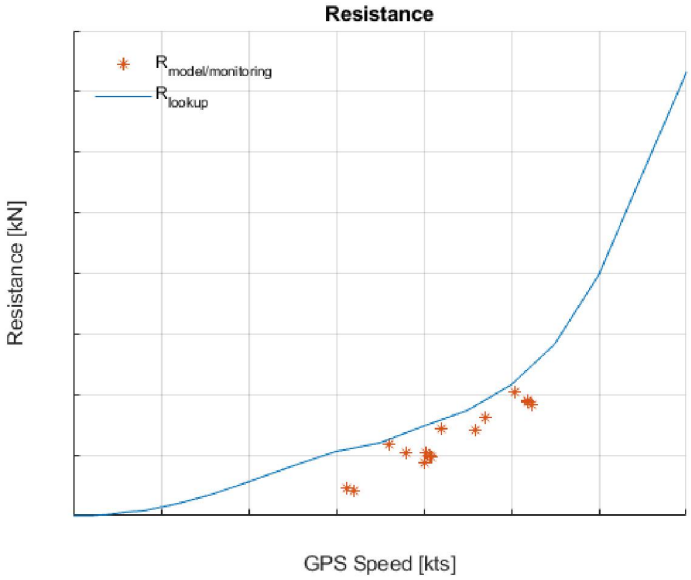

Figure 5.24: Resistance - GPS speed

The theoretical curve that is plotted in figure 5.24 represents the estimated resistance, calculated by Damen Shipyards. The resistance is estimated by the Damen Shipyards research and development department with the use of the Guldhammer resistance prediction method. This method is based on the admiralty coefficient to estimate the relationships between main particulars and calm water resistance [3]. The results from the estimation method are presented in the Damen power speed prediction documents where the estimated resistance is given for a range of different vessel speeds.

The orange markers in figure 5.24 represent the simulated value for an output of the propulsion line model. This output is the calm water resistance of the simulated vessel. The resistance depends on the vessel speed and is therefore plotted in figure 5.24 over a variety of vessel speeds. The propulsion line model discussed in chapter 5 uses the resistance as input for the model. Therefore an alternative modelling path, as discussed in chapter 5.2 must be used in order to obtain the resistance as an output from the model.

Now that both the theoretical expectation and simulation output are potted in the same figure, they can be compared. As mentioned earlier, the verification step focuses on the general shape and trend of the simulation result and not so much on the actual differences in values.

The first thing to notice is that the simulated resistance values are consistently below the theoretical curve. However the order of magnitude of both the theoretical prediction and the simulation output values seems the same. Second, despite the fact that due to the use of remote logged data as input for the model the simulation output of the resistance is only available for vessel speeds between 6 and 11 knots, the trend seems to follow the expected theoretical line.

Engine brake power - Engine speed
In figure 5.25 the brake engine power is plotted on the vertical axis and the engine speed is plotted on the horizontal axis. The brake engine power and engine speed of the port-side engine is presented in the left figure while the engine power and speed of the starboard engine is presented in the right figure. The orange markers represent the brake engine power calculated by the propulsion model. The solid blue line represents the theoretical line.

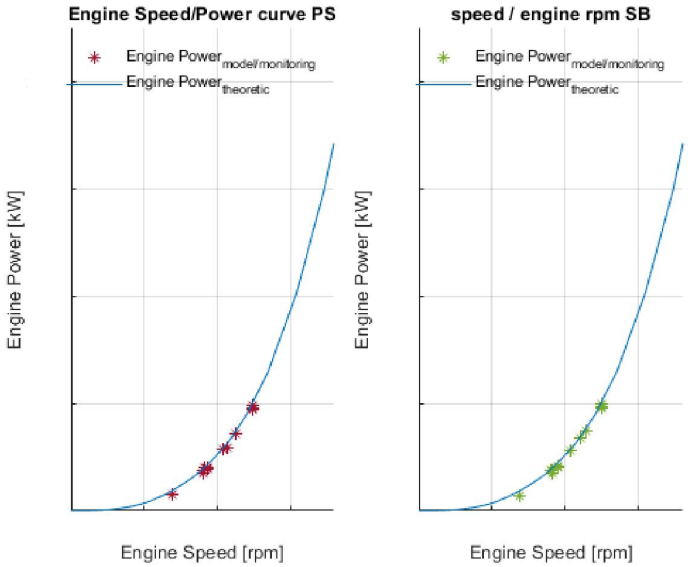

Figure 5.25: Engine brake power - Engine speed

The theoretical line is created by the use of formula 5.25. This formula shows the relation between the brake engine power and the engine speed. In the formula, engine speed is exponential to the 3rd power, this means that the theoretical curve will also have the shape of an exponential curve.

$$P_B = c_9 \cdot n_e^3 \tag{5.25}$$

In formula 5.25 the constant 'c9' is present. The value of this constant determines how steep the theoretical graph will be. A higher value for 'c9' makes the graph steeper. Formula 5.26 shows how the constant 'c9' can be determined.

$$c_9 = \frac{c_4}{\eta_{trm} \cdot k_e \cdot i_{gb}^3} \tag{5.26}$$

In formula 5.26 'c9' is determined with the use of the constant 'c4', the transmission efficiency, the amount of engines per shaft and the gearbox reduction ratio. The constant 'c4' can be determined by the use of formula 5.27.

$$c_4 = \frac{2\pi \cdot \rho \cdot D^5}{\eta_r} \cdot K_Q \tag{5.27}$$

Values for the transmission efficiency, relative rotative efficiency and torque coefficient must be assumed. All other variables are known and can be substituted into the formulas. By estimating the transmission efficiency, relative rotative efficiency and torque coefficient as it is done in the initial model, a value for 'c9' is determined. This value for 'c9' is substituted into formula 5.25 and the theoretical brake engine power is plotted in 5.25 with a solid blue line.

Now that both the theoretical expectation and simulation output are potted in the same figure, they can be compared. It seems that the simulation outputs are very close to the theoretical predicted line. For both higher and lower engine speeds the simulation output seem to follow the theoretical curve closely.

In addition to figure 5.25, figure 5.26 is made. In this figure both the starboard and port-side simulation

outputs are plotted into one graph. The red markers represent the port-side outputs and the green markers represent the starboard outputs. The difference between this figure and figure 5.25 is that the engine operating envelope of the installed engine is placed as background behind the plot.

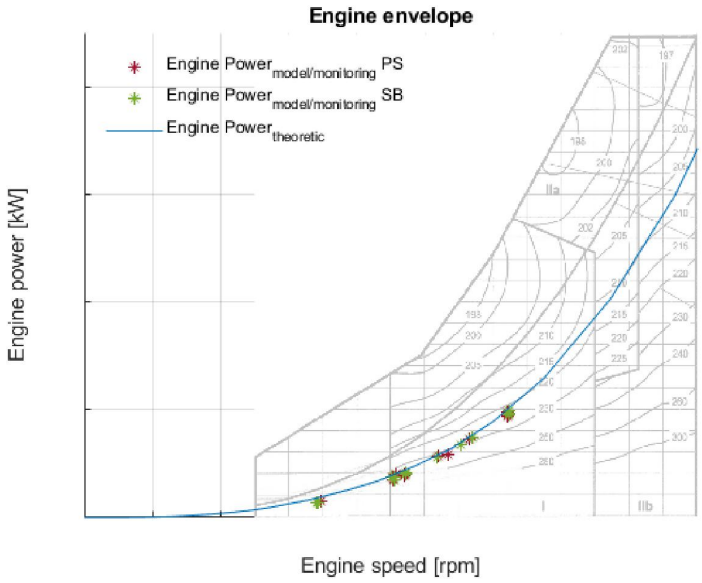

Figure 5.26: Engine operating envelope: Engine brake power - Engine speed

The engine operating envelope has several boundaries. The left boundary is the lower engine speed boundary at 500 rpm. The right boundary at 1800 rpm is the maximum engine speed. The upper boundary of the engine envelope represents the maximum power limit. It is important that all operating points are within those boundaries. As can be seen in the figure, the engine power - engine speed curve lies within the boundaries of the engine envelope. In the engine envelope the solid line that reaches the top right corner is the design load curve. Since the engine power - engine speed curve is less steep than the design load curve it intersects and thus is limited by the maximum diesel engine speed boundary. This is to be expected for a tug sailing in free sailing conditions.

Specific fuel consumption - Engine brake power
In figure 5.27 the specific fuel consumption is plotted on the vertical axis and the engine brake power is plotted on the horizontal axis. The specific fuel consumption and engine power of the port-side engine is presented in the left figure with red markers while the specific fuel consumption and engine power of the starboard engine is presented in the right figure with green markers. It can be seen that the starboard and port-side specific fuel consumption are different. This difference is not important in the verification, but will be discussed in the calibration.

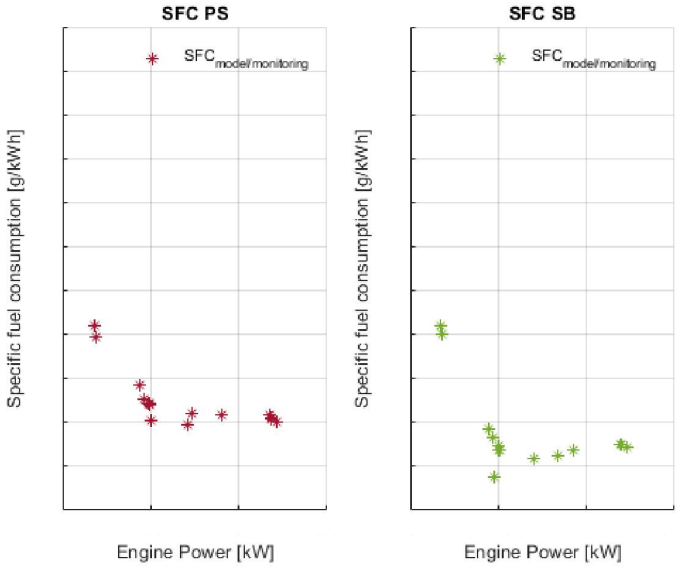

Figure 5.27: Specific fuel consumption - Engine brake power

As mentioned in the selection of the alternative modelling path, obtaining a theoretical prediction for the specific fuel consumption is not straightforward. That is why there is no blue line representing the theoretical expected curve plotted into figure 5.27. In order to compare the simulation outputs with the expected trend of the specific fuel consumption, a figure from Stapersma [48] is shown in figure 5.27. This figure shows the specific fuel consumption curves.

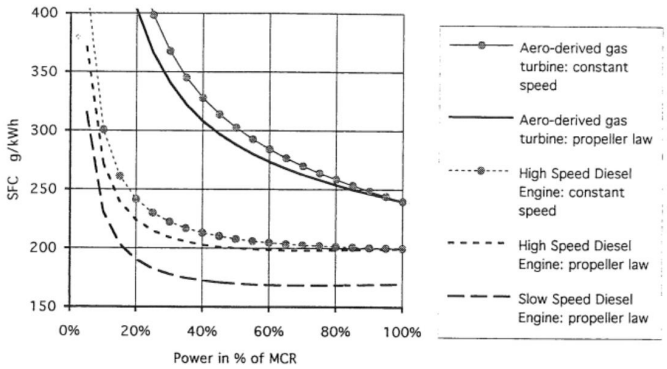

Figure 5.28: Specific fuel consumption curves

From figure 5.27 the general shape of the Specific fuel consumption - Engine brake power curve can be determined. The applicable curve is the 'high speed diesel engine: propeller law' curve from the figure since the speed of the diesel engine is not constant for different propeller loads. This curve shows the shape that is expected for the specific fuel consumption curve.

By comparing the 'high speed diesel engine: propeller law' curve from figure 5.27 with the simulation outputs plotted in figure 5.27, it can be seen that the simulation output seems to follow the shape of the expected specific fuel consumption curve well.

Engine brake power - GPS speed

In figure 5.29 the brake engine power is plotted on the vertical axis and the GPS speed is plotted on the horizontal axis. The engine power of the port-side engine is presented in the left figure with red markers and the engine power of the starboard engine is presented in the right figure with green markers.

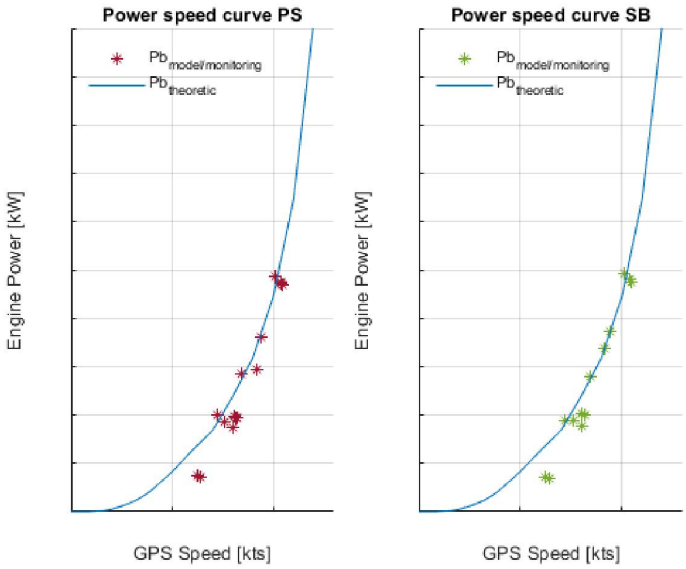

Figure 5.29: Engine brake power - GPS speed

In order to obtain the theoretical expected curve that is shown by a solid blue line in figure 5.29 formula 5.28 is used. First, formula 5.28 is used to obtain the relation between the brake engine power and propeller power. The transmission efficiency and number of engines per shaft are constant and known, so they can be used into the calculation.

$$P_B = \frac{P_p}{\eta_{trm} \cdot k_e} \tag{5.28}$$

Besides the transmission efficiency and amount of engines per shaft, formula 5.28 also includes the propeller power. Formula 5.29 is used to determine the propeller power. The propeller power depends on the constant 'c4' and the propeller rotational speed. The constant 'c4' can be calculated with the use of formula 5.30. Values for the transmission efficiency, relative rotative efficiency and torque coefficient must be assumed. All other variables are known and can be substituted into the formula.

$$P_p = c_4 \cdot n_p^3 \tag{5.29}$$

$$c_4 = \frac{2\pi \cdot \rho \cdot D^5}{\eta_r} \cdot K_Q \tag{5.30}$$

Formula 5.29 also includes the propeller rotational speed to the 3rd power. The propeller rotational speed is calculated with formula 5.31. This formula consist out of a constant 'c3' and the vessel speed. The constant 'c3' is determined by making an assumption for the wake factor and the advance ratio at the design condition.

$$n_p = c_3 \cdot v_s \tag{5.31}$$

$$c_3 = \frac{(1-w)}{J \cdot D} \tag{5.32}$$

Next, formula 5.31 can be substituted into formula 5.29 and finally formula 5.29 can be substituted into formula 5.28 in order to determine the relation between the engine brake power and the vessel speed. Formula 5.33 shows the substituted final formula that can now be used to create a theoretical curve.

$$P_B = \frac{c_4 \cdot (c_3 \cdot v_s^3)}{\eta_{trm} \cdot k_e} \tag{5.33}$$

Now that both the theoretical expectation and simulation outputs are potted in the same figure, they can be compared. For both the port-side and starboard simulation outputs the simulation output seem to follow the theoretical curve closely for higher speeds. For lower vessel speeds the simulation output lies below the expected curve. However, the shape of the simulated outputs seem to be the same as the theoretical curve.

Engine speed - GPS speed

In figure 5.30 the engine speed is plotted on the vertical axis and the GPS speed is plotted on the horizontal axis. As with previous figures, the left side shows the port-side engine speed with red markers and the right side shows the starboard engine speed with green markers.

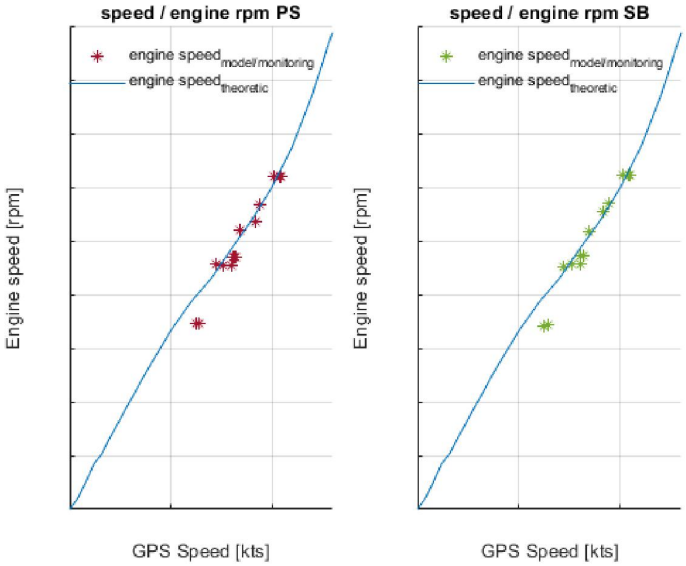

Figure 5.30: Engine speed - GPS speed

The relation between the propeller speed and the vessel speed is given by formula 5.34. This formula includes the constant 'c3' and the vessel speed. The constant 'c3' is determined with the use of formula 5.35. By making an assumption for the wake factor and the advance ratio, a value for the constant 'c3' can be derived.

$$n_p = c_3 \cdot v_s \tag{5.34}$$

$$c_3 = \frac{(1-w)}{J \cdot D} \tag{5.35}$$

Now that the relation between the propeller speed and the vessel speed is known, formula 5.36 can be used to determine the relation between the diesel engine speed and propeller speed. Since a fixed ratio reduction gearbox is present, the ratio between the diesel engine speed and propeller speed is also fixed. Substituting formula 5.36 into formula 5.34 results in formula 5.37 which shows the relation between the diesel engine speed and the vessel speed. Formula 5.37 is used to create the theoretical curve which is shown in figure5.30.

$$n_p = \frac{n_e}{i_{gb}} \tag{5.36}$$

$$n_e = i_{gb} \cdot c_3 \cdot v_s \tag{5.37}$$

Now that both the theoretical expectation and simulation outputs are potted in the same figure, they can be compared. The same can be seen here as the previous paragraph which showed brake engine power plotted against the GPS speed. For both the port-side and starboard simulation outputs the simulation output seem to follow the theoretical curve closely for higher speeds. For lower vessel speeds the simulation output lies below the expected curve. However, the shape of the simulated outputs seem to have the same linear behaviour as the theoretical curve.

Fuel rate - Engine speed

In figure 5.31 the fuel rate is plotted on the vertical axis and the engine speed is plotted on the horizontal axis. As with multiple previous figures, the left side shows the port-side fuel rate with red markers and the right side shows the starboard fuel rate with green markers.

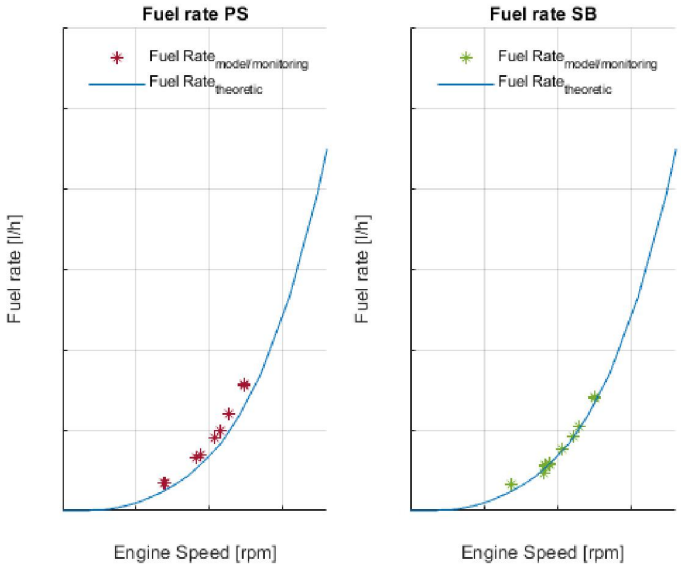

Figure 5.31: Fuel rate - Engine speed

The solid blue line in figure 5.31 shows the prediction of the fuel rate based on theoretical formulas. With formula 5.38 the fuel mass flow can be determined with the use of the specific fuel consumption and the engine brake power. Since the relation between the engine brake power and engine speed is known from previous calculations, the engine speed can be substituted into the formula. The specific fuel consumption is based on an assumption for the creation of the theoretical prediction.

$$\dot{m}_f = sfc \cdot P_B \tag{5.38}$$

$\dot{m}_f$ is expressed in kilogram per hour. In order to compare it with remote logged data which is expressed in litre per hour, the fuel mass flow must also be expressed in litre per hour. Therefore it must be divided by the density of fuel.

Now that both the theoretical expectation and simulation outputs are plotted in the same figure, they can be compared. The fuel rate follows the predicted line well. The fuel rate of the port-side diesel engine seems generally higher than the fuel rate of the starboard diesel engine. This difference is not important in the verification step. The order of magnitude and the shapes seem to match well.

5.4. Calibration

Now that the verification of the model is done, the model calibration is the next step. The model parameters are calibrated in order to increase the overlap between the remote logged data and the model prediction. With the use of an alternative modelling path, output variables can be created and used to take the place of some of the assumptions of the initial propulsion line model.

First, an alternative modelling path is chosen. Since the goal of the calibration is to change the initial propulsion model such way that the simulated outputs will match the remote logged data, it is preferred that the most of the remote logged data is used for calibration. Since alternative paths 5 to 11 use remote logged data for all three external model inputs, those paths are preferred. Besides using the remote logged data, it is also preferred to generate the output variables for the calibration with as less assumptions as possible. Therefore, combining output variables as is done in alternative modelling path 10 and 11, in order to reduce the number of required assumptions is preferred. Since alternative modelling path 11 combines the resistance with the thrust deduction factor and the specific fuel consumption with the transmission efficiency, this path requires the least amount of assumptions. Due to the fact that this path uses the least amount of assumptions and uses remote logged data for all three external inputs, alternative modelling path 11 is used to generate the output variables for the calibration. A debate can be had about the uncertainty in the measurements and therewith about the correctness of the choice. This uncertainty is discussed in more detail in the conclusions and recommendations. Path 11 is presented in figure 5.32.

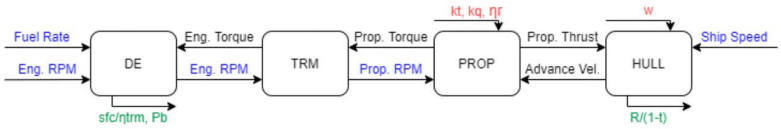

Figure 5.32: Possible Path 11

In modelling path 11 the formulas in the diesel engine, transmission and hull component are rewritten in such way that for all external input variables, the remote logged data can be used. The blue coloured variables in figure 5.32 represent the input variables. Those input variables are:

- Diesel engine Fuel rate
- Diesel engine speed
- Vessel GPS speed

Due to rewriting formulas within component models and by combining multiple output variables together the amount of assumptions reduce. The assumptions made for this modelling path are listed below.

- Thrust and torque coefficients are obtained from the open water propeller diagram of the corresponding propeller.
- Rotative efficiency is assumed to be constant.
- Wake factor is assumed to be constant.

When alternative modelling path 11 is used, the output variables are the engine brake power, the vessel resistance combined with the thrust deduction factor and the specific fuel consumption combined with the transmission efficiency. The combined outputs that are generated by using path 11 are in the form of $\frac{R}{(1-t)}$ and $\frac{sfc}{\eta_{trm}}$. For both combined outputs graphs are made. First the $\frac{R}{(1-t)}$ output is plotted on the y-axis against the GPS vessel speed on the x-axis. Second the $\frac{sfc}{\eta_{trm}}$ output is plotted on the y-axis against the engine power on the x-axis.

Resistance/(1-t) - GPS speed
In figure 5.33 the output containing the combination of the resistance and the thrust deduction factor is plotted on the vertical axis and the GPS speed is plotted on the horizontal axis.

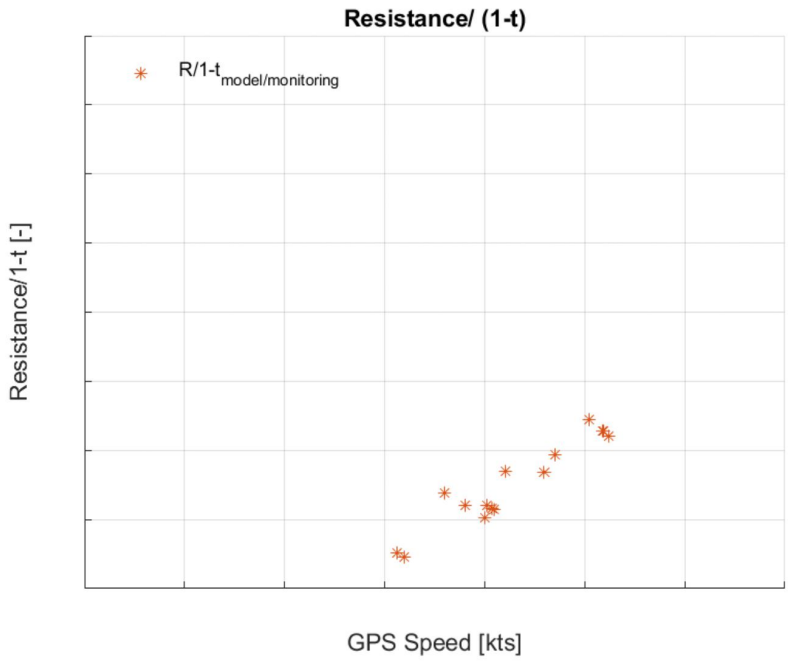

Figure 5.33: Resistance/(1-t) - GPS speed

As mentioned earlier, the goal of the model calibration is to change the initial propulsion model such way that the simulated outputs will match the remote logged data. In order to do so, reducing the amount of assumptions of the initial propulsion model by creating output variables that can take the place of some of the assumptions was proposed. Therefore, making trendlines that match and reproduce the values of the output variables is needed to be able to use it in the place of an assumption.

A trendline is made that fit to the output data of the resistance combined with the thrust deduction factor. This trendline is based on the relation between resistance and vessel speed. Klein Woud & Stapersma [10] state that for relative low speeds it is often acceptable to assume that the resistance is proportional to the square of the vessel speed. Formula 5.39 shows this relation.

$$R = c_1 \cdot v_s^2 \tag{5.39}$$

The combined output variable not only contains the resistance variable but also the thrust deduction factor. However, the thrust deduction factor is assumed to be a constant value. This value of the thrust deduction factor is often assumed to amount 0.06. Now that the resistance is combined with the thrust deduction factor, a value for the thrust deduction factor does not have to be assumed. The assumption that the thrust deduction factor is a constant is enough to be able to use the relation shown in formula 5.39 to make the trendline. The least squares method is used to find the best fit for the set of data points by minimising the sum of the offsets or residuals of points from the plotted curve. A value for 'c1' can be found such that the trendline has the best fit with the data set. This value of 'c1' amounts . The created trendline is presented in figure 5.34.

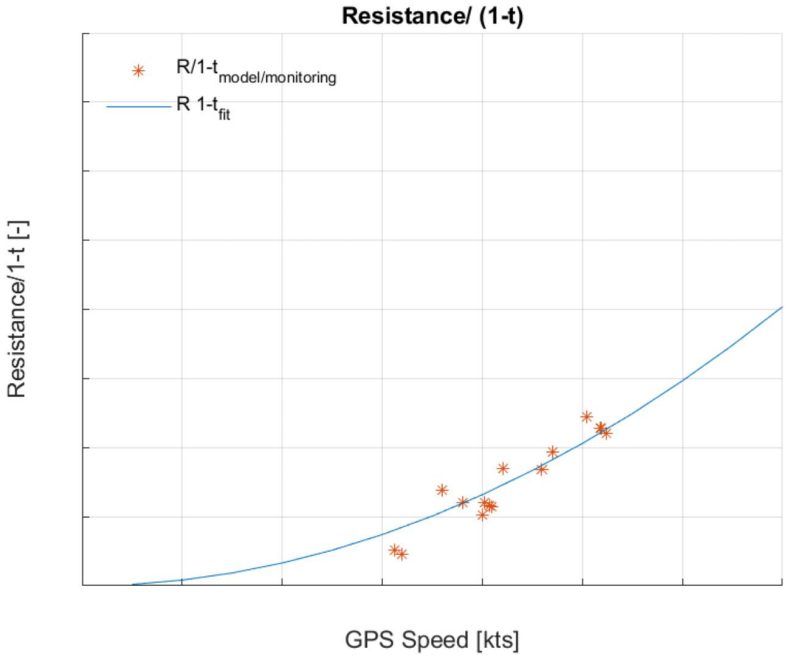

Figure 5.34: Curve fitting: Resistance/(1-t) - GPS speed

Specific fuel consumption/η_{trm} - GPS speed
In figure 5.35 the output containing the combination of the specific fuel consumption and the transmission efficiency is plotted on the vertical axis and the engine power is plotted on the horizontal axis.

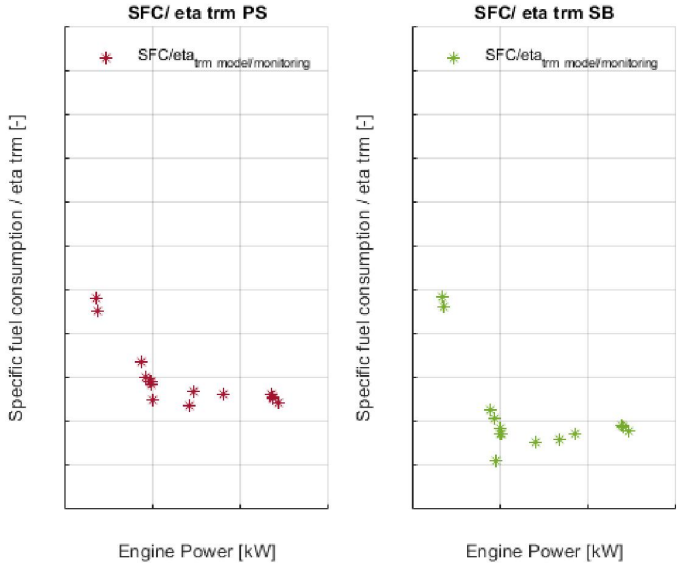

Figure 5.35: Specific fuel consumption/η_{trm} - GPS speed

From the specific fuel consumption combined with the transmission efficiency, both the port-side and starboard data is available. In figure 5.35, a difference between the port-side and starboard combined specific fuel consumption and transmission efficiency variable can be seen. Since the starboard azimuth thruster is identical to the port-side azimuth thruster, the starboard and port-side transmission efficiencies should be the same. The difference seen in figure 5.35 is caused by a difference in specific fuel consumption. One pos-

sible cause for this difference could be that the port-side diesel engine is actually less fuel efficient than the starboard diesel engine, resulting in a higher specific fuel consumption per delivered engine power. Another reason for the difference could be the inaccuracy of the sensor. Fuel sensors tend to be sensitive and therefore often inaccurate. Since both diesel engines are the same, we expect that the specific fuel consumption of those engines have to be the same. So to make a good fitting trendline for sfc/(η_{trm}) that is independent from the port or starboard side, the output values of the combined variable sfc/(η_{trm}) are averaged.

The combined sfc/(η_{trm}) variable consist out of two variables. For both variables methods are available to match a trendline with the output data. First a trendline for the transmission efficiency is made. This is done with a method produced by Godjevac, Drijver, de Vries and Stapersma [11]. Written in normalised notation, the torque loss can be determined with formula 5.40.

$$M^*_{loss} = a \cdot M^*_{in} + b \cdot N^*_{in} + c \tag{5.40}$$

Formula 5.40 consists out of three normalised values and three fit coefficients.M^*_{loss} is the normalised torque loss of the gearbox, 'a' is the fit coefficient related to the torque, M^*_{in} is the normalised torque going from the engine into the gearbox, 'b' is the fit coefficient related to the shaft speed, N^*_{in} is the normalised shaft speed going into the gearbox and 'c' is the fit coefficient related to the constant torque loss. Since the output variable is a combined term including this gearbox efficiency and the specific fuel consumption, a formula for the trendline of the specific fuel consumption is made next. The fit coefficients are determined when both trendlines are combined later.

Now that the formula that can be used to make a trendline of the transmission efficiency is discussed, the making of a trendline for the specific fuel consumption is addressed. Stapersma [48] described the typical shape of the specific fuel consumption curve with a formula. This formula is presented by formula 5.41.

$$SFC^* = \frac{FC^*}{P^*} = \frac{1 - d(1-P^*) + e(1-P^*)^2}{P^*} \tag{5.41}$$

Like with formula 5.40, normalised values and fit coefficients are used to shape the curve of the specific fuel consumption. With formula 5.41 the normalised specific fuel consumption (SFC^*) is calculated. This normalised specific fuel consumption is the fraction of the nominal specific fuel consumption. The nominal specific fuel consumption can be read from the diesel engine envelope presented in figure 5.26. At the point where the blue coloured theoretical expected propeller load line crosses the right boundary of the diesel engine envelope, a specific fuel consumption value of $\frac{g}{kWh}$ can be read from the figure. For this calculation, the normalised engine power (P^*) is required and the two fit coefficients 'd' and 'e' determine the shape of the trendline.

With a formula for the estimation of the gearbox losses and a formula for the estimation of the specific fuel consumption described, they can now be combined. Since the combined output variable is the specific fuel consumption divided by the transmission efficiency, the formulas regarding the specific fuel consumption and gearbox efficiency must be divided the same way. The least squares method is used to find the best fit for the set of data points by minimising the sum of the offsets or residuals of points from the plotted curve. With the use of the least squares method, the coefficients 'a', 'b' and 'c' for the gearbox efficiency and the fit coefficients 'd' and 'e' for the specific fuel consumption, can be found such that the combined trendlines has the best fit with the data set. The values for 'a', 'b', 'c', 'd' and 'e' are presented in table 5.3.

a	
b	
c	
d	
e	

Table 5.3: Values for the fit coefficients

In order to use the least squares method, the Excel solver is used. Since the Excel solver is used, multiple different values for the fit coefficients may be possible in the finding of the best fit of the trendline and the data points. In order to check if the values for the fit coefficients are indeed giving a trendline that has the best fit, the coefficients are checked in two ways.

First, the separate trendlines are examined. Both the trendline for the transmission efficiency with the fit coefficients 'a', 'b' and 'c' and the trendline for the specific fuel consumption with the fit coefficients 'd' and 'e' are analysed.

Second, the solution for the fit coefficients is checked on whether the solution is at a local or global minimum. The local minimum represents a minimum within a small area of the domain, whereas the absolute minimum of the whole domain is the global minimum. In order to check if the solution for the fit coefficients is the best solution, multiple start values for the solver are inserted. By changing the starting location of the solver, the best solution can be determined.

Now that all fit coefficients are determined, the trendline that fits the combined output variable sfc/(η_{trm}) is made. The trendline for this combined output variable is shown in figure 5.36. The red coloured markers is the combined output data from the initial model in combination with the use of alternative modelling path 11. The solid blue line is the trendline that has the best fit to this data.

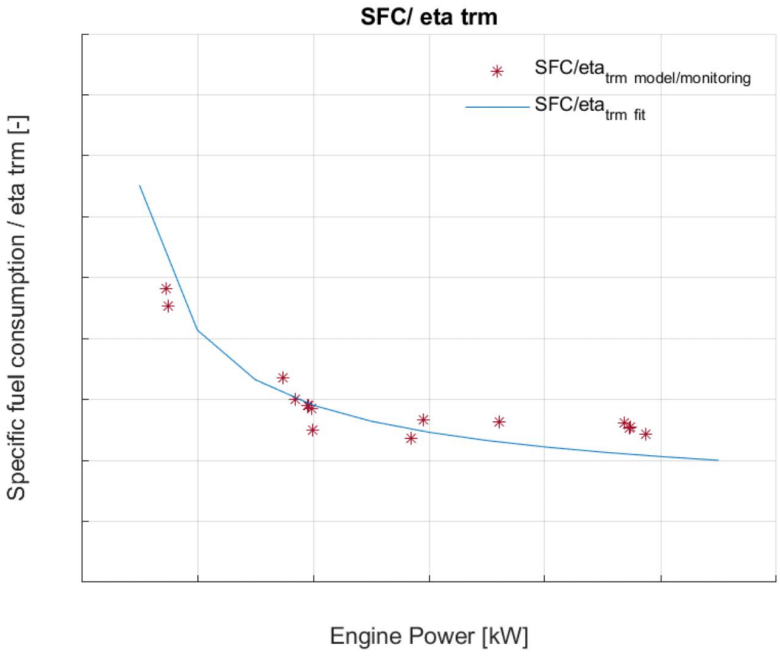

Figure 5.36: Curve fitting: Resistance/(1-t) - GPS speed

Using trendlines for calibration
Now that the trendlines for both combines output variables are made, they can be implemented to increase the overlap between the remote logged data and the model prediction and therewith to improve the model. When the initial model is used to simulate the propulsion system of the RSD tug, a lot of assumptions must be made. By replacing the assumptions for resistance, thrust deduction factor, specific fuel consumption and transmission efficiency with the two created trendlines, only 4 of the 8 assumptions for the initial model are left. The left over variables that need assumptions in the initial model are the thrust coefficient, the torque coefficient, the wake factor and the relative rotative efficiency.

With the use of lookup tables, the formulas for the trendlines are implemented into the initial propulsion line model. The initial propulsion line model has three output variables which are the diesel engine speed, diesel engine power and ship speed. The initial model needs the fuel rate as input variable to calculate the output variables. This means that by performing a simulation with the initial and improved initial propulsion model, the output variables can be compared with the remote logged data.

A comparison between the initial propulsion line model, the calibrated model and the remote logged data is made in order to see if the overlap between the remote logged data and the model is increased. The diesel engine speed and vessel speed are output variables of both models and are also remote logged variables. The output of these variables from the initial and calibrated model can directly be compared with the remote measured data. With the use of the steady state method, discussed in chapter 4, the vast amount of data is reduced to only 15 steady state operating points. For each steady state operating point, the remote logged value, the output from the initial model and the output from the calibrated model are compared. Figure 5.37 shows the output from the initial model, the output from the calibrated model and the remote logged data for the port-side diesel engine speed. Figure 5.38 shows the comparison between the initial propulsion line model, the calibrated model and the remote logged data for the starboard diesel engine speed. Finally, figure 5.39 shows the comparison between the initial propulsion line model, the calibrated model and the remote logged data for the vessel speed. The red markers represent the 15 steady state operating points, extracted from the remote logged data. The blue markers represent the calculated values from the initial model and the green markers represent the calculated values from the calibrated model. Since 15 steady state operating points are compared, the x- axis contains the index numbering from 1 to 15.

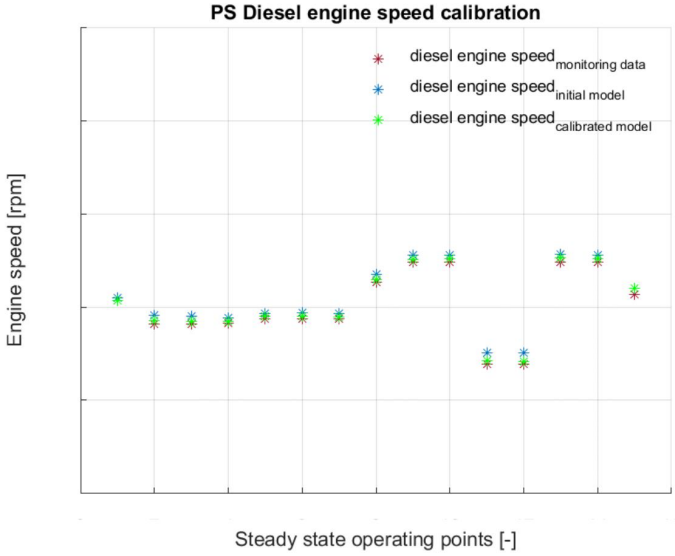

Figure 5.37: PS diesel engine comparison of the remote logged data, the initial model and the calibrated model

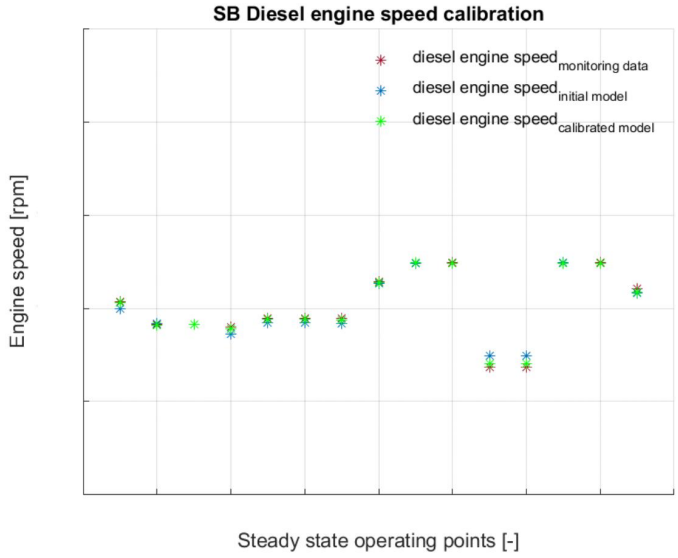

Figure 5.38: SB diesel engine comparison of the remote logged data, the initial model and the calibrated model

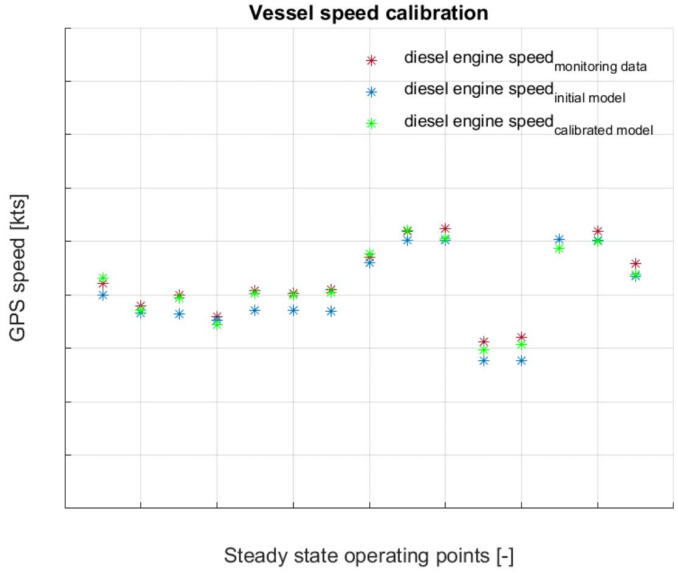

Figure 5.39: Vessel speed comparison of the remote logged data, the initial model and the calibrated model

From figures 5.37, 5.38 and 5.39 the conclusion can be drawn that the overlap between the remote logged data and the output of the calibrated model is better than the overlap between the remote logged data and the output of the initial model. This means that the calibrating method did increase the accuracy of the model. A closer look at figure 5.37 shows that the output values from the initial model are consistent below the values of the remote logged data. The output values from the calibrated model are more closer to the remote logged data.

Showing the initial model, the calibrated model and remote logged data for the 15 steady state points is useful to compare the output values and to check if the overlap between the remote logged data and the output of the model is improved due to the calibration. However, plotting these values for every steady state operating point does not show the behaviour of the model and the difference between the initial model and calibrated model. Instead of using 15 input values for the fuel rate, a range of values from 0 to the nominal value of the fuel rate is used in order to create output values for the full range of the diesel engine speed, diesel engine power and vessel speed. In order to evaluate the calibration even further, the full range of values for the output variables are plotted against each other. The 15 data steady state operating points of the corresponding variables are also included in these plots. The following plots are made:

- Engine speed - GPS speed
- Fuel rate - Engine speed
- Engine brake power - GPS speed
- Engine brake power - GPS speed (plotted over the engine envelope)

In figure 5.40 the diesel engine speed is plotted on the vertical axis and the vessel speed is plotted on the horizontal axis. The blue solid line represents full range of output values from the original model. The red solid line shows the output values from the calibrated model. The blue markers are the steady state operating points of the port-side diesel engine speed. The yellow markers are the steady state operating points of the starboard diesel engine speed. Figure 5.41 shows the fuel rate on the vertical axis and the engine speed on the horizontal axis with the same colour notation as figure 5.40. In figure 5.42 the engine power is presented on the vertical axis and the vessel speed is presented on the horizontal axis. Finally, in figure 5.43 the engine power is presented on the vertical axis and the engine speed is presented on the horizontal axis. The engine power in this figure is plotted over the engine envelope.

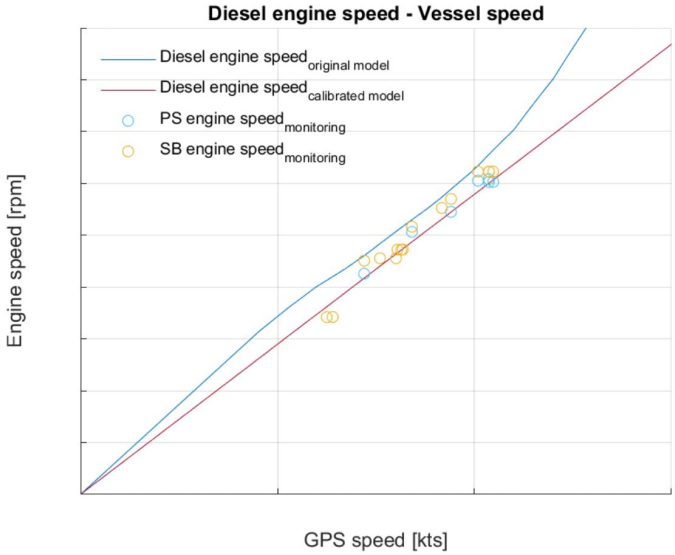

Figure 5.40: Comparison of the initial and calibrated model using an 'Engine speed - GPS speed' plot

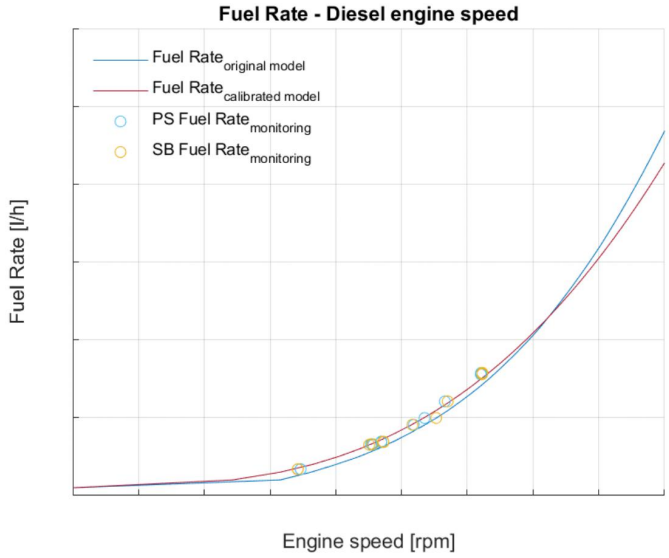

Figure 5.41: Comparison of the initial and calibrated model using a 'Fuel rate - Engine speed' plot

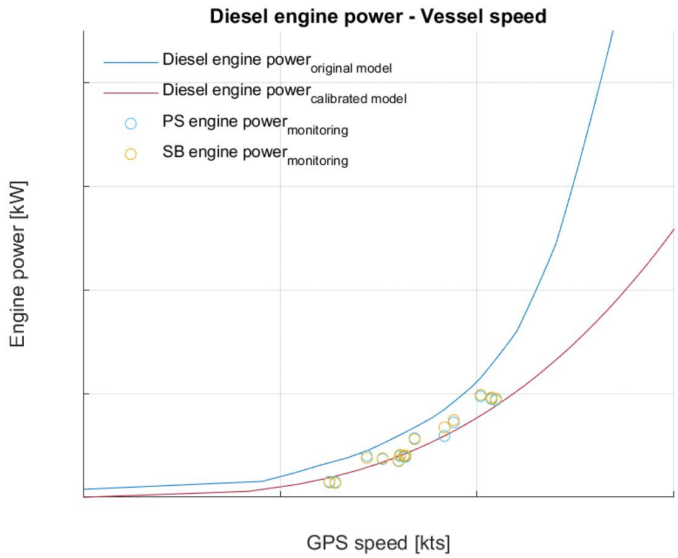

Figure 5.42: Comparison of the initial and calibrated model using an 'Engine power - GPS speed' plot

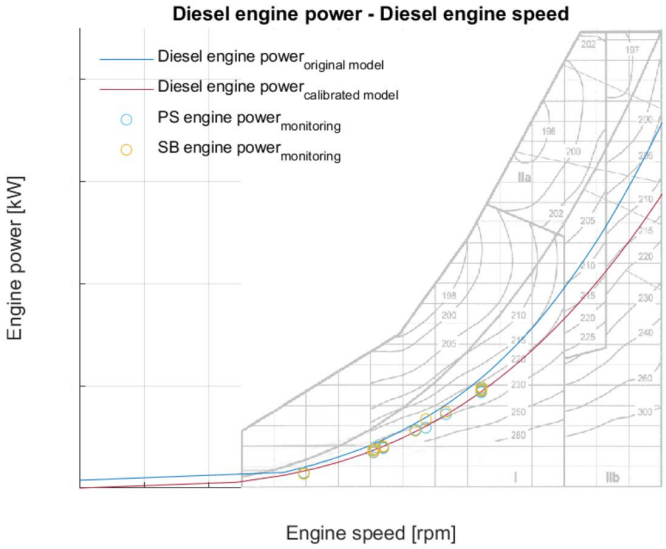

Figure 5.43: Comparison of the initial and calibrated model using an 'Engine power - Engine speed' plot in the engine envelope

As with figures 5.37 to 5.39 the conclusion can be drawn that the calibrated model has a better overlap between the remote logged data than the initial model. The improvement of the model was expected since the calibrated model is based on less assumptions and more on the remote logged data.

In figure 5.40 can be seen that there is only remote logged data for the vessel speed in the range from 6 to 10.5 knots. In figure 5.41 can be seen that there is only remote logged data of the diesel engine in the rotational speed range of 700 to 1250 rpm. Since the entire range of the diesel engine rotational speed lies between the lower speed limit of 500 rpm and the upper speed limit of 1800 rpm, the range where remote logged data is available is very limited. The same holds for the remote logged data of the vessel speed. If only sailing forward is considered, the entire vessel speed range lies between zero and the maximum speed of 13.8 knots. Remote logged data of the vessel speed is only available for 6 to 10.5 knots.

Since the calibrating is done with these remote logged values in those limited ranges, the model is in fact only calibrated for values between these limits. This means that the outputs from the model outside this range can not be considered accurate and calibrated. In figure 5.42 can be seen that above the limited range of the remote logged data the lines representing the initial model and calibrated model diverge. Since no remote logged data is available in the area where those lines diverge, the accuracy of neither of those lines can be determined.

5.5. Validation

The last step is the validation of the model. In order to perform the validation, independent remote logged data is required. This can be obtained in two ways. The first possibility is to use the remote logged data from only one vessel. When data originates from one vessel, some of the measurement must be used for the verification and calibration step, while the rest of the data is used for validation purposes. The other possibility is to use remote logged data from one vessel solely for verification and calibration purposes, while the remote logged data from another vessel is used for the validation. If two different vessel types are chosen, the application of the model on different vessel types is tested.

The available remote logging data for this project originates from six vessels. Those vessels are all tugs and three of them are even of the same series. since we have data from multiple vessels of the same series, the decision is made to use remote logged data from another vessel for validation purposes only. This way more data can be used for calibration, which can improve the accuracy of the model.

Remote logged data from the RSD tug with yardnumber 515002 is used in the same manner as the remote logged data from the tug with yardnumber 515001 was used. First, the data is loaded and processed into data which can be used further in the process. All steady state data points are extracted from this data. Thereafter, the same steady state criteria as for the 515001 is applied to the new data to obtain the steady state operating points of the new vessel. The steady state operating points from the new data for the vessel speed, diesel engine speed, propeller rotational speed and fuel rate are shown in table 5.4. Since verification and calibration of the model is only done with the first set of data points, the new set of data can solely be used for validation purposes. The validation is performed, the same way as the analysis of the calibration was done. The remote logged validation data is compared with the values of the output variables of the initial and the calibrated model.

GPS Speed [kts]	PS DE [rpm]	SB DE [rpm]	PS FR [l/h]	SB FR [l/h]	PS Prop [rpm]	SB Prop [rpm]

Table 5.4: Validation data steady state operating points

With the use of the method for obtaining the steady state data, the data of the RSD tug with yardnumber 515002 is reduced to only 5 steady state operating points. For each steady state operating point, the remote logged value, the output from the initial model and the output from the calibrated model are compared.

Figure 5.44 shows the output from the initial model, the output from the calibrated model and the remote logged validation data for the port-side diesel engine speed. Figure 5.45 shows the comparison between the initial propulsion line model, the calibrated model and the remote logged validation data for the starboard diesel engine speed. Finally, figure 5.46 shows the comparison between the initial propulsion line model, the calibrated model and the remote logged validation data for the vessel speed. The red markers represent the 5 steady state operating points, extracted from the remote logged data of the RSD tug with yardnumber 515002. The blue markers represent the calculated values from the initial model and the green markers represent the calculated values from the calibrated model. Since only 5 steady state operating points are compared, the x-axis contains the index numbering from 1 to 5.

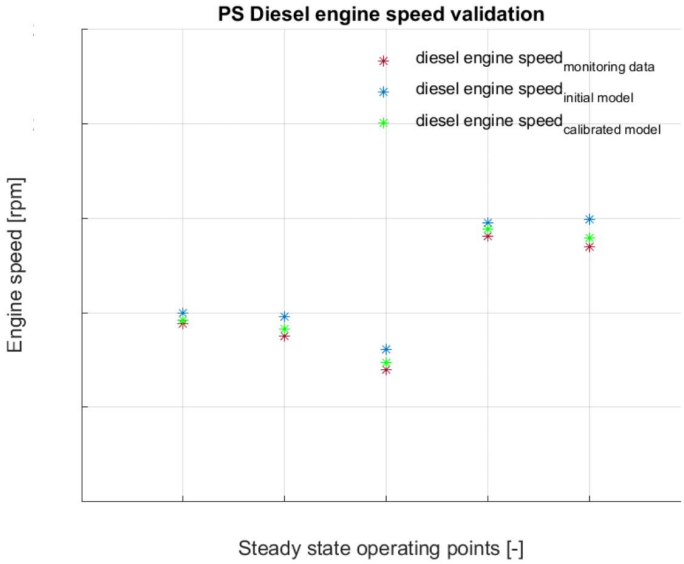

Figure 5.44: PS diesel engine comparison of the validation data, the initial model and the calibrated model

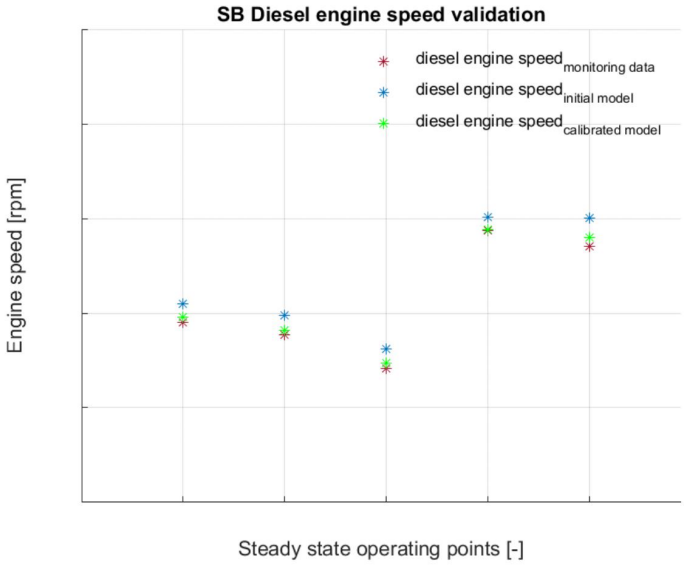

Figure 5.45: SB diesel engine comparison of the validation data, the initial model and the calibrated model

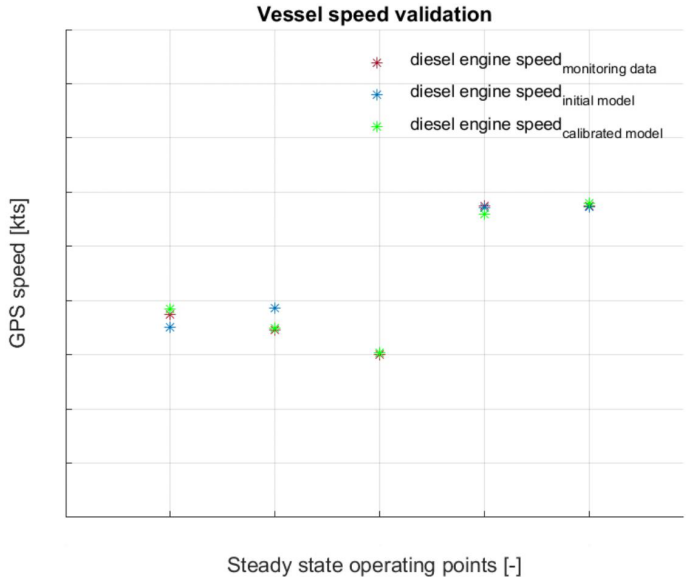

Figure 5.46: Vessel speed comparison of the validation data, the initial model and the calibrated model

When the values in figures 5.44, 5.45 and 5.46 are examined, it can be seen that the five steady state operating points lay closer to the calibrated model than to the initial model. This means that for a completely new data set, the calibrated model predicts the remote logged data better than the initial model. Like with the figures presented in the section regarding the calibration, plotting these values for 5 steady state operating points does not show the difference between the initial model and calibrated model with respect to the validation data. During the calibration of the model, the output variables are plotted and presented for the full range of the model and those variables are plotted against each other in the following plots:

- Engine speed - GPS speed
- Fuel rate - Engine speed
- Engine brake power - GPS speed
- Engine brake power - GPS speed (plotted over the engine envelope)

In figure 5.47 the diesel engine power is plotted on the vertical axis and the vessel speed is plotted on the horizontal axis. The blue solid line represents full range of output values from the original model. The red solid line shows the output values from the calibrated model. The blue markers are the 5 steady state operating points of the port-side diesel engine speed obtained from the reduction of the remote logged data of the RSD tug with yardnumber 515002. The yellow markers are the steady state operating points of the starboard diesel engine speed. Figure 5.48 shows the engine speed on the vertical axis and the vessel speed on the horizontal axis with the same colour notation as figure 5.47. In figure 5.49 the engine power is presented on the vertical axis and the engine speed on the horizontal. This plot is made on top of the engine envelope. Lastly, in figure 5.50 the fuel rate is presented on the vertical axis and the engine speed is presented on the horizontal axis.

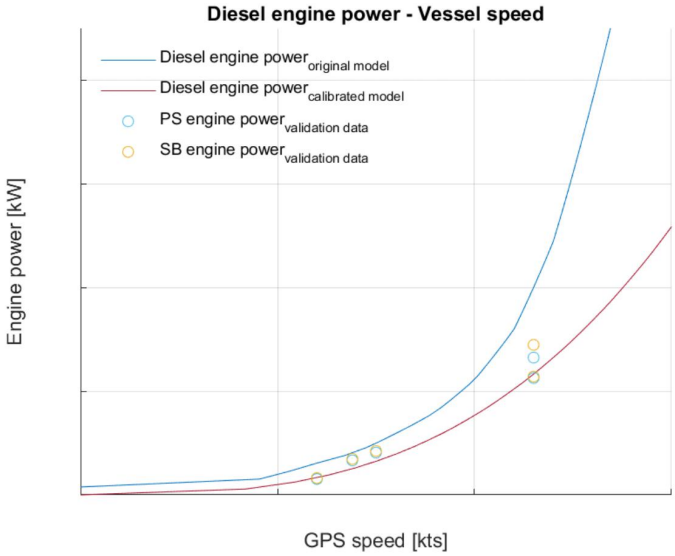

Figure 5.47: Comparison of the validation data with the initial and calibrated model using an 'Engine power - GPS speed' plot

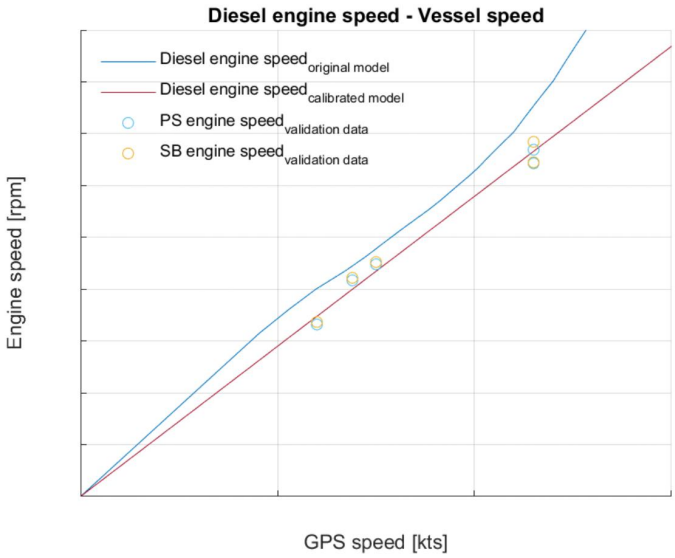

Figure 5.48: Comparison of the validation data with the initial and calibrated model using an 'Engine speed - GPS speed' plot

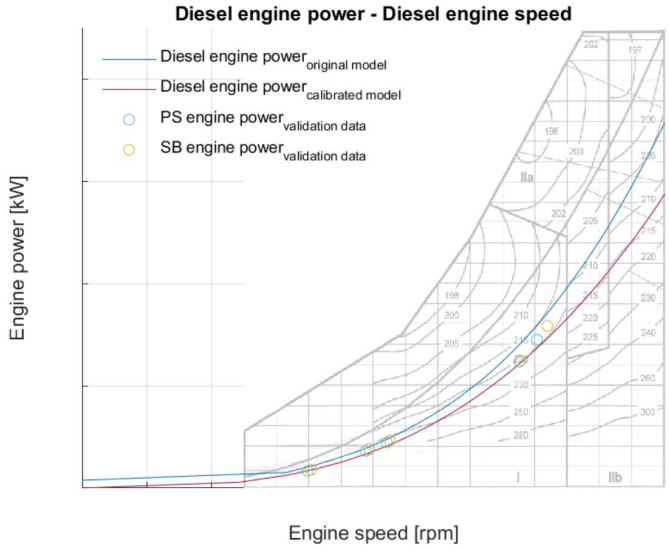

Figure 5.49: Comparison of the validation data with the initial and calibrated model using an 'Engine power - Engine speed' plot

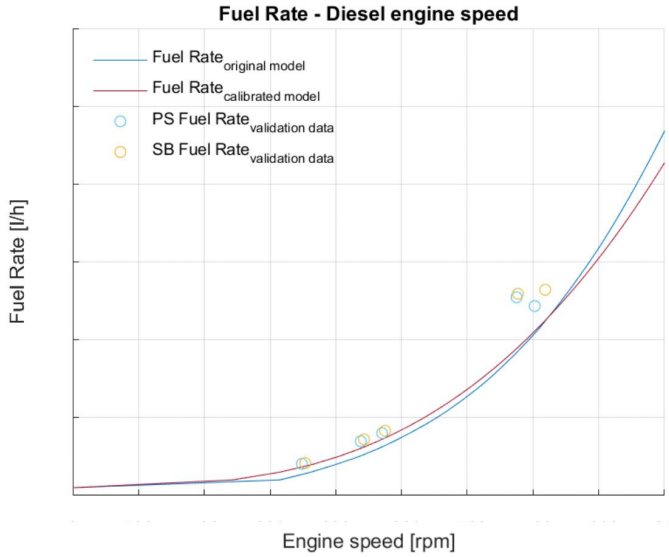

Figure 5.50: Comparison of the validation data with the initial and calibrated model using an 'Fuel rate - Engine speed' plot

In figure 5.48 can be seen that the remote logged data for the validation, overlaps with the red line representing the output of the calibrated model. When figure 5.47, 5.49 and 5.50 are examined, it can be seen that the overlap between the remote logged data for the validation and the output of the calibrated model holds for engine speeds between 700 and 900 rpm. in figure 5.50, the steady state operating points around a diesel engine speed of 1400 rpm are above the output of the model. This means that the by the calibrated model predicted fuel rate is less than the actual measured values. In the previous section, where the calibration of the model is done, the conclusion was drawn that the range of the available steady state operating points was limited and therefore the calibrated model can only be considered accurate for values within this limited range. Since the steady state operating points of the diesel engine speed of the validation data is around 1400 rpm, which is above the range explained in the calibration, a possibility of an inaccuracy of the calibrated model can be expected. Therefore the conclusion can be drawn that the calibrated model can only be used within the same range as the remote logged data that is used for the calibration.

6

Conclusions and recommendations

In this chapter conclusions and recommendations are discussed. First, conclusions are discussed regarding the main steps of the project, the data loading and processing, the data reduction and the modelling step including the verification, calibration and validation. Thereafter the research question and corresponding sub- research questions which were discussed in the introduction are answered. After the conclusions are discussed, recommendations for future research regarding the topic of this theses are discussed.

6.1. Conclusions

The initial plan was to use the remote logged data for a dynamic propulsion line model. By analysing and loading of the remote logged data a couple of limitations are discovered. One limitation is the amount of sensors that can be used to gather usable data for the propulsion line model. The majority of sensor data is about alarms, system errors, hatches, tank levels and electric systems. Only a few sensors are about the propulsion system. The other discovered limitation is that due to data transfer limitations, the maximum achievable sampling time is 10 seconds.
Due to the limited amount of sensors that are about the propulsion system and the maximum achievable sampling time of 10 seconds, building dynamic models is not possible at this stage with the available remote logged data.

The available remote logged data regarding the propulsion system is used by successfully extracting steady state operation points and use them for a simple non- dynamic propulsion line model. In the data reduction step 15 steady state operating points for seven different variables are extracted from the vast amount of data. Since sensor data regarding weather and water conditions are also available. With the use of this data it is possible to make criteria were the steady state data must comply with. By applying criteria in the form of maximum and minimum limits for water and weather data, the water and weather influences that have a significant effect on the vessel can be omitted from the data. By doing so, the water and weather effect can also be omitted from the model, resulting in a less complex model of the propulsion line.

By rewriting equations within the component blocks of the propulsion line model, input variables, output variables and assumptions can be switched. This way, multiple alternative modelling paths are made. Those paths were successfully used in the verification and calibration of the model. Using the alternative modelling paths made it possible to use the remote logged data in a new way to create model outputs for parameters that can be compared with theoretical calculations for model verification. With the use of alternative modelling paths, parameters can be combined. By calibrating the model with the use of these combined parameters, the simulated outputs not only have a better overlap with the remote logged data, but also simulate these values more accurate and based on less assumptions. Due to this calibration method were the combined parameters are calibrated, the model is based on three of the original eight assumptions.

Data from another vessel is used to validate the model. By comparing the simulation outputs from the initial model, the calibrated model and the remote logged data from this new vessel, the conclusion was drawn that the calibrated model overlaps the remote logged data better than the original model. The application of the discussed method to use the remote logged data for calibration purposes, resulted in an improvement of the propulsion line model.

In the introduction a main research question was given. This main research question was divided into multiple sub- research questions. Those sub- research questions that were discussed in the introduction are listed below. An answer to each question is given accordingly.

1. **How is the remote logged data collected and what processing must be done in order to use it?**
   Applying remote logged data for modelling purposes is not as straightforward as initially thought. Processing raw sensor measurements into data that can be used for modelling, verification, calibration or validation requires a lot of data processing. Analysing the remote logged data resulted in a selection of parameters that can be used for further processing. This further processing include the application of a suggested and discussed method to extract the steady state operating points from the vast amount of available remote logging data. By applying the data processing and steady state method, it becomes possible to use the remote logged data for verification, calibration and validation purposes

2. **What level of model complexity can be achieved by using the remote logged data and what corresponding variables are required?**
   As mentioned earlier, the remote logged data does have limitations. Since the frequency of data that can be transferred from vessel to shore is limited to only one sample per 10 seconds, the data cannot be used for dynamic models. Since dynamic models often include accelerations as for instance the acceleration of the propeller, shaft, diesel engine speed and sometimes even accelerations within the diesel engine, data with a frequency of 0.1 Hertz cannot be used to capture these accelerations. In previous chapters is shown that the remote logged data can successfully be used for a steady state model. The complexity of this steady state model depends on the available parameters. More available and a higher variety of remote logged sensors can increase the complexity of the model. From the data analysis the available sensors regarding the propulsion system are determined. The following list shows the variables that are available for further use.

   - GPS speed
   - PS & SB Diesel engine speed
   - PS & SB Propeller speed
   - PS & SB Propeller speed setpoint
   - PS & SB Fuel rate

   A model is made that use variables that matches the listed variables. Since the amount of variables in this list is limited, the level of complexity of the matching model is also limited. A simple model is made where engine speed, propeller speed, fuel rate and vessel speed are used within the model. Apart from the listed variables, eight assumptions are required for this model.

   If more data, such as temperatures and pressures within the diesel engine, rotational speed and pressures of the turbine and compressor and torque and power information between components are available, the complexity of the propulsion line model can be increased. Increasing the logging frequency makes it possible to add dynamic behaviour to the model.

3. **To what extend is the remote logged data suitable for the calibration and validation of the model?**
   Using the proposed and discussed method where alternative modelling paths are applied, it is possible to combine and create model output variables that can be used for the calibration and verification of the propulsion line model. 15 steady state operating points are used to calibrate the combined parameter and therewith improve the overlap between the model output and remote logged data and reduce the amount of assumptions needed for the model. Comparing the calibrated model with the original model and the remote logged data showed an improvement in accuracy of the model. In figure 5.42 the initial model, the calibrated model and the 15 steady state operating points from the remote logged data is shown. In this figure can be seen that the 15 steady state operating points are in the range from

6 to 10.5 knots vessel speed, which is just a small part of the total available speed range of the vessel. Since the calibration was done with the use of these 15 steady state operation points with a limited range, the calibrated model can only be considered accurate for values within this limited range.

4. **Can the application of validated models improve the accuracy and/or efficiency of the HIL tests?** Applying the discussed method to obtain the steady state operating points, and use them in combination with alternative paths to calibrate five combined variables result in a model that overlaps the remote logged data better than the initial model, and therefore we can say the calibrated and validated model is improved with respect to the initial model. With the calibration method it is possible to simulate the propulsion line more accurate than the initial model and also with less assumptions. Instead of eight assumptions, only four assumptions are left. Those four assumptions are the torque and thrust coefficients from the open water propeller diagram, the relative rotative efficiency and the wake factor. Using the discussed method in this thesis resulted in an improved model where the combined parameters sfc/η_{trm} and R/(1-t) are estimated and based on the remote logged data.

   If it becomes possible to log data with an higher frequency and with a higher variety, then the method can be applied to a more complex and dynamic model. When a dynamic model is considered, the parameters 'Vessel Mass' and 'Shaft line inertia' need to be determined. With an alternative path they may be combined in order to reduce the amount of assumptions.

6.2. Recommendations

In figure 5.40 we see the that the remote logged data that is used for the calibration has a vessel speed range of 7 to 11 knots and a diesel engine speed range of 700 to 1200 rpm. In the section where the calibration is discussed, the conclusion is drawn that the calibrated model is only valid for values within the range of the remote logged data, used for the calibration.

By increasing the overall logging period and therefore the amount of data, the chance of finding more steady state operating points increases. More steady state operation points over a larger range will result in a better calibrated model that is valid over a larger range. However, it seems that the majority of the steady state operating points are found around the cruise speed of the vessel. Since the steady state criteria only allow free sailing steady state operating points and most of the time this free sailing occurs when the vessel is on transit between harbour and a vessel that requires assistance, most of the steady state operating points are found around the cruise speed of the vessel. A method to obtain steady state operating points for vessel and engine speeds over the whole range is by deliberately sailing in a straight line at multiple different specified speeds for a short period. The duration must be long enough for the whole system to get in steady state. By starting slow and increasing the vessel speed in multiple steps, steady state operating points can be generated over the full speed range of the vessel and the diesel engine. This test must be performed in an area where there is no current, were no high waves are present, the water is deep enough to avoid shallow water effects and there is no hard wind. Otherwise, applying the steady state criteria will remove those steady state measurements.

The data that is used for this project is downloaded from the Damen digital portal. This means that data with a fixed amount of timestamp is used in the project. When a direct link to the database can be established, instead of downloading csv files, adjusting the amount of data can be done more easily. This way it becomes possible to use more data for calibration and validation purposed and therefore increase the accuracy of the model.

The steady state criteria are based on the water depth, wind speed and rate of turn. To improve the method of finding steady state operating points, the amount of criteria can be increased. When a sensor is available to measure the speed through water, it becomes possible to use this sensor alongside the GPS speed measurements to determine the water current. Wave height and diction influence the resistance of the vessel. If a sensor is present that can log the wave height, a maximum wave height can be added to the criteria. With the current criteria it may be possible that the vessel moves in a straight line, but with the thruster not pointing in the same direction as the course. The vessel speed can then deviate from the expected speed due to fact that the overall delivered thrust is not pointing in the direction in which the vessel is travelling. Another scenario where the vessel speed deviates from the expected speed is when the tug is towing another vessel. If a sensor is present that logged when the vessel is towing, this can be included into the criteria.

When the model is calibrated, alternative modelling path 11 is used. This path is chosen since it required the least amount of assumptions and the assumptions that are left are considered to be variables that can be correctly assumed. A sensitivity study to the effect of a change of an assumption on different outputs variables of the model could make clear which assumptions play a more important role than others. This way, the choice for alternative modelling path 11 for the calibration can be criticised.

To validate the model, remote logged data from another vessel of the same series and the same vessel type is used. The results from the calibration show that the calibrated model overlaps the measured data better than the initial model and the results from the validation show that the calibrated model predicts the measured data from another vessel better than the initial model. When data from different types of vessels is used in the model validation, the modularity of the model can be tested and the application of the model becomes possible for multiple different hardware-in-the-loop tests.

A

Appendix

A.1. Sensor list

AQM PS ACTIVE CONTROL STATION	timestamp	TANK 2 PERCENTAGE ALARM HIGH	SERVICE BATTERY CHARGING CURRENT
AQM PS AUTOPILOT CONTROL STATE	yardnumber	TANK 2 PERCENTAGE ALARM HIGH HIGH	SERVICE BATTERY VOLTAGE
AQM PS DP/JOYSTOCK CONTROL STATE	SPEEDLOG (VBW) LONGITUDIAL WATER SPEED	TANK 2 PERCENTAGE ALARM LOW	SHORE ACTUAL KVAR LOAD
AQM PS LOAD LIMIT CURRENT MAX ALLOWED	ECHO (DPT) DEPTH IN METERS	TANK 2 PERCENTAGE ALARM LOW LOW	SHORE ACTUAL KW LOAD
AQM PS LOAD LIMIT SET VALUE	METEO (MWV) SPEED REL. TO VESSEL HEADING	TANK 2 WEIGHT	SHORE AVAILABLE KVAR CAPABILITY
AQM PS LOAD MEASUREMENT ACTUAL VALUE	METEO (MWV) WIND REL. TO VESSEL HEADING	TANK 3 INHIBIT HIGH	SHORE BREAKER CLOSED
AQM PS PITCH CMND SET VALUE	METEO (MWV) WIND TRUE TO VESSEL HEADING	TANK 3 INHIBIT HIGH HIGH	SHORE CB TRIPPED (ANY/ALL CAUSE)
AQM PS PITCH MEASUREMENT ACTUAL VALUE	METEO (XDR) BAROMETRIC PRESSURE	TANK 3 INHIBIT LOW	SHORE DISPLAY - GENERATOR COSPHI
AQM PS PROPELLER RPM ACTUAL VALUE	METEO (XDR) HUMIDITY	TANK 3 INHIBIT LOW LOW	SHORE IO-BOARD NOT PRESENT
AQM PS RPM COMMAND SET VALUE	METEO (XDR) TEMPERATURE	TANK 3 PERCENTAGE ALARM HIGH	SHORE IOBOARD/DISPLAY -OUT BUS FREQ
AQM PS RPM MEASUREMENT ACTUAL VALUE	GPS (PSAT) HEADING - GPS DERIVED	TANK 3 PERCENTAGE ALARM HIGH HIGH	SHORE IOBOARD/DISPLAY -OUT BUS VOLT
AQM PS SLIPPING CLUTCH CMND SET VALUE	GPS (PSAT) PITCH	TANK 3 PERCENTAGE ALARM LOW	SHORE IOBOARD/DISPLAY -OUT GEN CB
AQM PS STEERING COMMAND SET VALUE	GPS (PSAT) ROLL	TANK 3 PERCENTAGE ALARM LOW LOW	SHORE IOBOARD/DISPLAY -OUT GEN FREQ
AQM PS STEERING MEAS. ACTUAL VALUE	GPS [ROT] RATE OF TURN	TANK 3 SPECIFIC GRAVITY	SHORE IOBOARD/DISPLAY -OUT GEN VOLT
AQM SB ACTIVE CONTROL STATION	GPS (ROT) STATUS (A=65/V=86)	TANK 3 WEIGHT	SHORE PROGRAM NOT RUNNING
AQM SB AUTOPILOT CONTROL STATE	GPS (VTG) COURSE OVER GROUND - TRUE	TANK 4 INHIBIT HIGH	START BATTERY CHARGING CURRENT
AQM SB LOAD LIMIT CURRENT MAX ALLOWED	GPS (VTG) SPEED OVER GROUND (KNOTS)	TANK 4 INHIBIT HIGH HIGH	START BATTERY VOLTAGE
AQM SB LOAD LIMIT SET VALUE	GYRO (HDT) HEADING	TANK 4 INHIBIT LOW	Winch - Brightness of Touch Screen
AQM SB LOAD MEASUREMENT ACTUAL VALUE	GYRO (ROT) RATE OF TURN	TANK 4 INHIBIT LOW LOW	Winch - Engine Speed 1 ME PS
AQM SB PITCH CMND SET VALUE	GYRO (ROT) STATUS (A=65/V=86)	TANK 4 PERCENTAGE ALARM HIGH	Winch - Engine Speed 2 ME SB
AQM SB PITCH MEASUREMENT ACTUAL VALUE	MAGNETIC COMPAS (HDG) DEV. (E=69/W=87)	TANK 4 PERCENTAGE ALARM HIGH HIGH	Winch - Hydraulic Oil level low / to low
AQM SB PROPELLER RPM ACTUAL VALUE	MAGNETIC COMPAS (HDG) MAGNETIC DEVIATION	TANK 4 PERCENTAGE ALARM LOW	Winch - Leds to full brightness
AQM SB RPM COMMAND SET VALUE	MAGNETIC COMPAS (HDG) MAGNETIC HEADING	TANK 4 PERCENTAGE ALARM LOW LOW	Winch - PTO1 PRESS OK
AQM SB RPM MEASUREMENT ACTUAL VALUE	MAGNETIC COMPAS (HDG) MAGNETIC VARIATION	TANK 4 SPECIFIC GRAVITY	Winch - PTO2 PRESS OK
AQM SB SAFETY OVERRIDE FUNC. ACTIVATED	MAGNETIC COMPAS (HDG) VAR. (E=69/W=87)	TANK 4 WEIGHT	Winch - q3742 Group Alarm PLC Fault
AQM SB SLIPPING CLUTCH CMND SET VALUE	DG PS GENERATOR KW LOAD (%)	TANK 7 PERCENTAGE ALARM HIGH HIGH	Winch - q3770 Group Alarm General hydr
AQM SB STEERING COMMAND SET VALUE	DG PS GENERATOR RATED CURRENT	TANK 13 INHIBIT HIGH	Winch - q3772 Group Alarm PTO pumps
AQM SB STEERING MEAS. ACTUAL VALUE	DG PS IOBOARD -RATED KW POWER [100%]	TANK 13 INHIBIT HIGH HIGH	Winch - q3774 Group Alarm Hydr Epumps
ME PS Act Max Avail Eng Perc Torque	DG PS IOBOARD/DISPLAY -OUT BUS FREQ	TANK 13 INHIBIT LOW	Winch - q3776 GroupAlarm Hydr RetPresLow
ME PS Clutch Press	DG PS IOBOARD/DISPLAY -OUT GEN CB	TANK 13 INHIBIT LOW LOW	Winch - q3778 Group Alarm Hydr LevelLow
ME PS Coolant Press	DG PS PROGRAM NOT RUNNING	TANK 13 PERCENTAGE ALARM HIGH	Winch - q3780 Group Alarm Hydr FiltClogg
ME PS Crankcase Press	PS FUEL SEPERATOR 1 DIESEL CONSUMERS	TANK 13 PERCENTAGE ALARM HIGH HIGH	Winch - q3782 GroupAlarm Hyd OilTempHigh
ME PS Engine Air Inlet Temp	PS FUEL SEPERATOR 2 DIESEL CONSUMERS	TANK 13 PERCENTAGE ALARM LOW	Winch - q3784 Group Alarm EmergStopWinch
ME PS Engine Coolant Temp	PS generator apparent power	TANK 13 PERCENTAGE ALARM LOW LOW	Winch - spare
ME PS Engine Exhaust Gas Temp Average	PS generator average current	TANK 13 SPECIFIC GRAVITY	WHEELHOUSE RED SWITCH DIM DOWN
ME PS Engine Fuel Delivery Press	PS generator average voltage	TANK 13 WEIGHT	N.A. >HVAC AC FAN CTRL IN AUTO MODE
ME PS Engine Fuel Filter Diff Press	PS Generator Coolant Temp	TANK 14 INHIBIT HIGH	N.A. >HVAC COOL MODE CTRL IN AUTO MODE
ME PS Engine Main Bearing 1 Temp	PS Generator Coolant Temp Alarm	TANK 14 INHIBIT HIGH HIGH	AUTO MODE - FAN PS
ME PS Engine Main Bearing 2 Temp	PS Generator Coolant Temp Sens Failure	TANK 14 INHIBIT LOW	AUTO MODE - FAN SB
ME PS Engine Oil Filter Diff Press	PS generator current L1	TANK 14 INHIBIT LOW LOW	EMERGENCY BATTERY CHARGING CURRENT
ME PS Engine Oil Press	PS generator current L2	TANK 14 PERCENTAGE ALARM HIGH	EMERGENCY BATTERY VOLTAGE
ME PS Engine Oil Temp	PS generator current L3	TANK 14 PERCENTAGE ALARM HIGH HIGH	EM-STOP GENERAL RESET COMMAND
ME PS Engine Speed	PS generator DC supply term. 1-2	TANK 14 PERCENTAGE ALARM LOW	Engine 1 running ME PS
ME PS Engine Turbocharger Oil Temp	PS generator DC supply term. 98-99	TANK 14 PERCENTAGE ALARM LOW LOW	Engine 1 Sensor Failure ME PS
ME PS Fuel Rate	PS Generator Exh Gas Temp	TANK 14 SPECIFIC GRAVITY	Engine 2 running ME SB
ME PS Fuel Temp	PS Generator Exh Gas Temp Alarm	TANK 14 WEIGHT	Engine 2 Sensor Failure ME SB
ME PS FuelLevel1_Norm	PS Generator Exh Gas Temp Sens Failure	BILGE LEVEL SWITCH ER DIRECT BILGE PS	ENGINE ROOM FAN 1 HIGH SPEED
ME PS FuelLevel2_Norm	PS generator frequency	BILGE LEVEL SWITCH VOID BELOW ROPE STORE	ENGINE ROOM FAN 1 RUNNING
ME PS Max. Scale Fuel Consumpt.l/h	PS Generator Fuel Pressure	BILGE LEVEL SWITCH VOID BELOW SWBD ROOM	ENGINE ROOM FAN 2 HIGH SPEED
ME PS Percent Load At Current Speed	PS Generator Fuel Pressure Alarm	BILGE WATER TANK LEVEL SWITCH	ENGINE ROOM FAN 2 RUNNING
ME PS Trip Average Fuel Rate	PS Generator Fuel Pressure Sens Failure	FLUSH HATCH ER	ENGINE ROOM FAN 2 SELECTION
ME PS Trip Engine Running Time	PS generator generator Speed	FO ALARM TANK HIGH	ESCAPE HATCH AFT DECK
ME PS Eng Exhaust Gas Port 1 Temp	PS Generator High Coolant	FO HEADER TANK LEVEL LOW	ESCAPE HATCH FORE DECK
ME PS Eng Exhaust Gas Port 2 Temp	PS Generator High Coolant Shutdown	FO SYSTEM OVERFLOW TANK3 LEVEL HIGH	FIRE - FIRE - ALARM LED
ME PS Eng Exhaust Gas Port 3 Temp	PS GENERATOR HT TANK LOW LEVEL	FO SYSTEM OVERFLOW TANK3 LEVEL LOW	Fire alarm panel XP41 Not Present
ME PS Eng Exhaust Gas Port 4 Temp	PS Generator Low Oil Press	FO TRANSFER SYSTEM BUNKER VALVE OPEN	FLC.Value_Actual_Pay_Out_W1D1
ME PS Eng Exhaust Gas Port 5 Temp	PS Generator Low Oil Press Shutdown	FO TRANSFER SYSTEM WATER IN OIL	FLC.Value_ATFB_W2D1
ME PS Eng Exhaust Gas Port 6 Temp	PS Generator Low Oil Temp	GMDSS BATTERY CHARGING CURRENT	FLC.Value_ATFB_W2D2
ME PS Eng Exhaust Gas Port 7 Temp	PS Generator Low Oil Temp Shutdown	GMDSS BATTERY VOLTAGE	Options.W1_ANCHORS
ME PS Eng Exhaust Gas Port 8 Temp	PS GENERATOR LT TANK LOW LEVEL	CO2 24Vdc POWER FAIL	Options.W2_RES1
ME PS Eng Exhaust Gas Port 11 Temp	PS Generator Oil Pressure	CO2 RELEASE	Options.W2_RES2
ME PS Eng Exhaust Gas Port 12 Temp	PS Generator Oil Pressure Alarm	NMEA: Autopilot No Communication	PANEL.IP_NR__Fore2
ME PS Eng Exhaust Gas Port 13 Temp	PS Generator Oil Pressure Sens Failure	NMEA: Echo No Communication	PMS-1 panel XP61 Not Present
ME PS Eng Exhaust Gas Port 14 Temp	PS generator power	NMEA: GPS No Communication	PMS-2 panel XP62 Not Present
ME PS Eng Exhaust Gas Port 15 Temp	PS generator power factor	NMEA: Gyro No Communication	PMS-3 panel XP63 Not Present
ME PS Eng Exhaust Gas Port 16 Temp.	PS generator reactive power	NMEA: Meteo Sensor No Communication	HVAC AC FAN FAIL
ME PS Eng Exhaust Gas Port 17 Temp	PS generator Remote	NMEA: Speedlog No Communication	HVAC COOL MODE FAIL
ME PS Eng Exhaust Gas Port 18 Temp	PS generator Running	Server_1 Active	HYDR SYSTEM COOLING WATER PUMP SELECTION
ME SB Act Max Avail Eng Perc Torque	DG SB GENERATOR KW LOAD (%)	Server_1 out of order	KEYB AUTO MODE - FAN PS
ME SB Clutch Press	DG SB GENERATOR RATED CURRENT	Server_2 Active	LoadPin_AxleW1.RawValue
ME SB Coolant Press	DG SB HEATER CONTROL FAILURE	Server_2 out of order	LoadPinW1D2.RawValue
ME SB Crankcase Press	DG SB HOUR COUNTER	XP02- Board 2 Earth Fault	LoadPinW2D1.RawValue
ME SB Engine Air Inlet Temp	DG SB IOBOARD -RATED KW POWER [100%]	PS generator Abs. run hours	LoadPinW2D2.RawValue
ME SB Engine Coolant Temp	DG SB IOBOARD/DISPLAY -OUT BUS FREQ	MBM_TCP: Winch System No Communication	Parameters.W1D2_DIAMETER.def
ME SB Engine Exhaust Gas Temp Average	DG SB IOBOARD/DISPLAY -OUT GEN CB	AUTOPILOT ON	Parameters.W1D2_DIAMETER.max
ME SB Engine Fuel Delivery Press	DG SB MIMIC - PB HEATER OFF	AUTOPILOT (HSC) HEADING MAGNETIC	Parameters.W1D2_DIAMETER.min
ME SB Engine Fuel Filter Diff Press	DG SB PROGRAM NOT RUNNING	AUTOPILOT (HSC) HEADING TRUE	Parameters.W1D2_DIAMETER.value
ME SB Engine Main Bearing 1 Temp	SB FUEL SEPERATOR 1 DIESEL CONSUMERS	REVERSE COMMAND FOR RR AND AUTOPILOT	Parameters.W1D2_LENGTH.value
ME SB Engine Main Bearing 2 Temp	SB FUEL SEPERATOR 2 DIESEL CONSUMERS	EAS Chief Eng - Ethernet Port A No Comm.	_FLCParameters.W1D1.Down
ME SB Engine Oil Filter Diff Press	SB generator Abs. run hours	EAS Chief Eng - Ethernet Port B No Comm.	_FLCParameters.W1D1.Tonnage
ME SB Engine Oil Press	SB generator apparent power	EAS Mess - Ethernet Port A No Comm	_FLCParameters.W1D1.Up
ME SB Engine Oil Temp	SB generator average current	EAS Mess - Ethernet Port B No Comm	_FLCParameters.W1D2.Tonnage
ME SB Engine Speed	SB generator average voltage	EAS Mess Port C No Comm Client_2 Port A	_FLCParameters.W2D2.Tonnage
ME SB Engine Turbocharger Oil Temp	SB Generator Coolant Temp	ACTIVE ANTI FOULING SYSTEM FAILURE	_PRAXIS.VAL_BrakeW1D1
ME SB Fuel Rate	SB Generator Coolant Temp Alarm	Alarm01 [3422] Emergency stop	_PRAXIS.Val_Joystick_W1_W2
ME SB Fuel Temp	SB generator current L1	Alarm16 [1093] Filter 2 clogged	CalcWire.ActualFittedLength_W1D2.value
ME SB FuelLevel1_Norm	SB generator current L2	SB MAIN ENGINE COMMON ALARM	
ME SB FuelLevel2_Norm	SB generator current L3	PS MAIN ENGINE COMMON ALARM	
ME SB Max. Scale Fuel Consumpt.l/h	SB generator DC supply term. 1-2	WT DOOR ER	
ME SB Percent Load At Current Speed	SB generator DC supply term. 98-99	WT DOOR MAIN DECK PS	
ME SB Trip Average Fuel Rate	SB Generator Exh Gas Temp	WT DOOR MAIN DECK SB	
ME SB Trip Engine Running Time	SB Generator Exh Gas Temp Alarm	WT DOOR WHEELHOUSE	
ME SB Eng Exhaust Gas Port 1 Temp	SB generator frequency	TRIP COUNTER AC COOLING PUMP	
ME SB Eng Exhaust Gas Port 2 Temp	SB Generator Fuel Pressure	TRIP COUNTER BILGE STRIPPING PUMP	
ME SB Eng Exhaust Gas Port 3 Temp	SB Generator Fuel Pressure Alarm	TRIP COUNTER CLEAN OIL PUMP	
ME SB Eng Exhaust Gas Port 4 Temp	SB generator generator Speed	TRIP COUNTER DG PS	
ME SB Eng Exhaust Gas Port 5 Temp	SB Generator High Coolant	TRIP COUNTER DG SB	
ME SB Eng Exhaust Gas Port 6 Temp	SB GENERATOR HT TANK LOW LEVEL	TRIP COUNTER DIRTY OIL PUMP	
ME SB Eng Exhaust Gas Port 7 Temp	SB Generator Low Oil Press	TRIP COUNTER DISPERSANT PUMP	
ME SB Eng Exhaust Gas Port 8 Temp	SB Generator Low Oil Temp	TRIP COUNTER FO SEPERATOR 1	
ME SB Eng Exhaust Gas Port 11 Temp	SB GENERATOR LT TANK LOW LEVEL	TRIP COUNTER FO SEPERATOR 2	
ME SB Eng Exhaust Gas Port 12 Temp	SB Generator Oil Pressure	TRIP COUNTER FUEL OIL TRANSFER PUMP	
ME SB Eng Exhaust Gas Port 13 Temp	SB Generator Oil Pressure Alarm	TRIP COUNTER GENERAL SERVICE PUMP #1	
ME SB Eng Exhaust Gas Port 14 Temp	SB generator power	TRIP COUNTER GENERAL SERVICE PUMP #2	
ME SB Eng Exhaust Gas Port 15 Temp	SB generator power factor	TRIP COUNTER HYDR COOL WATER PUMP	
ME SB Eng Exhaust Gas Port 16 Temp.	SB generator reactive power	TRIP COUNTER HYDR HPU MAIN PUMP	
ME SB Eng Exhaust Gas Port 17 Temp	SB generator Remote	TRIP COUNTER SEWAGE PUMP	
ME SB Eng Exhaust Gas Port 18 Temp	SB generator Running	TRIP COUNTER SHORE	

Table A.1: Sensor list

A.2. RSD Product sheet

REVERSED STERN DRIVE TUG 2513

"INNOVATION"

GENERAL

Yard number	515001
Delivery date	April 2018
Basic functions	Towing and mooring
Classification	Bureau Veritas I ✠ HULL ● MACH Tug Coastal Service AUT UMS COMF-NOISE 3, COMF-VIB 3
Owner	Damen Marine Services
Flag	The Netherlands

DIMENSIONS

Length overall	24.73 m
Beam overall	13.13 m
Depth at sides	4.95 m
Draught aft	5.50 m
Displacement (98% consumables)	525 t

TANK CAPACITIES

Fuel oil	77.4 m^3
Fresh water	10.2 m^3
Bilge water	6.0 m^3
Sewage	6.0 m^3
Dirty oil	2.5 m^3
Lubrication oil	2.5 m^3

PERFORMANCES

Bollard pull ahead	75.3 t
Bollard pull astern	71.2 t
Speed ahead	13.0 kn
Speed astern	12.8 kn

PROPULSION SYSTEM

Main engines	2x MTU 16V 4000 M63L
Total power	4480 bkW (6008 bhp) at 1800 rpm
Thrusters	Rolls Royce US 255
Propeller diameter	2700 mm
Forced ventilation	60.000 m^3/h

AUXILIARY EQUIPMENT

Generator set	2x Caterpillar C4.4 TA, 81 kVA, 400/230 V, 50 Hz
General service pumps	2x Azcue CA 50/3A 20 m^3/h at 2.35 bar
Bilge pump	Azcue CA 32/0.5 3.6 m^3/h at 1.1 bar
Fuel pump	Azcue BR-41-10 12 m^3/h at 1 bar
Fuel oil purifier	2x CJC, PTU3 3x FA/BLA 27/27, 1920 l/h each
Cooling system	Closed box cooling system
Fresh water pressure set	Sterling AOHA HBK 111
Hydraulic system	Main engine driven pumps

DECK LAY-OUT

Anchor	1x 360 kg Pool (High Holding Power)
Anchor winch	Electric 10 m/min
Towing winch	Hydraulically driven split drum 31 ton pull up to 11 m/min, reduced pull up to 38 m/min, 175 ton brake
Fendering	Cylinder + block bow fender, D-fender side/aft

ACCOMMODATION

For 4 persons, completely insulated and finished with durable modern linings, sound absorbing ceiling in the wheelhouse and floating floors. Air-conditioned wheelhouse, accommodation and switchboard room. Accommodation above main deck with a captain's cabin, chief engineer's cabin, one double crew cabin, pantry, mess/dayroom and sanitary facilities. The superstructure is mounted resiliently to reduce noise levels.

NAUTICAL AND COMMUNICATION EQUIPMENT

Searchlight	1x Norselight, 2000 W
Radar system	1x Furuno FAR-1518-BB
Compass	Cassens & Plath Reflecta 11
Autopilot	Simrad AP-70
Satellite compass/GPS	Simrad GN70/HS80A
Echosounder	Furuno FE-800
Speed log	Furuno DS-80
VHF	2x Sailor 6222
VHF hand-held	Jotron TR-20
Navtex	Furuno NX-700
AIS	Furuno FA-170
EPIRB	Jotron Tron-60S
SART	Jotron Tronsart20
Anemometer	Gill Instruments GMX 500
VSAT	Intellian v60G

DAMEN

REVERSED STERN DRIVE TUG 2513

"INNOVATION"

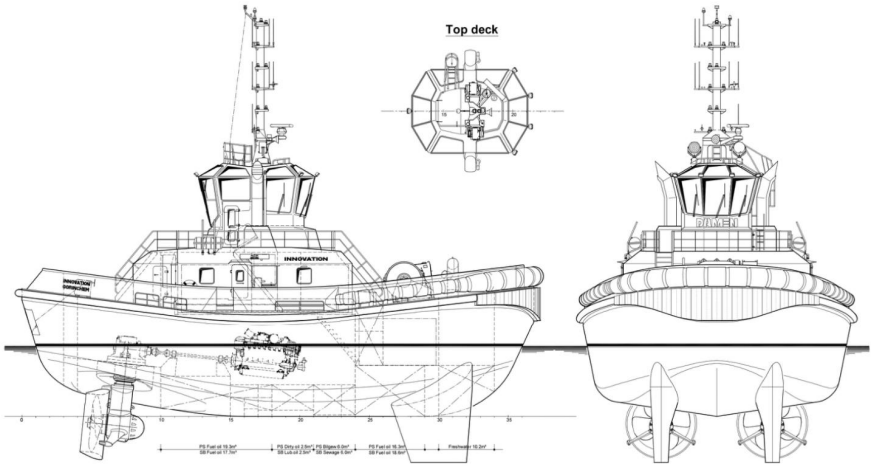

Top deck

Main deck

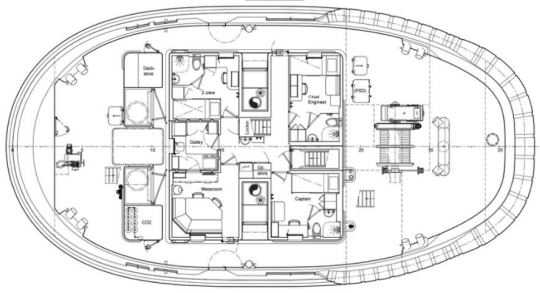

Bridge deck

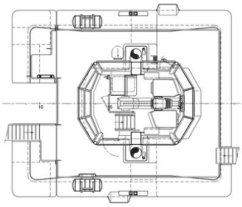

Below Main deck

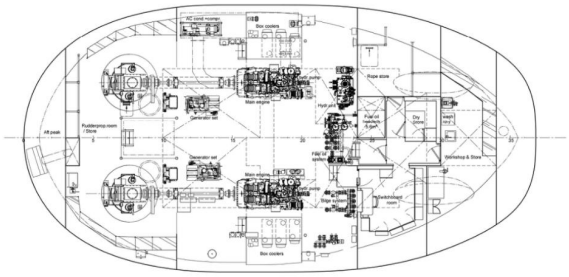

DAMEN

DAMEN SHIPYARDS GROUP

Avelingen-West 20
4202 MS Gorinchem
The Netherlands

P.O. Box 1
4200 AA Gorinchem
The Netherlands

phone +31 (0)183 63 99 22
fax +31 (0)183 63 21 89

info@damen.com
www.damen.com

A.3. Steady state vectors

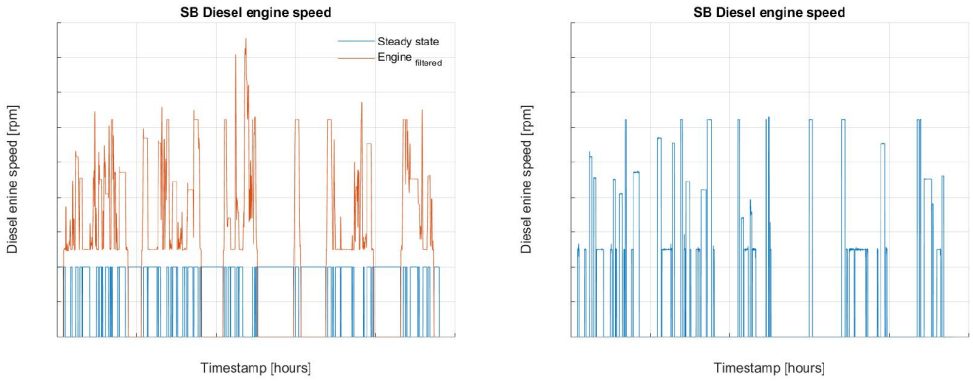

(a) (b)

Figure A.1: SB Diesel engine speed

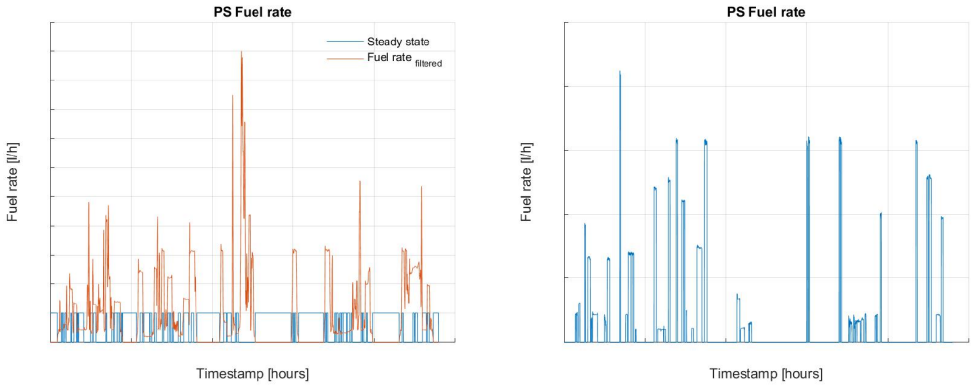

(a) (b)

Figure A.2: PS Fuel rate

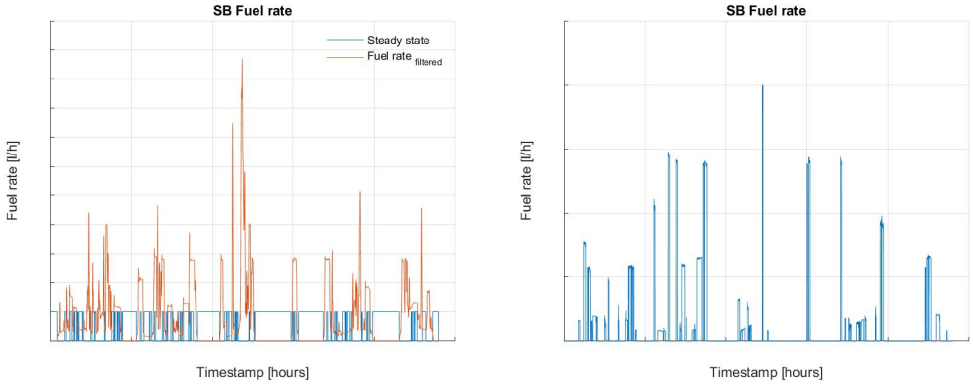

(a) (b)

Figure A.3: SB Fuel rate

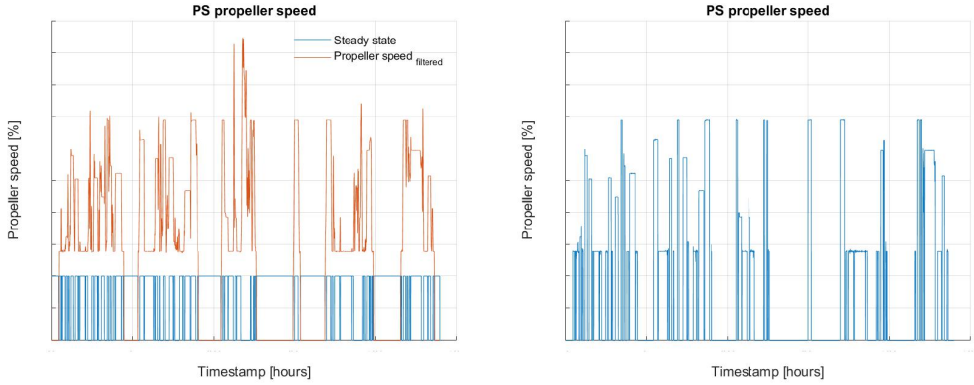

(a) (b)

Figure A.4: PS Propeller speed

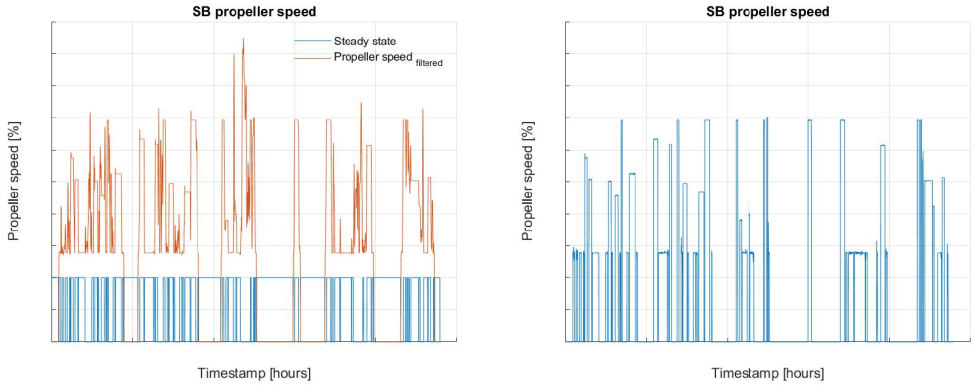

(a) (b)

Figure A.5: SB Propeller speed

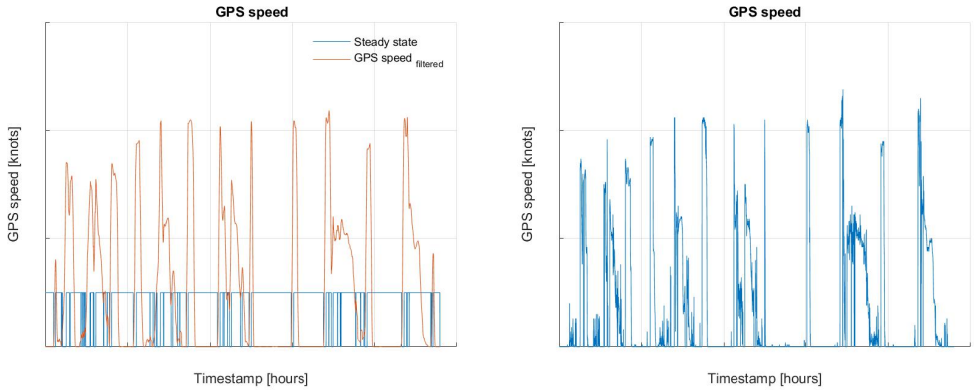

(a) (b)

Figure A.6: GPS speed

,

A.4. Steady state script

```
clear all; clc; clear figures; close all;

%import processed remote logged data
open('515001_sensor_215.fig');
a = get(gca,'Children');
xdata = get(a, 'XData');
ydata = get(a, 'YData');
close

%find steady state data
%tune parameters
bigstep_tune        =   5;          % forward range check step
spread_range_tune   =   40;         % forward check max deviation
derivative_tune     =   1.5e-04;    % max slope threshold
minconnect_tune     =   5;          % minimal connected output points

%moving-average digital filter
windowSize          =   10;
bfilter             =   (1/windowSize)*ones(1,windowSize);
afilter             =   1;
ydata_filtered      =   filter(bfilter,afilter,ydata);

%get derivative of dataset
y_derivative = gradient(ydata_filtered(:)) ./ gradient(xdata(:));

%check for max slope and difference over max step
ss = zeros(1,length(ydata));
for i = 1:(length(ydata_filtered)-bigstep_tune)
    if y_derivative(i) < derivative_tune && ydata_filtered(i)-
        abs(ydata_filtered(i+bigstep_tune)) < spread_range_tune
        ss(i) = 1;
    end
end

%remove too small connected output points
transitions = diff([0 ;ss' == 1; 0]);
runstarts   = find(transitions == 1);
runends     = find(transitions == -1);
runlengths  = runends - runstarts;
runstarts(runlengths > minconnect_tune-1)   = [];
runends(runlengths > minconnect_tune-1)     = [];
indices     = arrayfun(@(s, e) s:e-1, runstarts,
 runends, 'UniformOutput', false);
indices     = [indices{:}];
ss(indices) = [0];

%save steady state vector for a specific sensor
de_ps_steadystate           = ss.*ydata;
de_ps_steadystate_vector    = ss;
save('steady_state_515001\de_ps','de_ps_steadystate',
'de_ps_steadystate_vector')
```

Bibliography

[1] A. Dubey, A. Subramanian. (2020). Hardware in the loop simulation and control design for autonomous free running ship models. *Defence science journal.* 10.14429/dsj.70.14926.

[2] D. Stapersma, A. Vrijdag. (2017). Linearisation of a ship propulsion system model. *Ocean Engineering.* 10.1016/j.oceaneng.2017.07.014.

[3] L. Birk. *Fundamentals of Ship Hydrodynamics: Fluid Mechanics, Ship Resistance and Propulsion.* John Wiley & Sons, 1st edition, (2019). https://doi.org/10.1002/9781119191575.ch31.

[4] Y. Marchesse, F. Ville, P. Velex, C. Changenet. (2011). Investigations on cfd simulations for predicting windage power losses in spur gears. *Journal of Mechanical Design.* 10.1115/1.4003357.

[5] S. Akyurek, G.S. Ozden, B. Kurkcu, U. Kaynak, C. Kasnakoglu. (2015). Design of a flight stabilizer for fixed-wing aircrafts using h loop shaping method. *2015 9th International Conference on Electrical and Electronics Engineering (ELECO).* 10.1109/ELECO.2015.7394579.

[6] D. Durante, G. Dubbioso, C. Testa. (2013). Simplified hydrodynamic models for the analysis of marine propellers in a wake-field. *Journal of Hydrodynamics, Volume 25).* 10.1016/S1001-6058(13)60445-X.

[7] J. Carlton. *Marine Propellers and Propulsion.* Butterworth-Heinemann, 3rd edition, (2012). 10.1016/S1001-6058(13)60445-X.

[8] R.D. Reitz, C.J. Rutland. (1995). Development and testing of diesel engine cfd models. *Engine Research Center. University of Wisconsin-Madison.*

[9] A. Palladino, G. Fiengo, F. Giovagnini, D. Lanzo. (2009). A micro hardware-in-the-loop test system. *2009 European Control Conference (ECC).* 10.23919/ECC.2009.7074997.

[10] H. Klein Woud, D. Stapersma. *Design of Propulsion and Electric Power Generation Systems.* Institute Of Marine Engineers, 1st edition, (2002).

[11] M. Godjevac, J. Drijver, L de Vries, D. Stapersma. (2015). Evaluation of losses in maritime gearboxes. *Proceedings of the Institution of Mechanical Engineers Part M Journal of Engineering for the Maritime Environment 230(4).* 10.1177/1475090215613814.

[12] P. de Vos. (2015). Design of a new ship propulsion system fundamentals course. *Conference: International Marine Design Conference.* https://www.researchgate.net/publication/284646715_Design_of_a_New_Ship_Propulsion_System_Fundamentals_course/comments.

[13] Dieselnet. Eu: Fuels: Automotive diesel fuel. retrieved from `https://dieselnet.com/standards/eu/fuel_automotive.php`, n.d. (2015). accessed 01-01-2020.

[14] E. Wright. Powershell - split large log and text files. retrieved from `https://gallery.technet.microsoft.com/scriptcenter/PowerShell-Split-large-log-6f2c4da0`, n.d. (2011). accessed 01-01-2020.

[15] F. Concli. (2012). Oil squeezing power losses in gears: A cfd analysis. *Advanced in fluid mechanics IX (WIT Transactions on Engineering Sciences).* 10.2495/AFM120041.

[16] M. Ishida, H. Ueki, N. Matsumura, M. Yamaguchi, G. Luo. (1996). Diesel combustion analysis based on two-zone model : Comparison between model analysis and experiment. *JSME International Journal Series B Fluids and Thermal Engineering.* 10.1299/jsmeb.39.185.

[17] J. Holtrop, G.G.J. Mennen. (1982). An approximate power prediction method. *International Shipbuilding Progress.*

[18] L. Huijgens, A. Vrijdag, H. Hopman. (2018). Propeller-engine interaction in a dynamic model scale environment. *ISOPE 2018: 28th International Ocean and Polar Engineering*.

[19] V.R. Aparow, K. Hudha, H. Jamaluddin. (2014). Model-in-the-loop simulation of gap and torque tracking control using electronic wedge brake actuator. *Int. J. Vehicle Safety, Vol. 7*. 10.1109/ICAL.2007.4338984.

[20] M.Fritz, S. Winter, J. Freund, S. Pflueger, O. Zeile, J. Eickhoff, H. Roeser. (2015). Hardware-in-the-loop environment for verification of a small satellite's on-board software. *Aerospace Science and Technology*. 10.1016/j.ast.2015.09.020.

[21] J. Du, Y.Wang, C. Yang, H. Wang. (2007). Hardware-in-the-loop simulation approach to testing controller of sequential turbocharging system. *Automation and Logistics, 2007 IEEE International Conference*. 10.1109/ICAL.2007.4338984.

[22] J.C. Refsgaard, H.J. Henriksen. (2003). Modelling guidelines—terminology and guiding principles. *Advances in Water Resources Volume 27, Issue 1, January 2004, Pages 71-82*. https://doi.org/10.1016/j.advwatres.2003.08.006.

[23] H. Jasak, V. Vulkcevic, I. Gratin, I. Lalovic. (2019). Cfd validation and grid sensitivity studies of full scale ship self propulsion. *Int. J. Nav. Archit. Ocean Eng.* 10.1016/j.ijnaoe.2017.12.004.

[24] C. Fernandes, P. Marques, R. Martins, J. Seabra. (2015). Gearbox power loss. part iii: Application to a parallel axis and a planetary gearbox. *Tribology International*. 10.1016/j.triboint.2015.03.029.

[25] R.D. Geertsma, R.R. Negenborn, K. Visser, M.A. Loonstijn, J.J. Hopman. (2017). Pitch control for ships with diesel mechanical and hybrid propulsion: Modelling, validation and performance quantification. *Applied Energy, 206, 1609-1631*. 10.1016/j.apenergy.2017.09.103.

[26] H. Nguyen, Y. Besanger, Q.T. Tran, T.L. Nguyen, C. Boudinet, R. Brandl, F. Marten, A. Markou, P. Kotsampopoulos, A.A. van der Meer, E. Guillo-Sansano, G. Lauss, T. Strasser, K. Heussen. (2017). Real-time simulation and hardware-in-the-loop approaches for integrating renewable energy sources into smart grids. *IEEE PES IGST Asia 2017*.

[27] Y. Tsai, S. Chin, G. Lee, S. Goh, K. Low. (2015). Hardware-in-the-loop validation of gps/gnss based mission planning for leo satellites. *International Symposium on GNSS 2015*.

[28] H. Yamasaki, T. Matsumoto, K. Itakura, S. Miyamoto, K. Yonemoto. (2013). Development of a hardware-in-the-loop simulator and flight simulation of a subscale experimental winged rocket. *2013 IEEE/ASME International Conference on Advanced Intelligent Mechatronics*. 10.1109/AIM.2013.6584309.

[29] L. Chang, G. Lui, L. Wu. (2011). Research on vibration influence chart of planetary gear systems. *Applied Mechanics and Materials)*. 10.4028/www.scientific.net/AMM.86.747.

[30] M. Altosole, U. Campora, M. Figari, M. Laviola, M. Martelli. (2019). A diesel engine modelling approach for ship propulsion real-time simulators. *Journal of Marine Science and Engineering*. 10.3390/jmse7050138.

[31] S. Chesi, O. Perez, M. Romano. (2015). A dynamic hardware-in-the-loop three-axis simulator of nanosatellite dimensions.

[32] F. Perabo, M. Zadeh. (2020). Modelling of a shipboard electric power system for hardware-in-the-loop testing. *IEEE Transportation Electrification Conference & Expo (ITEC)*. 10.1109/ITEC48692.2020.9161719.

[33] M.A. Loonstijn. (2017). Diesel a-m (a-modular) model proposal expanding the diesel a model for advanced turbocharging capabilities.

[34] Z. Ahmad, S. Papadakis, A.D. Guerra, L. Jose, M.A M.M. van der Meijden. (2020). Hardware-in-the-loop based testing of wind turbine controllers for transient stability enhancement. *29th IEEE International Symposium on Industrial Electronics*. 10.1109/ISIE45063.2020.9152436.

[35] Damen Magazine. (2019). Smart sensor mapping breaks new ground in maritime remote monitoring. *invullen*. URL `https://magazine.damen.com/innovation/smart-sensor-mapping-breaks-new-ground-in-maritime-remote-monitoring`.

[36] C. Coopmans, M. Podhradsky, N.V. Hoffer. (2015). Software- and hardware-in-the-loop verification of flight dynamics model and flight control simulation of a fixed-wing unmanned aerial vehicle. *2015 Workshop on Research, Education and Development of Unmanned Aerial Systems (RED-UAS)*. 10.1109/RED-UAS.2015.7440998.

[37] R. Skjetne, O. Egeland. (2005). Hardware-in-the-loop simulation for testing of dp vessels. *International Conference on Technology & Operation of Offshore Support Vessels*.

[38] M.W.C Oosterveld. (1970). Wake adapted ducted propellers.

[39] R. Bhandia, J. Chavez, M. Cvetkovic, P. Palensky. (2018). High impedance fault detection in real-time and evaluation using hardware-in-loop testing. *Proceedings IECON 2018 - 44th Annual Conference of the IEEE Industrial Electronics Society*. 10.1109/IECON.2018.8591824.

[40] R. Abdulhamid, N.M.F. de Oliveira, R. d'Amore. (2016). Proposal of hardware-in-the-loop control platform for small fixed-wing uavs. *2016 Annual IEEE Systems Conference (SysCon)*. 10.1109/SYSCON.2016.7490637.

[41] A.T. Al-Hammouri, L. Nordström, M. Chenine, L. Vanfretti, N. Honeth, R. Leelaruji. (2012). Virtualization of synchronized phasor measurement units within real-time simulators for smart grid applications. *IEEE Power and Energy Society General Meeting*. 10.1109/PESGM.2012.6344949.

[42] I. Lugo-Cárdenas, S. Salazar, R. Lozano. (2016). The mav3dsim hardware in the loop simulation platform for research and validation of uav controllers. *2016 International Conference on Unmanned Aircraft Systems (ICUAS)*. 10.1109/ICUAS.2016.7502657.

[43] D. Aregger, H. Hesse, F. Gohl, J. Heilmann, C. Houle, R.S. Smith, R.H. Luchsinger. (2015). Hardware in the loop testing for autonomous airborne wind energy systems. *Airborne Wind Energy Conference 2015*.

[44] Z. Luman, M. Roh, S. Ham. (2016). Hardware-in-the-loop simulation for a heave compensator of an offshore support vessel. *ASME 2016 35th International Conference on Ocean, Offshore and Arctic Engineering*. 10.1115/OMAE2016-54709.

[45] C. Kamal, S. Jain. (2016). Hardware in the loop simulation for a mini uav. *IFAC-PapersOnLine*. 10.1016/j.ifacol.2016.03.138.

[46] S. Sankararaman, S. Mahadevan. (2015). Integration of model verification, validation, and calibration for uncertainty quantification in engineering systems. *Reliability Engineering & System Safety Volume 138, June 2015, Pages 194-209*. https://doi.org/10.1016/j.ress.2015.01.023.

[47] S. Raman, N. Sivashankar, W. Milam, W. Stuart, S. Nabi. (1999). Design and implementation of hil simulators for powertrain control system software development. *Proceedings of the 1999 American Control Conference (Cat. No. 99CH36251)*. 10.1109/ACC.1999.782919.

[48] D. Stapersma. (1994). The importance of (e)mission profiles for naval ships. *INEC 94, Cost Effective Marine Defence*.

[49] D. Stapersma. *A fundamental approach to performance analysis, turbocharging, combustion, emissions and heat transfer*. NLDA & Delft UT, 7th edition, (2010).

[50] M. Blanke, K. Lindegaard, T. Fossen. (2000). Dynamic model for thrust generation of marine propellers. *IFAC Proceedings Volumes 33)*. 10.1016/S1474-6670(17)37100-8.

[51] A. Vrijdag, D. Stapersma, T. van Terwisga. (2009). Systematic modelling, verification, calibration and validation of a ship propulsion simulation model. *Proceedings of IMarEST - Part A - Journal of Marine Engineering and Technology*. https://doi.org/10.1080/20464177.2009.11020223.

[52] M. Altosole, G. Benvenuto, M. Figari, U. Campora. (2008). Real-time simulation of a cogag naval ship propulsion system. 10.1243/14750902JEME121.

[53] A. Vrijdag. (2016). Potential of hardware-in-the-loop simulation in the towing tank. *In S. Farr, J. Zande, & B. Kirkwood (Eds.), Proceedings OCEANS 2016 MTS/IEEE Monterey Piscataway, NJ, USA: IEEE*. https://doi.org/10.1109/OCEANS.2016.7761060.

[54] W. Froude. (1955). The papers of william froude.

[55] K. Qi, L. Feng, X. Leng, B. Du, W. Long. (2010). Simulation of quasi-dimensional combustion model for predicting diesel engine performance. *Applied Mathematical Modelling Volume 35, Issue 2, February 2011, Pages 930-940.* 10.1016/j.apm.2010.07.047.

[56] Y. Zhang, H. Yang, Z. Jiang, F. Hu, W. Zhang. (2015). Rapid construction of hardware-in-the-loop simulation and control system validation for the thx rocket. *Proceedings of the 22nd ESA Symposium on European Rocket and Balloon Programmes and Related Research.* 2015ESASP.730..227Z.

[57] A.W. Wemekamp, Y. Luo. (2014). Efficiency and thermal gearbox calculation. 10.1533/9781782421955.1069.

[58] S.A. Miedema, Z. Lu. (2002). The dynamic behavior of a diesel engine. *WEDA TAMUAt: Denver, Colorado, USA.*